

**Integration of EGFR and LIN-12/Notch signaling in Vulval Precursor Cell fate  
specification in *Caenorhabditis elegans***

**Ryan Underwood**

Submitted in partial fulfillment of the  
requirements for the degree of  
Doctor of Philosophy  
in the Graduate School of Arts and Sciences

COLUMBIA UNIVERSITY

2018

© 2018

Ryan Underwood

All rights reserved

## ABSTRACT

### Integration of EGFR and LIN-12/Notch signaling in Vulval Precursor Cell fate specification in *Caenorhabditis elegans*

Ryan Underwood

Cellular differentiation is the cornerstone of metazoan development. Cell-cell signaling mechanisms are responsible for the specification of many cell fates. The response of a particular cell to a given signal is highly context dependent allowing signaling mechanisms to be reused to produce a variety of different outcomes. The EGFR and LIN-12/Notch signaling pathways are well-conserved across metazoan species and govern many fate-specification events. The specification of *C. elegans* Vulval Precursor Cells (VPCs) offers a powerful system to investigate how these signaling mechanisms specify cell-fates, and previous studies of VPC fate patterning have identified several forms of crosstalk between these two critical signaling mechanisms.

In this thesis, I investigate how input from both the EGFR and LIN-12/Notch signaling pathways is integrated by the VPCs. I provide evidence that VPCs respond to the relative levels of LIN-12/Notch and EGFR signaling. I show that LIN-1/Elk1 is critical for VPCs to adopt discrete cell fates. In addition, I show that the Mediator components SUR-2/Med23 and the CDK-8 kinase module (CKM), in cooperation with LIN-1/Elk1, are required for an EGFR-mediated resistance to LIN-12/Notch activity.

I also used CRISPR/Cas9 techniques to generate endogenous, fluorescently-tagged LAG-1 proteins. Characterization of tagged LAG-1 accumulation in the VPCs and in the somatic gonad show that LAG-1 is present in all VPCs at low levels in a *lin-12/Notch* independent manner. Activation of LIN-12/Notch is correlated with higher levels of LAG-1 accumulation compared to cells that do not have activated LIN-12/Notch. These findings suggest a potential autoregulation mechanism for *lag-1* in certain contexts. They also suggest that endogenously-tagged LAG-1 may be a useful molecular marker of LIN-12/Notch activation.

## Table of Contents

List of Figures and Tables .....	vi
Acknowledgements .....	viii
Chapter 1. General Introduction .....	1
Vulval development of <i>Caenorhabditis elegans</i> .....	2
Establishment and maintenance of the vulval competency group .....	3
VPC specification.....	4
Inductive signal .....	4
Identification of the inductive signal.....	4
EGFR-Ras-ERK signaling in P6.p .....	6
Effectors and regulators of EGFR-RAS-ERK .....	6
<i>ln-1</i> – Ets-domain-containing transcription factor .....	7
Lateral signal .....	8
Identification of the lateral signal .....	8
LIN-12 signaling.....	9
Lateral signaling targets .....	10
<i>lag-1</i> – CSL transcription factor .....	10
Drosophila Su(H) .....	12
Structure of CSL and the Notch ternary complex.....	13
Summary .....	14
Chapter 1. Figures.....	16
Chapter 2. Integration of EGFR and LIN-12/Notch signaling by LIN-1/Elk1, the Cdk8 kinase module, and SUR-2/Med23 in Vulval Precursor Cell fate patterning in <i>C. elegans</i> .....	21

Abstract.....	22
Introduction .....	22
Materials and Methods .....	25
Results.....	27
The CKM negatively regulates <i>lin-12</i> activity in uninduced VPCs.....	27
The CKM is not required for EGFR- and SUR-2-promoted transcription of the lateral signal gene <i>lag-2</i> in P6.p.....	29
Resistance to activated LIN-12 in P6.p depends on the relative balance of EGFR and LIN-12 activity and allows for robust expression of lateral signal gene reporters .....	30
The CKM and SUR-2/Med23 are required for resistance of P6.p to signal transduction by expression of constitutively active LIN-12/Notch.....	32
Loss of LIN-1 leads to ectopic LIN-12 signal transduction in all VPCs .....	33
LIN-1 coordinates crosstalk between the inductive and lateral signaling pathways .....	34
Discussion .....	35
The CKM and basal activity of LIN-12/Notch in VPCs .....	36
Different requirements for SUR-2, the CKM, and LIN-1 in P6.p for different functions relevant to LIN-12/Notch and VPC patterning .....	38
Integrating the EGFR-Ras-ERK inductive signaling and LIN-12/Notch lateral signaling pathways.....	39
Acknowledgments.....	41
Chapter 2. Figures.....	42
Chapter 2. Supplemental Material.....	54
Effect of <i>lin-1(gf)</i> on 2 <sup>o</sup> -fate marker expression.....	55

Examination of requirement for additional Mediator components in EGFR-mediated resistance to LIN-12 activity .....	58
Characterization of <i>lin-31</i> mutants on 2 <sup>o</sup> -fate marker expression .....	60
Chapter 3. Characterization of expression and patterning of LAG-1 .....	62
Abstract.....	63
Introduction .....	63
Materials and Methods .....	66
Results.....	69
An N-terminally tagged LAG-1-mCherry translational fosmid reporter rescued <i>lag-1(0)</i> lethality, but did not produce visible expression .....	69
C-terminally tagged LAG-1-GFP translational fosmid reporters were visible and not patterned during VPC specification .....	70
Endogenous CRISPR-engineered translational reporters of LAG-1 display a dynamic expression pattern in the VPCs .....	71
LAG-1-mKate2 levels and patterning in the VPCs are dependent on <i>lin-12</i> signaling.....	72
Strong constitutive LIN-12 activity elevates LAG-1-mKate levels in all VPCs.....	73
LAG-1-mKate2 levels are not affected by removal of <i>sel-10</i> or <i>cdk-8</i> .....	75
Weak forms of constitutively active LIN-12 influence LAG-1 accumulation .....	75
LAG-1-mKate2 is regulated in a <i>lin-12</i> dependent manner during the AC/VU decision .....	77
Discussion .....	79
Implications of LAG-1 fosmid reporter results .....	80
Use of endogenously-encoded reporters of LIN-12 activity .....	82
Regulating LIN-12 activity in the VPCs through control of LAG-1 levels or subcellular localization .....	83

Further investigation of LAG-1 regulation.....	84
Chapter 3. Figures .....	86
Chapter 4: Characterization of cis-regulatory sequences of the LIN-12 target gene <i>lst-5</i> and <i>in vivo</i> analysis of LAG-1 target binding in the VPCs: successes and complications.....	95
Abstract.....	96
Introduction .....	96
Materials and methods .....	98
Results and Discussion .....	100
The regulatory sequence of <i>lst-5</i> as a tool to study regulation of <i>lin-12</i> signaling .....	100
The first exon and first intron of <i>lst-5</i> are sufficient to drive expression in 2 <sup>o</sup> VPCs.....	101
Deletion analysis of <i>lst-5p</i> transcriptional reporters.....	102
Nuclear Spot Assay .....	103
Chapter 4. Figures .....	106
Chapter 5. Discussion .....	114
Summary .....	115
EGFR-mediated resistance to LIN-12 activity in P6.p.....	116
Interactions of EGFR and LIN-12/Notch signaling in other contexts.....	117
LIN-1 function in VPC specification .....	121
LIN-1 integrates EGFR and LIN-12/Notch signaling in the VPCs .....	122
Potential for autoregulation of <i>lag-1</i> .....	122
Potential for different LAG-1 isoforms to affect VPC .....	124
Issues resulting from use of multi-copy arrays .....	126
Chapter 5. Figures .....	128

References ..... 132



## List of Figures and Tables

Chapter 1. Figures .....	16
Figure 1. Overview of vulval development.....	17
Figure 2. EGFR-Ras-ERK activation in VPCs.....	18
Figure 3. Canonical LIN-12/Notch activation.....	19
Figure 4. LIN-12 domain organization and structure of transcriptional activation complex.....	20
Chapter 2. Figures .....	44
Figure 1. VPC fate specification.....	45
Figure 2. The CKM acts in a kinase dependent manner to negatively regulate <i>lin-12</i> activity...47	
Figure 3. Resistance to constitutively active LIN-12 signal transduction in P6.p.....	49
Figure 4. Activated LIN-12 expressed from single-copy transgenes overcomes resistance in P6.p and leads to repression of lateral signal gene expression.....	50
Figure 5. Loss of LIN-1 results in ectopic LIN-12 activity in all VPCS, and abrogates LIN-12-GFP endocytic downregulation in P6.p.....	52
Figure 6. Resolution of cell fate in different genotypes.....	54
Figure 7. Summary and models for the roles of LIN-1, SUR-2, and the CKM in P6.p.....	55
Chapter 2. Supplementary Material .....	56
Figure S1. 2 <sup>o</sup> -fate marker expression in putative <i>lin-1</i> gain-of-function background.....	59
Figure S2. 2 <sup>o</sup> -fate marker expression in Mediator component loss-of-function mutants.....	61
Figure S3. 2 <sup>o</sup> -fate marker expression in <i>lin-31</i> mutant backgrounds.....	63
Chapter 3. Figures .....	88
Figure 1. Schematics of VPC specification and formation of LIN-12 transcriptional activation complex.....	89

Figure 2. Diagram of <i>lag-1</i> genomic locus and mCherry-LAG-1 fosmid reporter.....	90
Figure 3. LAG-1-GFP from transgenic and endogenous sources.....	91
Figure 4. LAG-1-mKate2 accumulation in the VPCs from L2 stage to Pn.pxx stage.....	92
Figure 5. LAG-1-mKate2 accumulation in the VPCs is dependent on <i>lin-12</i> activity. ....	93
Figure 6. LAG-1-mKate2 accumulation is sensitive to the presence of weak LIN-12. ....	94
Figure 7. LAG-1-mKate2 accumulation increases in somatic gonadal cells that receive <i>lin-12</i> signaling during the AC/VU. ....	95
Chapter 4. Figures.....	108
Figure 1. The gene <i>Ist-5</i> is a direct target of LIN-12.....	109
Figure 2. 5' exon and first intron of <i>Ist-5</i> are sufficient to drive expression in P5.p and P7.p. .	110
Figure 3. Deletions analysis of <i>Ist-5</i> 5' exon and first intron.....	111
Figure 4. Deletion analysis of <i>Ist-5</i> 5' exon and first intron in the presence of LIN-12(intraΔP). .....	112
Figure 5. <i>Ist-5p</i> transcriptional reporter with SunTag. ....	113
Figure 6. Nuclear Spot Assay.....	114
Table 1. Summary of target arrays used in dot experiments and results.....	115
Chapter 5. Figures.....	130
Figure 1. Summary of <i>arls116[Ist-5p::2xnl5-yfp]</i> expression. ....	131
Figure 2. Summary of LAG-1-mKate2 accumulation.....	132

## Acknowledgements

I would like to thank my advisor, Dr. Iva Greenwald, for her supervision and guidance, both inside and outside the laboratory. She is a superb scientist with a penchant for asking insightful biological questions and an unwavering dedication towards scientific rigor. I am privileged to have learned from her over six years and incredibly grateful for her support throughout my graduate career.

I thank Dr. Oliver Hobert and Dr. Gary Struhl for serving on my qualifying exam and thesis committees and for the helpful feedback they provided over the years. Additionally, I thank Dr. Alicia Melendez and Dr. Andrew Tomlinson for reading my dissertation and for serving on my thesis committee.

Thank you to my bay-mates Claire de la Cova and Michelle Attner: I appreciate the time you two spent going over presentations, discussing experiments, and any of the hundreds of other things that you two did for me over the years, but most of all, thank you for the encouragement that you provided during my final year-long sprint to the finish, it made a world of difference. The old guard, Xantha Karp, Dan Shaye, and Maria Sallee, thank you for the help when I first stepped foot into the lab and your continued assistance since then. Yuting Deng, my class mate and commiserating buddy, Claudia Tenen, Jessica Chan, Hana Littleford, Justin Benavidez, Katherine Luo, Catherine O'Keeffe, and Justin Shaffer, thank you for your friendships and making the lab an enjoyable place to be; I expect big things from all of you! Gleniza Gomez, thank you for the technical support and for looking out for me. I am also grateful for the past support of Richie Ruiz, Cindy Zhou, and Orquidea Cardenas.

Thanks to my friends and family for their continued support. To my parents Jeanne and Scott, brother Eric, step-mother Susan, and the Nagle clan: I am very appreciative of the constant check-ins and encouragement I received from all of you. Paul, Seth, Naps, Kevin, Brendan, Lizelle, and Roshan, I couldn't have asked for better friends and drinking buddies. Finally, I thank my fiancée, Liz Nagle, for her patience, support, and around-the-clock encouragement even when, especially when, we were 3,000 miles apart.

# **Chapter 1. General Introduction**

## **Vulval development of *Caenorhabditis elegans***

The nematode species *Caenorhabditis elegans* has proved to be a valuable tool for studying the many biological processes necessary for multicellular life. *C. elegans* was chosen as a model organism to study development of the nervous system due to its practicality in a laboratory setting and its relative biological simplicity (Brenner 1974). This was a sound choice when it was made, but several defining features were only learned of during the subsequent years. One such feature of *C. elegans* is the virtually invariant cell lineages that give rise to the 959 somatic cells found in every adult hermaphrodite (Sulston and Horvitz 1977; Kimble and Hirsh 1979; Sulston *et al.* 1983).

The cellular response to any given developmental signal is generally highly context dependent. During *C. elegans* development, cells or groups of cells offer paradigms to study cellular signaling and how cellular contexts affect signaling. Investigating cells of different contexts that receive the same signal, but respond differently, is one tactic. Another is through the examination of groups of cells that are functionally equivalent but receive different signals. We can investigate how cells in the same context respond to different signals. One such cellular group comprises the precursor cells that give rise to the adult vulva.

The development of the *C. elegans* vulva has been extensively characterized and provides a powerful paradigm to study cell-cell communication and how cells integrate multiple signaling pathways to produce discrete outcomes. Vulva development is a multi-step process that occurs over several larval stages: beginning in the first larval (L1) stage, with the birth and establishment of the vulval precursor cells (VPCs); during the second larval (L2) stage, several intercellular signals maintain VPC competency; VPCs commit to vulval fates during the third larval (L3) stages; finally, during the third and fourth larval (L3 and L4) stages, descendants of specified VPCs differentiate into adult vulva cell-types and undergo morphogenesis to generate the adult vulva [reviewed in Sternberg (2005)]. The work described herein uses the paradigm of *C. elegans* vulva development, and specifically the patterning of the VPCs, to study how cells integrate two important signaling pathways.

### **Establishment and maintenance of the vulval competency group**

The VPCs are born during the L1 stage (Fig. 1). Twelve cells, numbered P1-12, migrate to the ventral side of the animal. P1-P11 undergo a round of division and the anterior (Pn.a) daughters become neuroblasts that produce ventral cord neurons, while the posterior (Pn.p) daughters become hypodermal cells; P12 does not follow this pattern and undergoes its own distinct lineage. Six of the Pn.p cells, P3.p-P8.p, become VPCs while the remaining Pn.p cells, P.p1, P2.p and P9.p-P11.p, fuse to the hypodermal syncytium, hyp7, before the L1 stage ends (Sulston and Horvitz 1977). The six VPCs form the “vulval competency group” and can respond to intercellular signals to adopt vulval fates (Sulston and Horvitz 1977; Sulston and White 1980; Kimble 1981). During normal development, descendants of P5.p, P6.p, and P7.p will generate the vulva, while descendants of P3.p, P4.p, and P8.p will fuse to the hypodermis (Sternberg and Horvitz 1986).

The Hox gene *lin-39*, the *C. elegans* ortholog of *Sex combs reduced* and *Deformed*, is required for establishment of the VPCs (Clark *et al.* 1993; Wang *et al.* 1993). *lin-39* mutants are Vul, and mosaic analysis indicated that *lin-39* functions cell autonomously in the P3.p-P8.p cells (Clark *et al.* 1993). Analysis of transcriptional reporters suggested that *lin-39* expression is limited to P3.p-P8.p (Salser *et al.* 1993). Many transcription factors appear to work in combination to regulate *lin-39* expression (Liu *et al.* 2014). LIN-39 was found to repress transcription of the fusogen gene *eff-1* in P3p-P8.p (Shemer and Podbilewicz 2002). EFF-1 promotes the cellular fusion of P1, P2, and P9-P11 to hyp7. P3.p-P8.p express *eff-1* in the absence of LIN-39, and fuse to hyp7 during the L1 stage similar to *lin-39* mutants (Mohler *et al.* 2002).

WNT and EGFR signaling are critical to prevent the VPCs from inappropriately fusing with the hypodermis during the L2 stage. The WNT ligand genes *cwn-1* and *egl-20* are expressed by the surrounding tissues and are required to prevent premature VPC fusion with the hypodermis (Gleason *et al.* 2006; Myers and Greenwald 2007). These ligands most likely activate expression of WNT target genes through *bar-1*, a  $\beta$ -catenin homolog, as VPCs in BAR-1/ $\beta$ -catenin mutants will similarly prematurely fuse to the hypodermis (Eisenmann *et al.* 1998). Loss

of EGF ligand produced by the somatic gonad (Myers and Greenwald 2007) or EGFR-Ras activity in the VPCs (Eisenmann *et al.* 1998; Maloof and Kenyon 1998) can cause a failure of VPC maintenance. Many of these signals help to regulate the expression of *lin-39*. During the L2 stage, continued *lin-39* expression is critical for maintenance of VPCs (Eisenmann *et al.* 1998; Maloof and Kenyon 1998), and the eventual induction of VPCs (Maloof and Kenyon 1998; Wagmaister *et al.* 2006; Roiz *et al.* 2016).

### **VPC specification**

The VPCs adopt one of three fates—primary (1°), secondary (2°), or tertiary (3°)—in an invariable 3°-3°-2°-1°-2°-3° pattern (Sulston and White 1980; Sternberg and Horvitz 1986)(Fig. 1). The three 1° and 2° VPCs will generate the vulva, while the 3° VPCs will fuse with the hypodermis. Two signaling events occur sequentially to specify VPC fates. First, an inductive signal is sent by the somatic gonad causing the nearest cell, P6.p, to adopt the 1° fate. The subsequent lateral signal causes the flanking VPCs, P5.p and P7.p, to adopt the 2° fate. The outer VPCs, P3.p, P4.p, and P8.p, do not receive either signal, and adopt the default 3° VPC fate. All VPCs undergo a single round of division, except for P3.p, which fuses with the hypodermis ~50% of the time prior to division.

Two classes of mutant phenotypes have been used extensively to characterize genes involved in the generation of the vulva. In Vulvaless (Vul) mutants, the VPCs are not induced, and fuse with the hypodermis, thus, no vulva is generated. In Multivulva (Muv) mutants, the additional VPCs are induced to adopt the 1° or 2° fate, and adult animals will have ventral protrusions along the ventral side of their body. These categories are not inclusive and other vulval phenotypes exist. Additionally, phenotypes of the same category are not necessarily equivalent and there are many subdivisions with important distinctions.

### **Inductive signal**

#### **Identification of the inductive signal**

The anchor cell (AC), located in the somatic gonad, was implicated in vulval development through laser ablation experiments. When the gonad primordium is ablated at the time of hatching, the

VPCs adopt the 3<sup>o</sup> fate, and animals are Vul (Sulston and White 1980). When all gonadal cells except for the AC were eliminated during the L2 stage, animals produced a normal vulva. In the reciprocal experiment, only the AC was eliminated, and these animals failed to generate a vulva and were Vul (Kimble 1981), indicating that signaling from the AC was necessary and sufficient to induce vulval fates. Ablation experiments indicated that if the AC was eliminated near the first round of VPC divisions, the VPCs may only be partially specified (Kimble 1981). Temperature-shift experiments suggested that the VPCs were specified during the L3 stage, just prior to the first-round of VPC division (Greenwald *et al.* 1983a). Additional laser ablation experiments were consistent with this finding (Greenwald *et al.* 1983a; Sternberg and Horvitz 1986).

In a *lin-3* mutant, the VPCs are not induced and animals are Vul, despite the presence of the AC (Horvitz and Sulston 1980; Sulston and Horvitz 1981; Ferguson and Horvitz 1985). The *lin-3* locus was cloned and molecular analysis indicated that *lin-3* encoded an epidermal growth factor (EGF)-like protein (Hill and Sternberg 1992). Observations of a LIN-3-LacZ translational fusion reporter suggested that *lin-3* was expressed in the AC (Hill and Sternberg 1992). Animals carrying a transgene containing the *lin-3* genetic locus had a Muv phenotype, proposed to be due to excessive vulval induction caused by the over-production of LIN-3. Ablation experiments revealed this Muv phenotype did not require the AC (Hill and Sternberg 1992), indicating that vulval induction caused by transgenic LIN-3 production bypassed the requirement for an AC. VPCs in *let-23* mutants are not induced and animals are Vul. Molecular analysis of *let-23* revealed that it encoded an EGF receptor (EGFR)-family receptor tyrosine kinase (RTK), suggesting that *let-23* was the receptor that transmitted the inductive AC signal to the VPCs (Aroian *et al.* 1990). When the *lin-3* transgene was combined with a *let-23* mutant, nearly all animals had a Vul phenotype, indicating that *lin-3* functioned upstream of *let-23* (Hill and Sternberg 1992). These experiments indicated that LIN-3/EGF was the inductive signal produced by the AC.



### **EGFR-Ras-ERK signaling in P6.p**

Upon EGF ligand binding, EGFR dimerizes and autophosphorylates at the C-terminal domain (Lemmon and Schlessinger 2010), and it had been assumed that the same would be true for LET-23 (Sundaram 2013). More recent data, however, suggests that LET-23 is constitutively dimeric unlike other EGFR-family RTKs (Freed *et al.* 2015). This study proposes that LIN-3 binding induces an allosteric conformational change in the LET-23 dimer that triggers autophosphorylation. Ultimately, the scaffold protein SEM-5 associates with the phosphorylated intracellular tyrosine residues of the LET-23 dimer (Clark *et al.* 1992), and recruits the guanine nucleotide exchange factor SOS-1 (Chang *et al.* 2000); SOS-1 binds and activates LET-60/Ras (Han and Sternberg 1990). Activated LET-60/RAS initiates a phosphorylation cascade of LIN-45/RAF (Han *et al.* 1993), MEK-2/MEK (Kornfeld *et al.* 1995), and MPK-1/ERK (Lackner *et al.* 1994)(Fig. 2). Activation of the EGFR-Ras-ERK pathway activates expression of later signal genes (Chen and Greenwald 2004; Zhang and Greenwald 2011).

### **Effectors and regulators of EGFR-RAS-ERK**

Many downstream effectors of MPK-1/ERK have been identified. MPK-1/ERK has two identified substrates: the forkhead-like transcription factor LIN-31 (Miller *et al.* 1993; Tan *et al.* 1998), and the ETS domain containing protein LIN-1 (Jacobs *et al.* 1998; Tan *et al.* 1998). In addition, the BTB-zinc finger transcription factor EOR-1 has been shown to be phosphorylated *in vitro* by murine ERK (Howell *et al.* 2010), and *in vivo* experiments suggest that LIN-45/RAF phosphorylated in a MPK-1/ERK-dependent manner (de la Cova and Greenwald 2012). The Mediator complex subunits SUR-2 (Singh and Han 1995) and LIN-25 (Tuck and Greenwald 1995; Nilsson *et al.* 1998), homologs of Med23 and Med24 respectively, function together downstream of LET-60/Ras, and potentially downstream of MPK-1 (Lackner and Kim 1998), to promote vulval induction. The uncharacterized protein EOR-2 binds with EOR-1; this complex functions to promote MPK-1/ERK 1<sup>o</sup>-fate induction redundantly with SUR-2/LIN-25 (Howard and Sundaram 2002; Howell *et al.* 2010).

Activation of EGFR-RAS-ERK in P6.p promotes expression of lateral signal genes, including *lag-2* (Chen and Greenwald 2004). In its unphosphorylated state, LIN-1 directly represses transcription of lateral signal genes in all VPCs (Zhang and Greenwald 2011). Upon ERK activation, LIN-1-mediated repression is relieved, and *lag-2* is transcriptionally activated. Expression of lateral signal genes requires the presence of SUR-2 (Chen and Greenwald 2004). The requirement for SUR-2 for transcriptional activation of *lag-2* is independent of LIN-1 (Zhang and Greenwald 2011). Regulation of *lag-2* expression is discussed further in Chapter 2.

### ***lin-1* – Ets-domain-containing transcription factor**

*lin-1* is critical for the appropriate cell fate pattern of the VPCs. LIN-1 is an ETS-domain containing protein of the Elk1 subfamily (Beitel *et al.* 1995), and biochemical analyses have determined that LIN-1 is directly phosphorylated by ERK (Tan *et al.* 1998; Jacobs *et al.* 1999). The loss of *lin-1* activity leads to gonad-independent ectopic vulval induction and a strong Muv phenotype (Ferguson and Horvitz 1985; Ferguson *et al.* 1987). Genetic epistasis experiments placed *lin-1* downstream of *let-60/Ras* and *mpk-1/MAPK*, and indicated that *lin-1* acted to antagonize *let-60/Ras* signaling (Lackner *et al.* 1994; Wu and Han 1994).

Lineage analysis of VPCs in *lin-1(0)* animals suggested that P6.p preferentially adopts the 1° fate in the presence of the AC. In the absence of the AC, P6.p appeared to adopt non-1°-fate lineages at a higher frequency (Beitel *et al.* 1995). Another study showed that a LIN-45-YFP fusion protein was degraded in P6.p through an ERK-dependent mechanism; loss of *lin-1* activity did not affect the downregulation of LIN-45-YFP (de la Cova and Greenwald 2012). Overall, these observations indicate that *lin-1* activity negatively regulates a branch of the EGFR-Ras-ERK pathway.

The role of *lin-1* in VPC development has been challenging to decipher. Lineage analysis in the *lin-1(0)* background described many VPCs as being “hybrid” fates, showing some 1°- and 2°-fate character. Analysis of *lin-12(d); lin-1(0)* suggests that VPCs were more 2°-like compared to *lin-1(0)* single mutant, while analysis of *lin-12(0); lin-1(0)* suggests that VPCs were more 1°-like, when compared to the *lin-1(0)* single mutant (Beitel *et al.* 1995), suggesting that *lin-1* may be

important in integrating the EGFR pathway with LIN-12 signaling. The role LIN-1 plays in integrating EGFR and LIN-12 is discussed further in Chapter 2.

Positive roles for *lin-1* have been described in VPC specification. A transcriptional reporter of the fibroblast growth factor gene, *egl-17*, is a reporter of 1<sup>o</sup>-fate adoption in the VPCs (Burdine et al. 1998). An analysis of this reporter, indicates *lin-1* activity is required for expression of *egl-17p::gfp* in P6.p (Tiensuu et al. 2005). Deletion analysis of the *egl-17* 5' cis-regulatory region, however, suggested that LIN-1 did not directly regulate *egl-17p::gfp* (Cui and Han 2003). As described above, the transcriptional reporters of the RHO kinase gene *let-502* appear to require direct binding by LIN-1 to drive expression in 2<sup>o</sup> VPCs (Farooqui et al. 2012). The dual role of LIN-1/Elk1, as both a transcriptional activator and repressor, may explain some of these observations.

In mammalian cells, Elk1 is a substrate for ERK (Gille et al. 1992; Marais et al. 1993). In its unphosphorylated state, Elk1 functions as a transcriptional repressor (Marais et al. 1993; Gille et al. 1995; Yang et al. 2001), and sumoylation of Elk1 can contribute to its role as a repressor (Yang et al. 2003). ERK-dependent phosphorylation switches Elk1 to function as a transcriptional activator and may recruit the Mediator complex through association with Med23 to activate target gene expression (Stevens et al. 2002; Wang et al. 2005). Sumoylated LIN-1 has been shown to function as a repressor as well (Leight et al. 2005; Leight et al. 2015). These studies proposed a model in which sumoylated unphosphorylated LIN-1 inhibits vulval cell fates, and phosphorylated LIN-1 recruits SUR-2 to promote P6.p to adopt the 1<sup>o</sup> fate. Observations suggest that this model is incomplete. Expression of *lag-2* transcriptional reporters do require SUR-2, but not LIN-1 (Zhang and Greenwald 2011). Furthermore, this model does not describe the role of *lin-1* in the 2<sup>o</sup> VPCs. The role of *lin-1* in VPC development is discussed further in Chapters 2 and 5.

## **Lateral signal**

### **Identification of the lateral signal**

Laser ablation experiments provided evidence for the presence of a lateral signal sent by the 1<sup>o</sup> VPC. In a *lin-15* loss-of-function background, now known to result in production of LIN-3/EGF

from the major hypodermal syncytium (Myers and Greenwald 2005; Cui *et al.* 2006; Myers and Greenwald 2007), all VPCs adopt either the 1<sup>o</sup> or 2<sup>o</sup> fate in an alternating 1<sup>o</sup>-2<sup>o</sup> pattern, and adjacent 1<sup>o</sup> VPCs were not typically seen (Sternberg 1988). This spatial pattern is similar to the lateral inhibition seen in *Drosophila* proneural clusters (discussed in more detail later). Additionally, if there is one VPC, this VPC will adopt the 1<sup>o</sup> fate; if there are two adjacent VPCs, they will adopt a 1<sup>o</sup>-2<sup>o</sup> or 2<sup>o</sup>-1<sup>o</sup> pattern with equivalent frequencies. Combined, these observations indicated that the 1<sup>o</sup> VPC signaled adjacent VPCs (Sternberg 1988).

Genetic analysis suggested that *lin-12* was the receptor for this signal. In *lin-12* null animals VPCs adopt either the 1<sup>o</sup> or 3<sup>o</sup> fate, but never the 2<sup>o</sup> fate. Semi-dominant hypermorphic *lin-12(d)* alleles cause all VPCs to adopt the 2<sup>o</sup> fate. Furthermore, *lin-12(d)* animals do not possess an anchor cell due to a cell-fate transformation in the gonad, indicating that *lin-12* activity is necessary and sufficient for 2<sup>o</sup> fate (Greenwald *et al.* 1983a). In *lin-12(null); lin-15* double mutants, all VPCs adopt the 1<sup>o</sup> fate (Sternberg and Horvitz 1989), suggesting that *lin-12* was required for later inhibition.

### **LIN-12 signaling**

*lin-12* encodes one of two Notch homologs in *C. elegans*, *glp-1* being the other (Yochem *et al.* 1988; Yochem and Greenwald 1989); the LIN-12 and GLP-1 proteins are functionally interchangeable (Fitzgerald *et al.* 1993). The receptor form of LIN-12/Notch is activated by binding to a DSL ligand which induces two proteolytic events (Fig.3). The first cleavage event is regulated and catalyzed by a disintegrin and metalloprotease (ADAM) at the S2 cleavage site (Tax *et al.* 1997; Wen *et al.* 1997). ADAM activity cleaves the Notch extracellular domain and leaves a small extracellular truncation. The second event is constitutive and cleavage at the S3 site is catalyzed by Presenilin of the  $\gamma$ -secretase complex (Levitan and Greenwald 1998b; Struhl and Greenwald 1999). The intracellular domain of LIN-12/Notch is released from the plasma membrane and translocated to the nucleus (Struhl and Adachi 1998). Within the nucleus, the intracellular domain of LIN-12/Notch will form a transcriptional activation complex with a CSL family (Fortini and Artavanis-Tsakonas 1994; Christensen *et al.* 1996) transcription factor and

member of the Mastermind family (Doyle *et al.* 2000; Petcherski and Kimble 2000; Wu *et al.* 2000).

### **Lateral signaling targets**

Activation of *lin-12* in P5.p and P7.p promotes specification of the 2° fate and promotes target gene expression. A number of these genes are transcriptional targets of LIN-12 and appear to negatively regulate EGFR-RAS-MAPK activity, including *lst-1*, *lst-2*, *lst-3*, *lst-4*, and *dpy-23* (Yoo *et al.* 2004). The gene *lip-1* encodes a phosphatase that negatively regulates MAPK (Berset *et al.* 2001), and *ark-1* encodes a tyrosine kinase that interacts with SEM-5 to negatively regulate LET-23/EGFR (Hopper *et al.* 2000; Yoo *et al.* 2004).

The RHO kinase gene *let-502* is expressed in 2° VPCs in response to LIN-12 activation, and is important for vulva morphogenesis (Farooqui *et al.* 2012). Analysis of *let-502* transcriptional reporters, however, suggest that it may transcriptionally activated by LIN-1 (Farooqui *et al.* 2012).

### ***lag-1* – CSL transcription factor**

LAG-1 is a member of the conserved class of transcription factors known as “CSL,” and is a core component of canonical Notch signaling; the CSL name is an initialism derived from three orthologs: mammalian CBF1; *Drosophila* Su(H); and *C. elegans* LAG-1. In general, CSL proteins are DNA-binding proteins that recruit co-activator or co-repressor proteins to Notch target genes. In this way, CSL can function as activators or repressors. The Notch intracellular domain (NICD) replaces these co-repressors, and the CSL-NICD functions as a transcriptional activator.

[reviewed by Bray (2016) ]

Animals containing loss-of-function mutations in both Notch genes, *lin-12* and *glp-1*, invariably arrest during the L1 stage with the distinctive Lag (*lin-12* and *glp-1*) phenotype (Lambie and Kimble 1991). The Lag phenotype of the *lin-12 glp-1* double was described as having three major anatomical defects: the lack of an excretory cell; the failure to develop a rectum; and a “twisted” nose. This phenotype was the basis for a genetic screen to identify core components of Notch signaling in *C. elegans*. Several *lag-1* loss-of-function alleles were generated during this

screen, and ranked in an allelic series based on the strength and penetrance of the Lag phenotype (Lambie and Kimble 1991). Notably, this screen also led to the identification of the first *C. elegans* DSL ligand gene *lag-2* (Lambie and Kimble 1991; Tax *et al.* 1994). Subsequent molecular analysis determined that the protein encoded by *lag-1* was homologous to *Drosophila* Suppressor of Hairless (Su(H)), and mammalian CBF1; biochemical assays suggested that LAG-1 bound DNA through a similar recognition motif (Christensen *et al.* 1996).

Few studies have explicitly investigated *lag-1* in *C. elegans*. Genetic experiments show that *lag-1* is required for several specification events during embryogenesis (Hermann *et al.* 2000; Neves and Priess 2005). A positive requirement for LAG-1 for transcription of the *ref-1* family of bHLH genes in early embryonic development has been described (Neves and Priess 2005). Subsequent *lag-1* RNAi knock-down experiments indicate that LAG-1 is required for transcriptional activation of *ref-1* family genes in combination with the GATA transcription factor, ELT-2, and LIN-12 activation (Neves *et al.* 2007). Mosaic analysis of *lag-1* RNAi treated animals suggests that *lag-1* is required for *lin-12* activity in the ventral M lineage for sex myoblast differentiation (Foehr and Liu 2008).

Other roles for *lag-1* were suggested by the phenotype caused by weaker *lag-1* alleles. These animals have lower penetrance of larval lethality and many survive to adulthood. Adult animals containing these weak *lag-1* alleles were reported to have reduced germline proliferation consistent with reduced *glp-1* activity (Lambie and Kimble 1991; Berry *et al.* 1997). These animals were not reported to have defects in vulval development (Lambie and Kimble 1991). Additional hypomorphic *lag-1* alleles that enhance a weak loss-of-function *glp-1* germline proliferation defect (Qiao *et al.* 1995) and suppress a weak *lin-12(d)* Vul phenotype (Katic *et al.* 2005) were identified in subsequent screens.

There is evidence to suggest a repressive role for LAG-1 during embryonic development of gland cells (Ghai and Gaudet 2008). LAG-1 was shown to directly repress reporter expression from a minimal *hlh-6* 5' cis-regulatory sequence (Ghai and Gaudet 2008). No co-repressor was

identified from this study, and thus far, no co-repressor that functions with LAG-1 has been identified in *C. elegans*.

### **Drosophila Su(H)**

Many co-repressors that interact with CSL have been identified. The Hairless-Su(H) repressor complex recruits the global repressors CtBP and Groucho. (Morel *et al.* 2001; Barolo *et al.* 2002; Nagel *et al.* 2005) In mammals, the CSL protein CBF1, has been found to interact with SHARP/MINT (Oswald *et al.* 2002; Kuroda *et al.* 2003), KyoT2 (Taniguchi *et al.* 1998), and CIR (Hsieh *et al.* 1999) to repress target gene transcription. Transcriptional repression is generally accomplished through the recruitment of chromatin modifiers such as histone deacetylases (Hsieh *et al.* 1999; Borggreffe and Oswald 2009; Mulligan *et al.* 2011). Although no co-repressor in *C. elegans* have been identified, there are several candidates based on homology, including: DIN-1 and GRLD-1 are homologs of MINT; GEI-1 is a homolog of SMRT; and CIR-1 is a homolog of Cir1.

The mechanosensory bristles of the adult peripheral nervous system are evenly spaced in a remarkably ordered pattern. The bristles arise from sense organ precursor cells (SOPs) that are specified in small populations of neural precursor cells called proneural clusters (PNCs). All cells of the PNC initially express the pro-SOP genes *achaete (ac)* and *scute (sc)* (Romani *et al.* 1989). The cell that accumulates the highest amount of Ac and Sc protein will become the SOP through lateral inhibition (Cubas *et al.* 1991). Ac and Sc activate expression of the “inhibitory” signal, the Notch ligand *delta* (Haenlin *et al.* 1994; Kunisch *et al.* 1994). Notch activation drives expression of inhibitory-SOP genes in cells of the PNC (Bailey and Posakony 1995; Lecourtois and Schweisguth 1995)

Su(H) regulates expression of both pro-SOP and inhibitory-SOP genes during lateral inhibition. Activation of Notch in non-SOP cells requires Su(H) to drive expression of SOP-inhibitory E(spl)-C genes (Bailey and Posakony 1995; Lecourtois and Schweisguth 1995). In the absence of activated Notch, Su(H) forms a repressor complex with Hairless (H) to inhibit

expression of the same SOP-inhibitory E(spl)-C genes (Castro *et al.* 2005). The SOP gives rise to four terminally differentiated cells that comprise the adult bristle [reviewed by (Schweisguth 2015)]. In a Notch-mediated binary cell-fate decision, two sister cells in the lineage differentiate to become the shaft cell and socket cell. Notch activation specifies the socket fate and produces high levels of Su(H) in this cell (Schweisguth and Posakony 1992; Gho *et al.* 1996). Analysis of cis-regulatory regions of a *su(H)* LacZ reporter gene identified Su(H) autoregulatory sites (Barolo *et al.* 2000). Su(H) autoinhibition is important for repression of Notch target genes and specification of the shaft cell. Positive autoregulation of Su(H) established by Notch activity is important for bristle function (Barolo *et al.* 2000; Liu and Posakony 2014).

### **Structure of CSL and the Notch ternary complex**

All Notch proteins are single-pass transmembrane proteins that are composed similar structural domains [reviewed by (Kovall and Blacklow 2010)]. The extracellular domain contains EGF-like repeats, the number of which vary by species and subtype, at the amino terminus. The EGF repeats are followed by three LIN-12/Notch repeat (LNR) modules and a heterodimerization (HD) domain. Together the LNR and the HD domains form the negative regulatory region (NRR), which functions to prevent premature activation in the absence of ligand. The intracellular domain contains an RBP-Jk associated molecule (RAM) domain, followed by seven ankyrin (ANK) repeats, a transactivation domain, and a PEST domain that promotes protein turnover (Fig. 4A).

CSL is composed of three general regions, a core region that is flanked by N- and C-terminal regions. The two flanking regions have little conservation between species and are not included in the crystal structures obtained so far. The core regions of all CSL proteins are well-conserved. Structural studies of mammalian CBF1 (Nam *et al.* 2006; Choi *et al.* 2012) and *elegans* LAG-1 (Kovall and Hendrickson 2004; Wilson and Kovall 2006; Friedmann *et al.* 2008) show a highly similar domain architecture and overall fold. The structure of the core region consists of three domains the N-terminal domain (NTD),  $\beta$ -trefoil domain (BTD), and C-terminal domain (CTD) separated by flexible linker strands. Specific NTD-BTD and NTD-CTD interactions contribute to a stable tertiary fold and these interactions are integral to the overall structure. CSL



proteins bind DNA monomerically through a large electropositive surface formed by segments of the NTD, BTD and their interdomain linker strand (Kovall and Hendrickson 2004). The protein-DNA interface contains several residues that contact DNA bases and specify the recognition sequence.

The core recognition sequence of CSL, GTGGGAA, was established biochemically in mammalian tissue (Tun *et al.* 1994), and subsequently confirmed in *Drosophila* (Brou *et al.* 1994) and *C. elegans* (Christensen *et al.* 1996). Studies indicate that CSL only has a moderate affinity for DNA, and that the specificity for this core recognition sequence is not particularly strong (Friedmann and Kovall 2010). This may represent a biochemical explanation for the requirement of low-affinity CSL sites for some cell differentiation (Swanson *et al.* 2011; Ramos and Barolo 2013; Liu and Posakony 2014), and may be an explanation for some of the difficulties encountered in computationally predicting LAG-1 targets discussed in (Choi 2009) and Chapter 4.

THE NICD and MAM bind with CSL to form the transcriptional activation complex (Fig. 4B). The RAM domain of NICD interacts with a conserved hydrophobic motif of CSL. This interaction stabilizes the relatively weak interaction between the ANK repeats and the CTD (Wilson and Kovall 2006). MAM binds the NICD-CSL through a roughly 60 amino acid “kinked”  $\alpha$ -helical structure that binds to the Notch ANK domain and the CSL CTD (Nam *et al.* 2006). This binding does not induce a conformational change in Notch or CSL (Nam *et al.* 2006; Wilson and Kovall 2006), and does not increase the DNA binding affinity of CSL (Friedmann *et al.* 2008). There is evidence suggesting that association by MAM may stabilize the ANK-CTD interface (Choi *et al.* 2012). The majority of MAM, however, has not been analyzed structurally.

## Summary

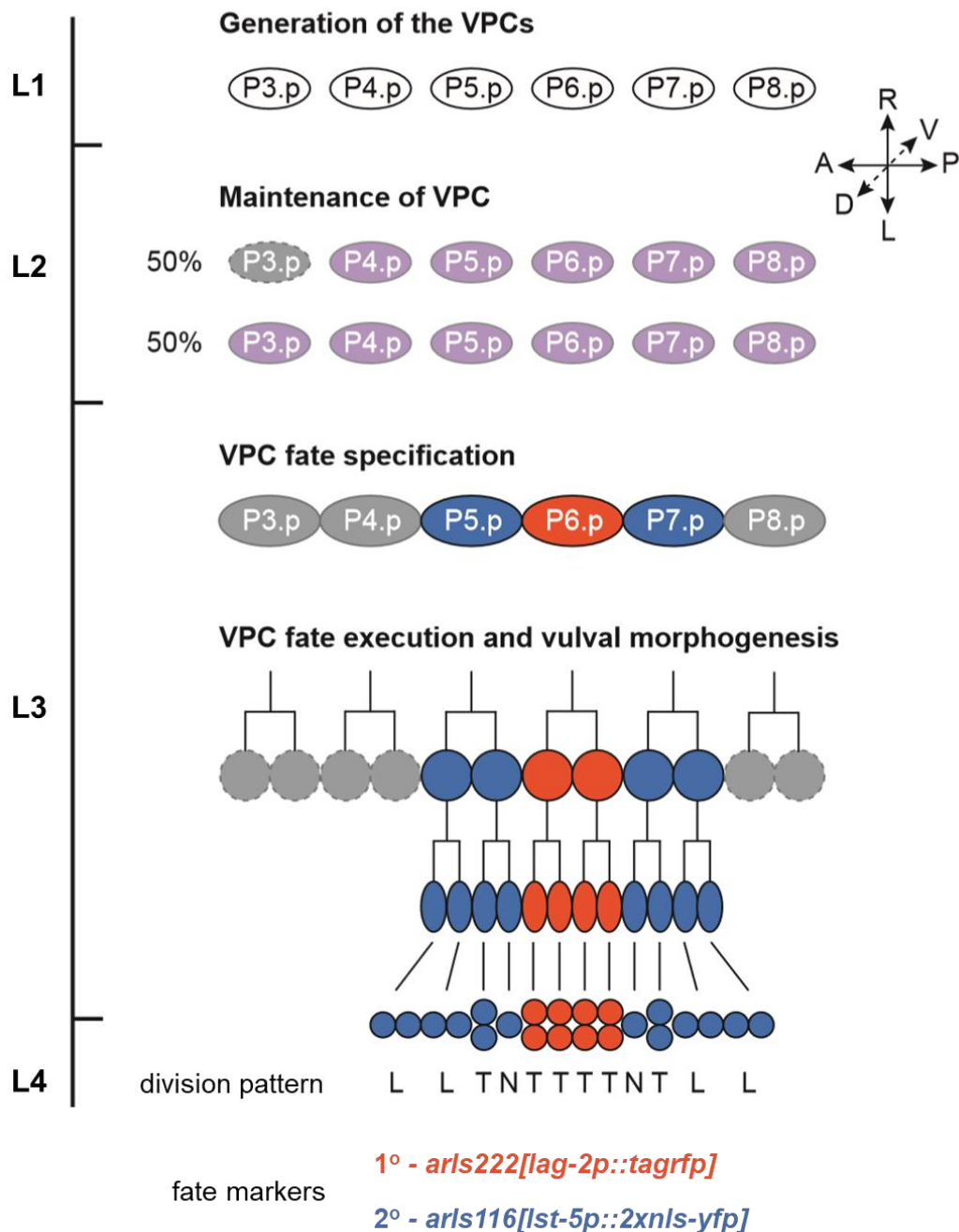
Here, I describe my investigations of regulatory mechanisms that contribute to the precise spatial patterning of VPC fate. In Chapter 2 I look at three factors—*lin-1*, *sur-2*, and the CDK-8 kinase module (CKM)—and find they interact in different combinations to regulate different aspects of 2<sup>o</sup> fate. In the presence of EGFR signaling, *lin-1* and *sur-2*, work in combination to promote endocytic downregulation of LIN-12-GFP in P6.p, while all three factors work in combination to

establish a mechanism to resist activated LIN-12 in P6.p. I find that the VPCs respond to the relative activity of LIN-12 and EGFR, and that *lin-1* is critical for proper integration of these two signals.

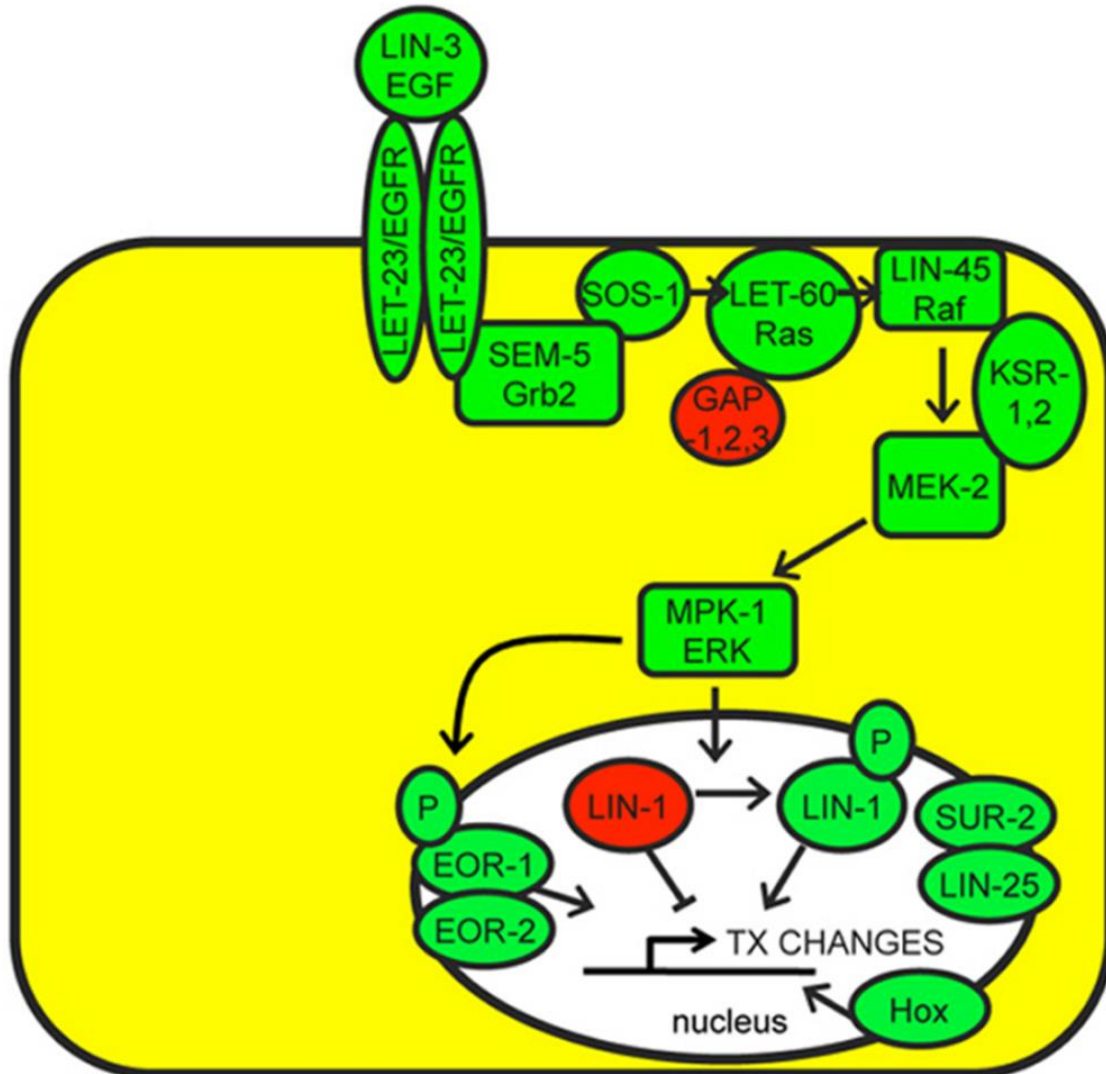
In Chapter 3, I discuss my work with tagged forms of the conserved CSL protein, LAG-1. I describe my observations using fosmid-based translational reporters. Ultimately, these reporters were contradicted by CRISPR-engineered, endogenously- tagged LAG-1 fusion proteins. These C-terminal LAG-1 fusions showed a dynamic pattern of LAG-1 protein accumulation in the VPCs. I observed that LAG-1 protein is present at a basal level uniformly in all VPCs, and LAG-1 accumulation increases in P5.p and P7.p compared to the other VPCs. Additional, experiments suggest that in the VPCs, LAG-1 accumulation increases in response to LIN-12 activity.

In Chapter 4, I discuss experiments designed to uncover trans-acting factors that contribute to EGFR-mediated resistance of LIN-12 activity in P6.p. I performed deletion analysis of the 5' regulatory region of *lst-5*, a direct LIN-12 transcription target. I also attempted to directly visualize the formation and activity of the LIN-12-LAG-1 transcriptional activation complex *in vivo*. Both experimental approaches had some successes but were ultimately limited by technical complications. I produced useful reagents during these experiments that were used in Chapters 2 and 3.

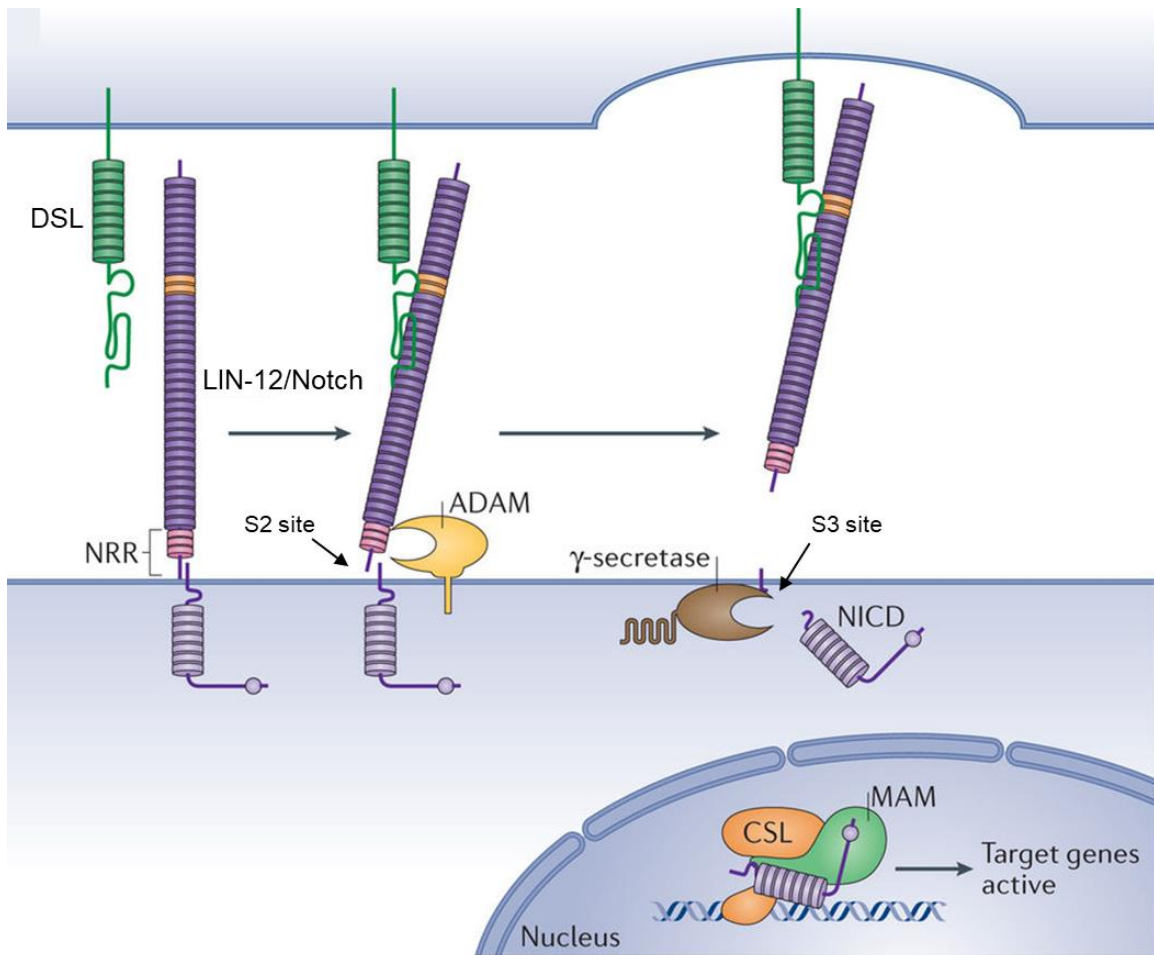
# Chapter 1. Figures



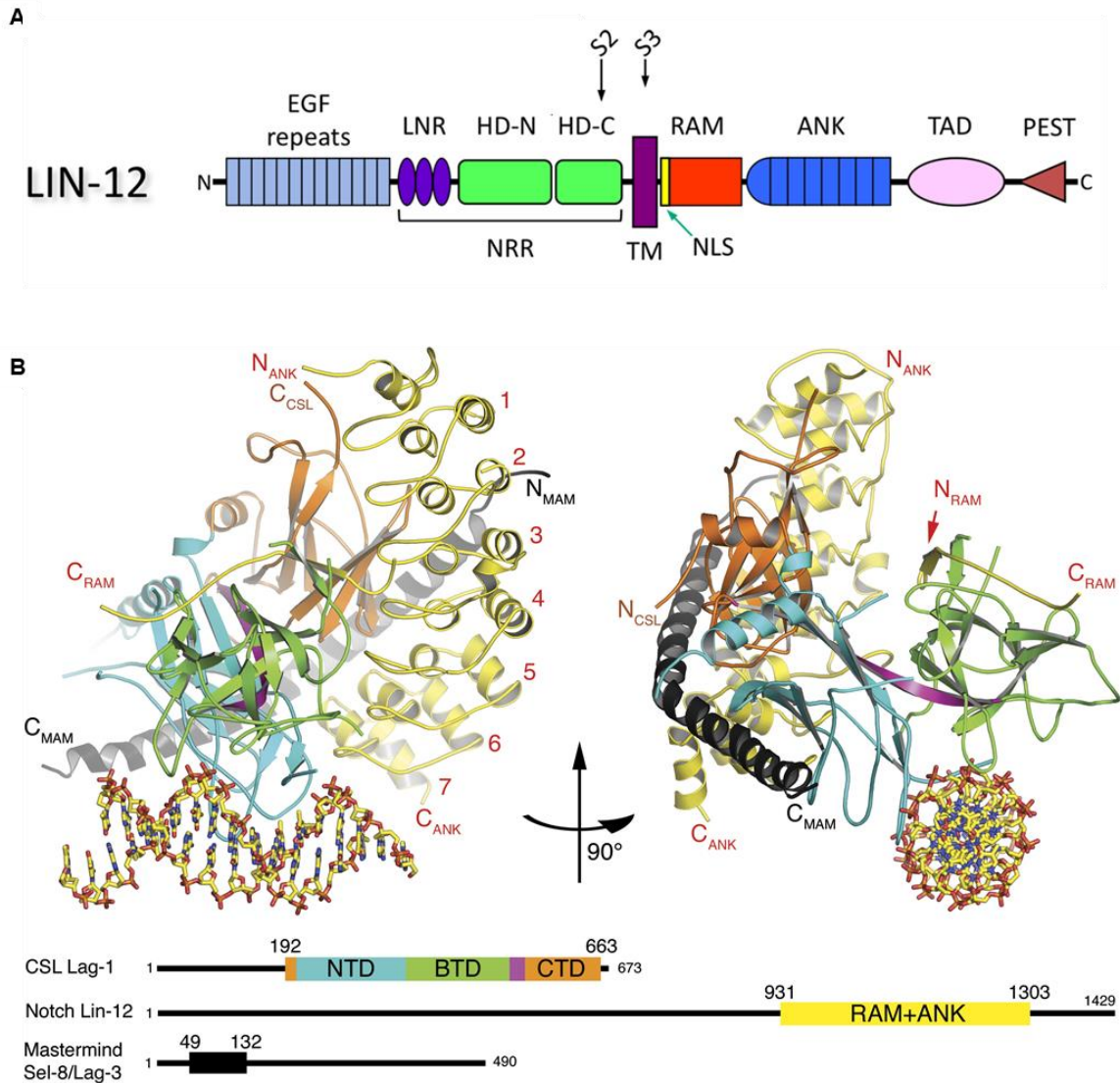
**Figure 1.** Overview of vulval development. During the L1 stage, the six VPCs, numbered P3.p-P8.p, are born. During the L2 stage, intercellular signals prevent the VPCs from prematurely fusing with the hypodermis; P3.p will fuse to the hypodermis during the L2 stage in ~50% of animals. During the L3 stage, the VPCs adopt vulval fates in an invariable 3°-3°-2°-1°-2°-3° pattern. 1° red; 2° blue; 3° grey. VPCs undergo one round of division and execute their programmed cell fate. The descendants of 1° and 2° VPCs will generate the vulva, and the daughters of the 3° VPCs will fuse to the hypodermis. Previously, the stereotypical lineage pattern was used to assign vulval fates: L longitudinal division (along anteroposterior axis); T transverse division (along left-right axis); N no division. Now, reporter gene expression is used (see Chapter 2). Larval stages are not to scale. Figure adapted from (Li 2011).



**Figure 2.** EGFR-Ras-ERK activation in VPCs. The anchor cell produces the inductive signal, an EGF-like ligand LIN-3 (not shown). Activation of LET-23/EGFR in P6.p, the nearest VPC, leads to activation of a canonical Ras-Raf-ERK pathway. Phosphorylated LIN-1 promotes 1<sup>o</sup>-fate. Based on mammalian Elk1, ERK-mediated phosphorylation of LIN-1 may switch it from a transcriptional repressor to activator, although direct targets of phosphorylated LIN-1 are not known. Evidence in *C. elegans* also indicates that it can relieve repression of lateral signal genes like *lag-2* (Zhang and Greenwald, 2011). Figure from (Sundaram 2013). In Chapter 2, I propose additional specific models to account for genetic interactions in different aspects of 1<sup>o</sup> fate.



**Figure 3.** Canonical LIN-12/Notch activation. The membrane-bound receptor form of LIN-12/Notch binds with a DSL-family ligand triggering two cleavage events. The cartoons represent mammalian Notch, where a cleavage at the S1 site leads to a heterodimeric Notch as shown. The ligand-dependent cleavage at the S2 site is mediated by a metalloprotease of the ADAM family. The cleavage at the S3 site is mediated by the  $\gamma$ -secretase complex. The untethered LIN-12/Notch intracellular domain (NICD) is translocated to the nucleus where it will form a transcriptional activation complex with LAG-1, a CSL protein, and SEL-8, a mastermind (MAM)-like protein. Figure adapted from (Bray 2016).



**Figure 4.** LIN-12 domain organization and structure of transcriptional activation complex. (A) Diagram showing modular organization of the full-length LIN-12 protein. The N-terminal extracellular region is composed of EGF repeats, LIN-12/Notch repeats (LNR), and the heterodimerization domains (HD). The negative regulator region (NRR) encompasses the LNR and HD domains. The C-terminal intracellular domain contains the RBPJ-associated module (RAM), Ankyrin (ANK) repeats, the transactivation domain (TAD), and a PEST domain. Figure 4A is adapted from (Greenwald and Kovall 2013). (B) Top panel shows ribbon diagram of the LIN-12-LAG-1-SEL-8 ternary complex bound to DNA. The NTD (blue) of LAG-1/CSL binds to DNA at the recognition sequence. The LAG-1/CSL BTM (green) and CTD (orange) bind to the RAM (yellow) and ANK (yellow) domains of LIN-12/Notch respectively. The seven ANK repeats are numbered sequentially starting from the N-terminus. A kinked helical domain of SEL-8/MAM (black) binds to the NTD and the CTD-ANK interface. Bottom panel shows color-coded diagram of the domains represented in this structure. Figure 4B is adapted from (Wilson and Kovall 2006).

## **Chapter 2. Integration of EGFR and LIN-12/Notch signaling by LIN-1/Elk1, the Cdk8 kinase module, and SUR-2/Med23 in Vulval Precursor Cell fate patterning in *C. elegans***

The following chapter contains a paper published in *Genetics* (Underwood *et al.* 2017).

I am responsible for all of the experiments and data presented in this chapter, with the exception of the analysis of *cdk-8(0); arls222[lag-2p::tagrfp]*, described in Figure 1C, and all experiments described in Figure 2. These experiments were performed by the co-author, Yuting Deng.



## Abstract

Six initially equivalent, multipotential Vulval Precursor Cells (VPCs) in *C. elegans* adopt distinct cell fates in a precise spatial pattern, with each fate associated with transcription of different target genes. The pattern is centered on a cell that adopts the “1<sup>o</sup>” fate through Epidermal Growth Factor Receptor (EGFR) activity, and produces a lateral signal composed of ligands that activate LIN-12/Notch in the two flanking VPCs to cause them to adopt “2<sup>o</sup>” fate. Here, we investigate orthologs of a transcription complex that acts in mammalian EGFR signaling—*lin-1/Elk1*, *sur-2/Med23*, and the Cdk8 Kinase module (CKM)—previously implicated in aspects of 1<sup>o</sup> fate in *C. elegans* and show they act in different combinations for different processes for 2<sup>o</sup> fate. When EGFR is inactive, the CKM, but not SUR-2, helps to set a threshold for LIN-12/Notch activity in all VPCs. When EGFR is active, all three factors act to resist LIN-12/Notch, as revealed by the reduced ability of ectopically-activated LIN-12/Notch to activate target gene reporters. We show that overcoming this resistance in the 1<sup>o</sup> VPC leads to repression of lateral signal gene reporters, suggesting that resistance to LIN-12/Notch helps ensure that P6.p becomes the robust source of lateral signal. In addition, we show that *sur-2/Med23* and *lin-1/Elk1*, and not the CKM, are required to promote endocytic downregulation of LIN-12-GFP in the 1<sup>o</sup> VPC. Finally, our analysis using cell fate reporters reveals that both EGFR and LIN-12/Notch signal transduction pathways are active in all VPCs in *lin-1/Elk1* mutants, and that *lin-1/Elk1* is important for integrating EGFR and *lin-12/Notch* signaling inputs in the VPCs so that the proper gene complement is transcribed.

## Introduction

The development of the *C. elegans* vulva is a valuable paradigm for studying signal transduction and how cells integrate multiple signaling inputs to regulate the expression of specific gene complements. Six Vulval Precursor Cells (VPCs), numbered P3.p-P8.p, each have the potential to adopt one of three fates, termed 1<sup>o</sup>, 2<sup>o</sup>, or 3<sup>o</sup> (Figure 1A). These fates are specified in the L3 larval stage and can be distinguished by division pattern, marker expression, and the terminal cell

types produced after the lineage is completed (Figure 1B). Patterning is initiated by an "inductive signal," the Epidermal Growth Factor (EGF)-like LIN-3 ligand produced by the anchor cell of the gonad. LIN-3/EGF activates EGF receptor (EGFR) and a canonical Ras-Raf-ERK cascade in P6.p, the VPC nearest the anchor cell, which causes P6.p to adopt the 1° fate. The EGFR-Ras-ERK cascade also promotes transcription of genes encoding Delta/Serrate/LAG-2 (DSL) family ligands for LIN-12/Notch in P6.p. These ligands constitute a "lateral signal" that activates LIN-12/Notch in the flanking VPCs, P5.p and P7.p, and causes these cells to adopt the 2° fate. EGFR-Ras may also support LIN-12/Notch activity in P5.p and P7.p via an alternate effector pathway, RalGEF-Ral (Zand *et al.* 2011). The remaining VPCs do not receive either the EGF or DSL signals and adopt the 3° fate. In addition to positive regulatory modes, like ligand production, the precise patterning of VPCs depends on negative regulatory modes as well. These include mechanisms that set high thresholds for response in all VPCs, as well as mutually inhibitory mechanisms for crosstalk between EGFR and LIN-12/Notch in the presumptive 1° and 2° VPCs [reviewed in Sundaram (2006)].

Activating the EGFR signal transduction pathway modulates the activity of transcription factors that change target gene expression. The transcription factor LIN-1 is a member of the Elk1 subfamily of ETS transcription factors (Hart *et al.* 2000; Shaye and Greenwald 2011), and is a key target of EGFR-Ras-ERK activation in VPCs (Beitel *et al.* 1995). LIN-1 (Jacobs *et al.* 1998) and Elk1 (Gille *et al.* 1992; Marais *et al.* 1993) are phosphorylated by ERK. For both LIN-1 (Leight *et al.* 2005; Leight *et al.* 2015) and Elk1 (Marais *et al.* 1993; Gille *et al.* 1995; Yang *et al.* 2003) the unphosphorylated, sumoylated transcription factor acts as a repressor, and the phosphorylated form acts as an activator. In mammalian cells, ERK-phosphorylated Elk1 associates with the Med23 component of the large multiprotein complex called Mediator, which links DNA-bound transcription factors to the basal transcription machinery (Allen and Taatjes 2015), to promote transcription of its targets. It has been proposed that the *C. elegans* ortholog, SUR-2/Med23 (Singh and Han 1995), as well as another Mediator component with which SUR-2 interacts, LIN-25/Med24 (Tuck and Greenwald 1995; Nilsson *et al.* 1998), work together with LIN-1/Elk1 to promote 1° fate in P6.p (Leight *et al.* 2015). Indeed, there are clear roles for these

genes in positively regulating 1<sup>o</sup> fate (Howard and Sundaram 2002; Tiensuu *et al.* 2005); however, the mechanisms by which SUR-2/Med23 and LIN-1/Elk1 regulate lateral signal gene transcription in VPCs do not conform to this model. SUR-2/Med23 is required for transcriptional activation of lateral signal genes in P6.p, likely via association with the Hox protein LIN-39, whereas LIN-1 is not required to activate transcription of lateral signal genes, only to repress transcription in all other VPCs (Zhang and Greenwald 2011).

Along with Elk1, Med23 also associates reversibly with the Cdk8 Kinase Module (CKM) (Boyer *et al.* 1999), a protein complex that modulates Mediator activity and consists of four subunits: Cdk8, Cyclin C, Med12, and Med13 [reviewed in Allen and Taatjes (2015)]. When associated with the Mediator core complex, the CKM can sterically prevent RNA Pol II binding to cause transcriptional repression of target genes, or can promote transcriptional activation via the kinase activity of Cdk8. In *C. elegans*, the CKM has been implicated in the control of cell cycle quiescence of VPCs (Clayton *et al.* 2008) and, when combined with mutations that activate EGFR pathway components or may have general effects on chromatin structure, in promoting ectopic vulval fate in VPCs that would normally adopt the 3<sup>o</sup> fate (Clayton *et al.* 2008; Grants *et al.* 2016). However, as discussed further herein, *cdk-8* and *cic-1*/Cyclin C null mutants are homozygous viable and have overtly normal vulval development, suggesting that they are not required for normal VPC fate patterning; in contrast, *dpy-22*/Med12 and *let-19*/Med13 null mutants are not viable, complicating the interpretation of their requirements in VPC fate patterning.

In this study, we analyze different combinations of *lin-1*, *sur-2*, and the CKM, and observe that they act in parallel to mediate different processes during VPC fate specification. Our analysis suggests that in the absence of EGFR signaling, the CKM, but not SUR-2, helps set a threshold to LIN-12/Notch activity in all VPCs. We also find that in the presence of EGFR signaling, all three factors are required to resist the response to ectopic LIN-12/Notch activity in P6.p, but only *sur-2*/Med23 and *lin-1*/Elk1 are required for endocytic downregulation of LIN-12-GFP in P6.p. Our further investigation of the role of *lin-1*/Elk1 in VPC patterning using cell fate reporters revealed that VPCs have characteristics of both 1<sup>o</sup> and 2<sup>o</sup> fate, suggesting that *lin-1*/Elk1 is

important for integrating EGFR and *lin-12*/Notch signaling inputs in the VPCs so that the gene complement for a specific cell fate is transcribed.

## Materials and Methods

### C. *elegans* genetics

Full genotypes are listed in Table S1. The following mutations were used and described fully in WormBase unless otherwise indicated: LGI: *cdk-8(tm1238)*, *sur-2(ku9)*. LGII: *let-19(os33)*, and a marked derivative of *mIn1[mIs14 dpy-10(e128)]*. LGIII: *lin-12(n302)*, *lin-12(n941)*, a marked derivative of *qC1 [dpy-19(e1259) glp-1(q339) qIs26]*, *cic-1(tm3740)*, *pha-1(e2123)*. LGIV: *lin-1(n304)*. LGV: *lin-25(ga67)*. LGX: *dpy-22(e652)*, *nre-1(hd20)* *lin-15b(hd126)* [isolated as a double mutant in Schmitz *et al.* (2007)].

The following transgenes were used: *arIs107[mir-61p::2xnlS-yfp]* (Yoo and Greenwald 2005); *arEx1080[lin-31p::lin-12(intraΔP)]* (Li and Greenwald 2010); *arIs131[lag-2p::2xnlS-yfp]* (Zhang and Greenwald 2011); *arEx1575[lin-12::gfp]* (Karp and Greenwald 2013); *arIs222[lag-2p::tagrpf]* (Sallee and Greenwald 2015); *arTi31[lin-31p::lin-45(AA, V627E)]* (de la Cova *et al.* 2017).

The *arIs116[Is1-5p::2xnlS-yfp]* transgene was described by (Choi 2009), and has been used as a LIN-12 target gene reporter and 2°-fate marker in other studies (Li and Greenwald 2010; Karp and Greenwald 2013; Keil *et al.* 2017). It is robustly expressed in the L3 stage, when 2° fate specification occurs, suggesting that LIN-12 activity is the main input into its expression in VPCs, in contrast to most other LIN-12 target gene reporters, which have a dynamic pattern of expression starting in the L2 stage (Yoo *et al.* 2004). We note that *arIs107[mir-61p::2xnlS-yfp]* (Yoo and Greenwald 2005), also used in this study, is specific to the L3 stage but is harder to visualize than *arIs116*.

### **Generation of single-copy insertion miniMos-based transgenes**

The *arTi102*, *arTi117*, *arTi120*, *arTi121*, and *arTi190* transgenes drive expression using regulatory elements from the *lin-31* promoter (Tan *et al.* 1998) and the *unc-54* 3'UTR. Each were cloned in the miniMos transgenesis vector pCFJ910 (Frøkjær-Jensen *et al.* 2014)(Addgene, #44481). Single-copy transgenes were generated by germline injection into N2 animals and insertions were isolated as described by Frøkjær-Jensen *et al.* (2014).

The transgenes *arTi102* and *arTi190* were modelled after *arEx1080* (Li and Greenwald 2010). They encode LIN-12(intra $\Delta$ P), the intracellular domain of LIN-12 protein (Wormbase sequence R107.8), from residues G931 to R1340. In *arTi102*, LIN-12(intra $\Delta$ P) is untagged; in *arTi190*, it is tagged at the C-terminus with mKate2.

The transgenes *arTi117*, *arTi120*, and *arTi121* encode CDK-8 protein (Wormbase sequence F39H11.3) in frame with the T2A peptide (Ahier and Jarriault 2014) and mCherry-H2B. *arTi117* encodes CDK-8(+), and *arTi120* and *arTi121* encode CDK-8(D182A).

### **RNAi**

Feeding RNAi was performed as described, using HT115-derived bacterial strains expressing *C. elegans* gene sequences (Kamath and Ahringer 2003) (Source BioScience) or *mCherry*. Briefly, eggs were prepared from *lin-12(n302); nre-1(hd20) lin-15b(hd126)* hermaphrodites maintained at 20°C using a bleach/sodium hydroxide protocol and placed on RNAi plates containing the appropriate bacterial strain. RNAi experiments were conducted at 25°C.

### **Assessment of Multivulva phenotype in the *lin-12(n302)* enhancement assay**

Strains containing *lin-12(n302)* were grown at 20°C. In RNAi experiments, eggs were placed on RNAi plates and the Multivulva phenotype of adults was assessed three to four days after egg preparation. Animals with three or more pseudovulvae were scored as Multivulva. When scoring conventional genotypes, L4 hermaphrodites were picked and the Multivulva phenotype of adults was assessed 24 hours later. Because *let-19(0)* homozygotes arrest during larval development,

homozygous progeny of a balanced *let-19(os33)/mIn1* strain were identified by loss of the *mIn1[mIs14 dpy-10(e128)]* balancer.

### **Scoring fluorescent reporter expression**

Strains were raised at 20° or 25° and scored at the L3 stage when VPCs were undivided (Pn.p), or had undergone either one cell division (Pn.px), or two cell divisions (Pn.pxx). Animals were immobilized in 10mM levamisole, mounted on a 2% agarose pad on a glass slide, and imaged at 40X on either a Zeiss Axio Imager D1 with an AxioCam MRm or a Zeiss Axio Imager Z1 with a Hamamatsu Orca-ER camera. Illumination was provided by an X-Cite 120Q light source (EXFO photonics solutions). Exposure times and scoring thresholds were established for individual reporters based on brightness of expression in control strains.

### **Data Availability**

All strains and reagents are available upon request. Please refer to Table S1 for full genotypes and strain names.

## **Results**

### **The CKM negatively regulates *lin-12* activity in uninduced VPCs**

*lin-12(d)* missense mutations cause ligand-independent constitutive activity (Greenwald and Seydoux 1990). All *lin-12(d)* mutants lack an anchor cell (AC) and therefore lack the cellular source of the LIN-3/EGF inductive signal. These mutants can be ranked in an allelic series (Greenwald *et al.* 1983b) based on their vulval phenotype: in a "weak" *lin-12(d)* mutant, exemplified by *lin-12(n302)*, all VPCs adopt the 3° fate, as in wild-type hermaphrodites when the AC is ablated; in a "strong" *lin-12(d)* mutant, higher constitutive *lin-12* activity causes all VPCs to adopt the 2° fate, causing a characteristic "Multivulva" phenotype (Figure 2A). Loss of a negative regulator such as *sel-10/Fbw7* boosts the activity of the weak *lin-12(d)* allele, such that all VPCs adopt the 2° fate instead of the 3° fate and the animals become Multivulva (Sundaram and Greenwald 1993; Hubbard *et al.* 1997).

Null alleles of *cdk-8* are homozygous viable and fertile, and have normal VPC fate specification based on marker gene expression and vulval anatomy (Figure 1C). We find that the null allele *cdk-8(tm1238)* enhances *lin-12(n302)* activity based on the characteristic Multivulva phenotype of adults (Figure 2B-C) and expression of *arls116[lst-5p::2xnl5-yfp]*, a direct transcriptional target of LIN-12/Notch (Li and Greenwald 2010)(Figure 2D). RNAi against *cdk-8* in a *lin-12(n302)* background sensitized for RNAi also enhances the Multivulva phenotype (Figure 2E). Thus, *cdk-8* behaves as a negative regulator of *lin-12* activity in this assay.

We evaluated the three other components of the CKM, *cic-1*/Cyclin C, *dpy-22*/Med12 and *let-19*/Med13 in the same assay. Null alleles of *cic-1* are homozygous viable and fertile, as is the hypomorphic allele *dpy-22(e652)*. Homozygous *let-19* null mutants can be obtained as sterile segregants from heterozygotes. Loss of activity of each of these genes enhances *lin-12(n302)*, based on the Multivulva phenotype or *arls116[lst-5p::2xnl5-yfp]* expression (Figure 2C-E). Thus, all four components of the CKM are required for negative regulation of *lin-12* activity in VPCs and are likely to work together in this process.

In human cells, Cdk8 kinase activity is dispensable when the CKM is associated with the Mediator core complex in repressing gene expression, implying that the CKM plays primarily a structural role in repressor mode (Knuesel *et al.* 2009a). In contrast, kinase activity appears to be essential when the CKM-Mediator complex promotes activation of target gene expression (Knuesel *et al.* 2009b). The mutation of a catalytic aspartate residue in the kinase domain to alanine (D173A) completely inactivates the kinase activity of mammalian Cdk8 (Akoulitchev *et al.* 2000). Sequence alignment of *C. elegans* CDK-8 protein with the human Cdk8 protein shows that this catalytic residue and its context are conserved in *C. elegans* (Figure 2F), so we infer that the corresponding D182A mutation should lack kinase activity as well.

We therefore investigated the requirement for kinase activity by examining the ability of wild-type CDK-8 or CDK-8(D173A), expressed in VPCs, to rescue the enhancement of *lin-12(n302)* by *cdk-8(0)*. To do so, we constructed single-copy insertion transgenes in which CDK-8(+) or CDK-8(D173A) is expressed in VPCs as part of a bicistronic transcript, made by fusing

mCherry-H2B via the viral T2A peptide, which causes ribosome skipping and works efficiently in *C. elegans* (Ahier and Jarriault 2014). The visualization of mCherry-H2B gives confidence that the upstream CDK-8 protein is expressed in the VPCs even when it has no rescuing activity. We find that CDK-8(+) efficiently rescues the Multivulva phenotype of *cdk-8(0); lin-12(n302)*, while two independent lines carrying transgenes that express the CDK-8(D173A) mutant are not rescued (Figure 2G). The inability of CDK-8(D173A) to rescue the enhancement of *lin-12(n302)* by *cdk-8(0)* supports the inference that the mutation abrogates kinase activity and suggests that kinase activity is essential for this role of the CKM.

We tested the requirement for *sur-2*/Med23 or *lin-25*/Med24 using null alleles and did not observe enhancement of *lin-12(n302)* (Figure 2C). This observation contrasts with the requirement for *sur-2* in the negative regulation of *lin-12* activity when EGFR-Ras-ERK is active, as described below.

### **The CKM is not required for EGFR- and SUR-2-promoted transcription of the lateral signal gene *lag-2* in P6.p**

Ligands for LIN-12 constitute the lateral signal, and the genes encoding these ligands are transcribed in P6.p in response to EGFR-Ras-ERK signaling (Chen and Greenwald 2004). Characterization of the upstream region of *lag-2* identified a cis-regulatory module composed of VPCrep, an element for repression in all VPCs, adjacent to VPCact, an element that is required for activation in all VPCs (Zhang and Greenwald 2011). The current model is that VPCrep is a binding site for LIN-1/Elk1, and VPCact is a binding site for a Hox protein, likely LIN-39. Both LIN-1 and LIN-39 are present in all VPCs (Wagmaister *et al.* 2006; Zhang and Greenwald 2011). When the inductive signal activates EGFR-Ras-ERK in P6.p, phosphorylation of LIN-1 by ERK relieves repression so that LIN-39 can promote transcription of *lag-2*. The Mediator components SUR-2/Med23 and LIN-25/Med24 are required for *lag-2* transcription even when VPCrep is deleted, consistent with Mediator acting in conjunction with LIN-39 to promote *lag-2* transcription through VPCact rather than acting with LIN-1/Elk1 to promote repression through VPCrep (Zhang and Greenwald 2011).



We assayed the effect of the CKM using null alleles for *cdk-8* and *cic-1* on the expression of the *lag-2* transcriptional reporter *arls222[lag-2p::tagrfp]*, which contains 7.2 kb of 5' flanking region (Sallee and Greenwald 2015). This reporter is strongly expressed in P6.p and its descendants in otherwise wild-type worms (Figure 1B), and is expressed normally in mutants lacking the CKM components *cdk-8* or *cic-1* (Figure 1C). Furthermore, the 2°-fate marker *arls116[lst-5p::2xnl5-yfp]* is expressed normally in CKM mutants, confirming that the lateral signal is produced (Figure 1C). These results suggest that *sur-2* and *lin-25* may promote transcription of lateral signal genes independent of the CKM, consistent with their distinctive abnormal vulval phenotypes. We also find that *arls222[lag-2p::tagrfp]* expression in P6.p, as well as the anchor cell, is greatly reduced in *let-19* animals, but such animals typically arrest prior to or during the L3 stage, so we cannot conclude that *arls222[lag-2p::tagrfp]* transcription requires LET-19.

### **Resistance to activated LIN-12 in P6.p depends on the relative balance of EGFR and LIN-12 activity and allows for robust expression of lateral signal gene reporters**

As described above, constitutive activation of LIN-12 in *lin-12(d)* mutants eliminates the anchor cell. When constitutively active forms of LIN-12 are expressed specifically in VPCs, and therefore do not prevent formation of the anchor cell, P6.p adopts and maintains the 1° fate (Shaye and Greenwald 2005; Li and Greenwald 2010), suggesting the existence of a mechanism for countering *lin-12* activity associated with 1° fate.

To ascertain if the CKM, SUR-2 and LIN-1 play a role in this mechanism, we first needed to characterize it further. To do so, we utilized transgenes that drive expression in VPCs using regulatory sequences from the *lin-31* gene ("*lin-31p*") (Tan *et al.* 1998) and the constitutively active form LIN-12(*intra*ΔP). This derivative of the intracellular domain ("*intra*") mimics the natural signal-transducing cleavage product (Struhl *et al.* 1993), but is stabilized by removal of a degron ("*ΔP*"), resulting in more potent constitutive activity (Li and Greenwald, 2010; Deng and Greenwald, 2016).

In the presence of the extrachromosomal array *arEx1080[lin-31p::lin-12(intraΔP)]*, all VPCs other than P6.p adopt the 2° fate, while P6.p still adopts the 1° fate (Figure 3A). The LIN-

12 target reporter *arls116[lst-5p::2xnl5-yfp]* is generally not transcribed in P6.p, consistent with implementation of a mechanism that resists constitutive *lin-12* activity (Figure 3A). In contrast, two independent, single-copy integrated transgenes that encode LIN-12(intra $\Delta$ P) lead to transcription of *arls116[lst-5p::2xnl5-yfp]* in P6.p (Figure 4A-C). We interpret this observation as indicating that these transgenes result in sufficient ectopic LIN-12 activity in P6.p to overcome resistance to LIN-12 activity in P6.p, thereby allowing us to examine the consequences of constitutive LIN-12 activity in a 1° VPC. To do so, we simultaneously scored *arls116[lst-5p::2xnl5-yfp]* and *arls222[lag-2p::tagrfp]* on a VPC-by-VPC basis in the presence of the single-copy insertion transgene *arTi102[lin-31p::lin-12(intra $\Delta$ P)]*. We observed that not only was *arls116[lst-5p::2xnl5-yfp]* expressed in P6.p, indicating that the resistance was overcome, but also that *arls222[lag-2p::tagrfp]* expression was concomitantly reduced in P6.p, suggesting that resistance is important for ensuring strong lateral signal gene expression (Figure 4A).

To test if this effect may be an artifact of the *arTi102[lin-31p::lin-12(intra $\Delta$ P)]* insertion site or *arls222[lag-2p::tagrfp]* reporter, we combined a different single-copy insertion transgene, *arTi190[lin-31p::lin-12(intra $\Delta$ P)-mkate2]*, and a different *lag-2* reporter, *arls131[lag-2p::2xnl5-yfp]* (Zhang and Greenwald 2011). We observed a similar reduction of *lag-2* reporter expression in this independent combination (Figure 4C), suggesting that reduced lateral signaling is a bona fide effect of ectopic LIN-12 activation in a 1° VPC.

We also tested whether LIN-12 activity from the *arEx1080[lin-31p::lin-12(intra $\Delta$ P)]* transgene, which appears to have lower constitutive activity, is sufficient to reduce transcription of *arls131[lag-2p::2xnl5-yfp]* in P6.p. We observed that *lag-2* reporter expression levels were initially reduced during the Pn.p stage (Figure 4C), consistent with the inference that lateral signaling in a 1° VPC is reduced by increased LIN-12 activity and further support the existence of a mechanism for countering *lin-12* activity in 1° VPCs. In this genotype, however, expression returned to wild-type levels by the Pn.px stage. We interpret the difference in the timing of the restoration of *lag-2* reporter expression between the two strains as reflecting the fact that expression driven by *lin-31p* regulatory sequences diminishes over the course of the lineage in

induced VPCs, while the anchor cell continues to produce LIN-3/EGF, so that the strength of *lin-12* activity and the number of copies of *lag-2* regulatory sequences in the reporters may come into play later in development.

In sum, our results suggest that 1°-fate associated resistance to activated LIN-12 depends on the relative balance of EGFR and LIN-12 activity and that this resistance helps ensure that P6.p becomes the robust source of lateral signal (Figure 4D). In the next section, we examine if the CKM and SUR-2 play a role in this resistance, and in the following section, describe how our investigation of a potential role for *lin-1* in this resistance led to novel observations about the role of *lin-1* in VPC patterning.

### **The CKM and SUR-2/Med23 are required for resistance of P6.p to signal transduction by expression of constitutively active LIN-12/Notch**

As described above, analysis of the role of the CKM in the absence of the inductive signal suggests that the CKM plays a role in setting a threshold by opposing LIN-12 activity in the VPCs. We therefore assessed whether the CKM also mediates the resistance to activated LIN-12 in P6.p in the presence of the inductive signal, when EGFR is activated. Additionally, we asked if *sur-2*, which acts in P6.p to promote lateral signal gene expression but does not enhance *lin-12(n302)* activity, is required for resistance to activated LIN-12 in P6.p. To do so, we removed the activity of individual genes using null alleles in the presence of *arEx1080[lin-31p::lin-12(intraΔP)]*, the “weak” transgene that does not overwhelm the resistance in P6.p, and assessed transcription of the LIN-12 target *arls116[lst-5p::2xnl5-yfp]*. We found that removal of any of these genes allowed *arls116[lst-5p::2xnl5-yfp]* transcription in P6.p, indicating that resistance to activated LIN-12 due to EGFR activation is relieved (Figure 3B-D).

We then assessed whether removal of *cdk-8* reduces *arls131[lag-2p::2xnl5-yfp]* expression in the presence of *arEx1080[lin-31p::lin-12(intraΔP)]*, as might be expected if loss of *cdk-8* increases constitutive *lin-12* activity. Although we could only assay a limited number of Pn.px-stage hermaphrodites due to the low brood size of the strain, we observed reduction of *lag-2* reporter expression in 4/8 *cdk-8(0); arls131 [lag-2p::2xnl5-yfp]; arEx1080[lin-31p::lin-*

*12(intraΔP)*] hermaphrodites as compared to *arls131[lag-2p::2xnl5-yfp]; arEx1080[lin-31p::lin-12(intraΔP)]* hermaphrodites (13/14), which is statistically significant by Fisher's Exact Test ( $p < 0.04$ ).

The requirement for the CKM for resistance to nuclear LIN-12 contrasts with the lack of a requirement for the CKM to promote *lag-2* transcription in the same VPC. These observations are consistent with independent function of different subcomplexes, e.g. a subcomplex containing both the CKM and SUR-2 for resistance to nuclear LIN-12, and a subcomplex that lacks the CKM (but may have LET-19/Med13) for expression of *lag-2*. We could not test if CDK-8 kinase activity is required for resistance to nuclear LIN-12 in P6.p because of synthetic lethality when we tried to construct strains containing *cdk-8(0)*, *arls116*, *arEx1080*, and any of the single-copy CDK-8-expressing transgenes, for reasons we did not investigate further.

### **Loss of LIN-1 leads to ectopic LIN-12 signal transduction in all VPCs**

Previous studies suggest that loss of *lin-1* does not affect production of the inductive signal by the anchor cell or activation of the EGFR-Ras-ERK phosphorylation cascade per se (Beitel *et al.* 1995; de la Cova and Greenwald 2012). We began to test if *lin-1* is required for resistance to activated LIN-12 in P6.p by constructing a control strain in which *lin-1(n304)*, a null mutant, and the LIN-12 target gene reporter *arls116[lst-5p::2xnl5-yfp]*, were combined. We observed that the reporter is expressed in all VPCs in this strain, even though it lacks any transgenic source of constitutively active LIN-12 (Figure 5A-B). To determine whether this unexpected expression of *arls116[lst-5p::2xnl5-yfp]* in all VPCs is a property of the reporter transgene, we tested a second LIN-12 target gene reporter, *arls107[mir-61p::2xnl5-yfp]* (Yoo and Greenwald 2005). Again, we observed ectopic expression in all VPCs in *lin-1(n304)* (Figure 5C), indicating that LIN-12 target genes may be generally derepressed in the absence of *lin-1* activity. We note that precocious derepression of *arls116[lst-5p::2xnl5-yfp]* is not observed during the L2 stage (Figure 5D), indicating that the temporal mechanism that normally restricts induction of this target to the L3 stage is not abrogated by loss of *lin-1*, and suggesting that the observed expression in all VPCs reflects a function of *lin-1* relevant to spatial patterning.

Due to the above observations, and because loss of *lin-1* leads to derepression of lateral signal gene expression (Zhang and Greenwald 2011), we hypothesized that LIN-12 signal transduction is ectopically activated in all VPCs in a *lin-1(0)* mutant background. We tested this hypothesis genetically by examining the effect of removing *lin-12* activity in a *lin-1(0)* background. If LIN-12 signal transduction occurs in all VPCs in a *lin-1(0)* background, then *lst-5* expression in the absence of LIN-1 would still require *lin-12* activity. When we examined *lin-12(0); lin-1(0); arls116[lst-5p::2xnl5-yfp]* hermaphrodites, we observed that *arls116[lst-5p::2xnl5-yfp]* was no longer expressed (Figure 5E), consistent with the possibility that LIN-12 signal transduction is ectopically activated.

Normally the EGFR-mediated inductive signal causes LIN-12 protein to be endocytosed and degraded in P6.p (Levitan and Greenwald 1998a; Shaye and Greenwald 2002)(Figure 5F-G), yet P6.p expresses LIN-12 target gene reporters in *lin-1(0)*. Thus, if loss of *lin-1* indeed causes ectopic LIN-12 signal transduction, we would predict that loss of *lin-1* also prevents LIN-12 downregulation in P6.p despite its 1° fate characteristics, such as *lag-2* expression and formation of a functional vulva. Indeed, when we assessed the presence of LIN-12-GFP in a *lin-1(0)* background, we observed that it is visible at the apical membrane of P6.p, as in the other VPCs, indicating that it has not been downregulated (Figure 5F-G). Furthermore, as described above, the 1° fate is normally associated with resistance to activated LIN-12, yet two different targets of LIN-12 are transcribed in P6.p and in all other VPCs in a *lin-1(0)* background, indicating that resistance is abrogated or overcome.

### **LIN-1 coordinates crosstalk between the inductive and lateral signaling pathways**

Cell lineage analysis suggested that in *lin-1(0)* mutants, VPCs commit to either the 1° or 2° fate and that VPCs are able to resolve the relative strength of the EGFR and LIN-12/Notch signaling inputs (Beitel *et al.* 1995). However, now, using direct targets of the inductive and lateral signaling pathways to assess the state of signal transduction in the VPCs, we instead observe highly penetrant expression of direct targets for both EGFR and LIN-12/Notch pathways in all VPC (Figure 6A-B). We interpret this observation as indicating that loss of *lin-1* activity

compromises at least some aspects of the ability of VPCs to integrate the signaling inputs from these pathways.

The simultaneous activation of EGFR and LIN-12/Notch signal transduction observed in *lin-1(0)* mutants contrasts with the mutually exclusive expression of the same targets when the Ras cascade per se is activated. We scored expression of the same signaling pathway reporters on a VPC-by-VPC basis in the presence of a transgene that expresses a constitutively active and stable form of LIN-45/Braf in all VPCs *arTi31[lin-31p::lin-45(AA, V627E)]* (de la Cova and Greenwald 2012; de la Cova *et al.* 2017). In contrast to *lin-1(0)*, we found that when the Ras cascade is activated, each VPC generally expresses one marker or the other, not both (Figure 6C-D). The innermost VPCs adopt their normal fates, indicating that the anchor cell inductive signal continues to center the pattern on P6.p. In addition, the outermost VPCs, which normally would adopt the 3<sup>o</sup> fate but instead form ectopic pseudovulvae away from the anchor cell, are patterned by their neighbors: P8.p always expresses only the *lag-2* reporter, because its neighbor P7.p always adopts its normal 2<sup>o</sup> fate; and P3.p and P4.p generally express one or the other reporter, but not both, implying that they retain the ability to resolve their fates through interactions between them. Thus, we interpret the difference in marker pattern as indicating that loss of *lin-1* not only causes all VPCs to behave as if they have been induced, but also abrogates coordination between the inductive and lateral signaling pathways.

## Discussion

In the *C. elegans* Vulval Precursor Cells (VPCs), multiple mechanisms coordinate LIN-12/Notch and EGFR signaling inputs to ensure a precise and robust spatial pattern of distinct cell fates. The pattern is centered on P6.p, in which EGFR-Ras-ERK is activated by an EGF-like ligand produced by the gonad, and subsequently produces a lateral signal composed of ligands that activate LIN-12/Notch. We examined how several parameters impacting the activity of *lin-12/Notch* in VPC fate patterning are affected by loss of three components that have biochemical relationships: LIN-1, the ortholog of the Elk1 subfamily of transcription factors, which regulates

lateral signal gene transcription in response to the inductive signal; SUR-2, the ortholog of Med23, which in mammalian cells links Elk1 to the core Mediator complex; and the facultative modulator of the Mediator complex, the Cdk8 kinase module (CKM).

We discuss here our three main conclusions and their implications. (i) The CKM, but not SUR-2/Med23, helps set a threshold for LIN-12/Notch activity in all VPCs. (ii) In P6.p, where EGFR is active and LIN-12/Notch is normally inactive, we find that the CKM, SUR-2 and LIN-1 are all required for EGFR-associated resistance to ectopically activated LIN-12/Notch, while only SUR-2 is required for lateral signal gene transcription. (iii) We extend the understanding of the integration of inductive and lateral signaling in view of our new insights into how loss of *lin-1* impacts *lin-12* activity, and how sufficient ectopic LIN-12 activity in P6.p can overcome EGF-promoted resistance and oppose 1° fate. Our results suggest that different configurations of the CKM, SUR-2 and LIN-1 operate simultaneously in VPCs to coordinate EGFR and LIN-12/Notch signaling to specify the 2° VPC fate, and emphasize the crucial role of *lin-1* in VPC fate patterning (Figure 7A-C).

### **The CKM and basal activity of LIN-12/Notch in VPCs**

We identified a requirement for the CKM and its associated kinase activity in negative regulation of *lin-12* activity. Loss of *cdk-8* strongly enhanced the mildly activated mutation *lin-12(n302)*, an allele which has two useful properties: (i) it affords a sensitized background for observing increased *lin-12* activity (Hubbard *et al.* 1997; de Souza *et al.* 2007), and (ii) it removes the anchor cell of the gonad, which serves as the cellular source of the EGF signal, and hence removed input from EGFR-mediated induction into VPC fate. Thus, the genetic interactions we observed with Mediator CKM components indicate that the CKM exerts a negative regulation on basal *lin-12* activity independent of EGFR-mediated input. We suggest that the CKM is important for setting a threshold in VPCs for response to *lin-12* activity.

In mammalian cells, (Fryer *et al.* 2004) found that Cdk8 and Cyclin C associate with the Notch nuclear complex, and that Cdk8 phosphorylates the Notch intracellular domain to promote its targeting by Fbw7 for ubiquitination and proteasome-mediated degradation. Based on these

observations and other supporting data, they proposed that Cdk8 activity promotes degradation of the Notch enhancer complex at target genes. Their biochemical observations were corroborated in a subsequent study, which further showed that *in vivo* Cyclin C is a haploinsufficient tumor suppressor for the *NOTCH1*-driven cancer T cell acute lymphoblastic leukemia (Li *et al.* 2014). Furthermore, a recent study of another *NOTCH1*-driven cancer, chronic lymphocytic leukemia, found that mutations in *MED12* correlate with increased levels of NOTCH1 intracellular domain, and that Cdk8 kinase activity negatively regulates its level in this cancer context, too (Wu *et al.* 2017). These findings are consistent with our conclusions that individual components of the CKM all contribute to the negative regulation of *lin-12* activity in a CDK-8 kinase dependent fashion.

*sel-10*, the *C. elegans* ortholog of Fbw7, was first implicated in negative regulation of Notch through genetic analysis in *C. elegans* (Sundaram and Greenwald 1993; Hubbard *et al.* 1997). The functional relationship of *sel-10* and *lin-12* parallels the functional relationship of *FBXW7* (the gene that encodes Fbw7) and *NOTCH1*: mutations that inactivate *sel-10* increase the activity of *lin-12(n302)*, and mutations that inactivate *FBXW7* increase the activity of oncogenic forms of *NOTCH1* with similar lesions (Gupta-Rossi *et al.* 2001; Öberg *et al.* 2001; Wu *et al.* 2001). However, in *C. elegans*, it is not clear that negative regulation of LIN-12 by CDK-8 is direct: although the intracellular domain of LIN-12/Notch must be able to assemble into the nuclear complex to be degraded by SEL-10/Fbw7 (Deng and Greenwald 2016), the Cdk8-dependent phosphorylation of the mammalian Notch1 intracellular domain occurs at serines that are not conserved in *C. elegans* LIN-12. It is possible that the CKM phosphorylates LIN-12 directly, but at a different site than in mammalian Notch1. Alternatively, the negative regulation of *lin-12* activity by the CKM in VPCs may occur by a different mechanism, such as phosphorylation of another component of the nuclear complex or more indirectly.



### **Different requirements for SUR-2, the CKM, and LIN-1 in P6.p for different functions relevant to LIN-12/Notch and VPC patterning**

The roles of SUR-2, the CKM, and LIN-1 are different in P6.p for three functions that are relevant to LIN-12/Notch signaling and VPC patterning: transcription of the lateral signal genes (Figure 7A), downregulation of the receptor form of LIN-12 (Figure 7B), and resistance to the nuclear form of LIN-12 (Figure 7C). Although the physical interactions cannot be known from this genetic analysis, we can make some hypotheses about complexes and mechanisms that mediate the different functions.

With respect to transcription of the lateral signal genes in P6.p, SUR-2/Med23 is required for expression (Chen and Greenwald 2004) and LIN-1/Elk1 is not, although *lin-1* plays an important role in VPC patterning by repressing the lateral signal genes in other VPCs (Zhang and Greenwald 2011). Our analysis of *cdk-8* and *cic-1* indicates that the CKM is not required for expression of the lateral signal genes. Thus, the LIN-39/Hox activator complex that promotes lateral signal gene transcription in P6.p may contain SUR-2 but not the CKM, and the LIN-1 repressor complex that prevents expression in other VPCs may not contain either SUR-2 or the CKM. We note that a small difference in penetrance of *lag-2* expression reported for a complex background that differed in *cdk-8* activity, interpreted as evidence that *cdk-8* partially contributes to LIN-1-mediated repression of lateral signal genes (Grants *et al.* 2016), is not statistically significant, so at present there is no unequivocal evidence for a partial contribution of the CKM to LIN-1-mediated repression of lateral signal genes.

The endocytic downregulation of a GFP-tagged receptor form of LIN-12 in P6.p was previously shown to require SUR-2 (Shaye and Greenwald 2002); we now find that LIN-1 is also required for this process, but the CKM is not. In addition, analysis of cis-acting sequences in the intracellular domain of LIN-12 suggested that kinases and ubiquitin ligases promote its internalization and degradation, leading to the hypothesis that one or more of these factors are under the transcriptional control of the EGFR-Ras-ERK pathway (Shaye and Greenwald 2005). Our analysis here suggests the further hypothesis that one or more direct transcriptional targets

are activated by ERK-phosphorylated LIN-1 recruitment of Mediator via SUR-2, as in mammals, although no direct targets regulated in this way have been identified in *C. elegans* as yet.

Finally, the CKM, SUR-2 and LIN-1 are all required for EGFR-associated resistance to a stabilized, nuclear form LIN-12/Notch that mimics the natural signal-transducing form after ligand-induced cleavage. Thus, we envisage that a complex containing all three components may mediate this function. In such complexes, a requirement for Cdk8 kinase activity is associated with transcriptional activation (Knuesel *et al.* 2009b) and the lack of a requirement for Cdk8 kinase activity, with repression (Knuesel *et al.* 2009a). However, we were unable to test if CDK-8 kinase activity was required for resistance because of synthetic lethality of the necessary genotype. It is possible that this complex functions in repressor mode to directly repress LIN-12 target genes; alternatively, it may function in activator mode to promote expression of one or more targets of EGFR-Ras-ERK that mediates resistance.

We note that there are differences in the contributions of the EGFR-Ras-ERK pathway to vulval development in other species when compared to *C. elegans* (Felix 2007; Sommer 2012). There also may be differences in the contributions of the components we have studied here to vulval development in the related species, *Caenorhabditis briggsae*: the ortholog of *lin-1* is critical for inhibiting ectopic vulval fate (Sharanya *et al.* 2015), but the ortholog of *sur-2* may not be essential for production of the lateral signal (Mahalak *et al.* 2017). Finally, these components function in different configurations and activate or repress different target genes in other developmental contexts in *C. elegans*, such the excretory system (Howard and Sundaram 2002; Rocheleau *et al.* 2002; Sundaram and Buechner 2016).

### **Integrating the EGFR-Ras-ERK inductive signaling and LIN-12/Notch lateral signaling pathways**

Our observations on the phenotype of *lin-1(0)* mutants and the resistance to activated LIN-12 in P6.p are relevant to how signaling inputs are integrated during VPC specification. *lin-1* has been viewed as an “inhibitor of vulval fate”, because loss of *lin-1* causes ectopic vulval induction (Ferguson *et al.* 1987; Beitel *et al.* 1995), while missense mutations near phospho-acceptor sites

prevent the generation of additional vulval cells even in the presence of activated Ras (Jacobs *et al.* 1998). In terms of molecular mechanism, it has been proposed that sumoylated LIN-1 recruits transcriptional repressors to inhibit the 1<sup>o</sup> fate, and ERK-mediated phosphorylation of LIN-1 converts it into a transcriptional activator to promote 1<sup>o</sup> fate in P6.p (Leight *et al.* 2015). This model accounts for a positive role for *lin-1* in promoting 1<sup>o</sup> fate as inferred from a requirement for expression of *egl-17*, a marker for 1<sup>o</sup> fate in VPCs (Howard and Sundaram 2002; Tiensuu *et al.* 2005), and is compatible with the regulation of *lag-2* expression by loss of LIN-1 repression in response to the inductive signal. The later role of *lin-1* in descendants of 2<sup>o</sup> VPCs during vulval morphogenesis (Farooqui *et al.* 2012) is distinct from the role in VPC fate specification considered here.

In classic cell lineage analysis, VPC fates were assigned using the best criteria available at the time--the plane of the final division in the lineage and adhesive properties of the terminal cells (Sternberg and Horvitz 1986). Such analysis suggested that in a *lin-1(0)* mutant, each VPC adopts a 1<sup>o</sup> or 2<sup>o</sup> fate, depending on the relative input of competing inductive and lateral signaling pathway activity (Beitel *et al.* 1995); however, it was also noted that many of the lineages were abnormal. Here, using markers that directly report the activities of the EGFR and LIN-12/Notch pathways, we observed that both EGFR-Ras-ERK and LIN-12/Notch signal transduction is active in VPCs in *lin-1(0)* mutants, likely accounting for the abnormal lineages previously observed. We observed that expression of these reporters persists throughout the lineage in *lin-1(0)* mutants, in contrast to their clean resolution by the Pn.px stage when LIN-45/Braf, the first kinase in the Ras cascade, is constitutively activated. We interpret these findings as indicating that *lin-1* is required for crosstalk between the EGFR and LIN-12 signal transduction pathways, such that loss of *lin-1* not only leads to ectopic 1<sup>o</sup> fate, but also abrogates the normal mechanisms that mediate crosstalk between the EGFR-Ras and LIN-12/Notch, such as downregulation of LIN-12.

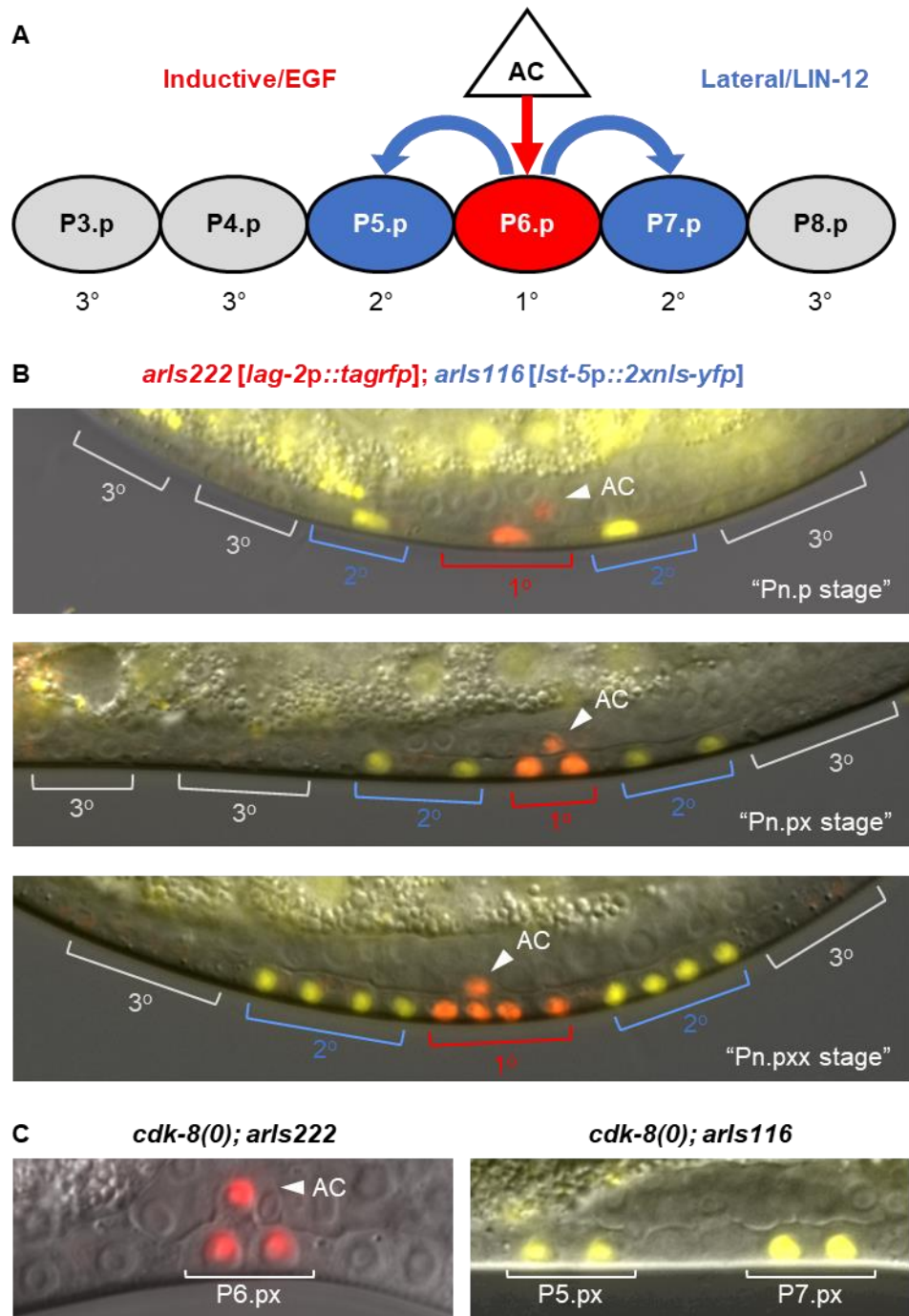
In previous reports it had been briefly noted that in response to EGFR activity, P6.p appears to be refractory to an activated form of LIN-12 lacking the extracellular domain (Shaye and Greenwald 2005; Li and Greenwald 2010). We have now characterized this phenomenon

further using a stabilized form of the untethered intracellular domain, which mimics the ultimate cleavage product after ligand binding, and transcriptional reporters for EGFR-Ras-ERK and LIN-12 target genes. Our observation that *lag-2* expression can be repressed when *lin-12* activity is sufficiently high in the presence of the inductive signal is evidence that “high” LIN-12 can oppose EGFR-Ras-ERK in presumptive 1° VPCs, suggesting that EGFR-promoted resistance to activated LIN-12 is a mechanism for preventing inappropriate activation of 2°-fate genes that would otherwise inhibit adoption of 1° fate. How high constitutive *lin-12* activity overcomes resistance may be mechanistically related to what normally occurs in 2° VPCs, where activation of LIN-12 leads to expression of negative regulators of EGFR-Ras-ERK activity (Berset *et al.* 2001; Yoo *et al.* 2004) and positively reinforces *lin-12* activity through a microRNA-mediated double negative feedback loop (Yoo and Greenwald 2005). We speculate that LIN-1, SUR-2 and the CKM work together to promote expression of one or more target genes that implement resistance to LIN-12.

## **Acknowledgments**

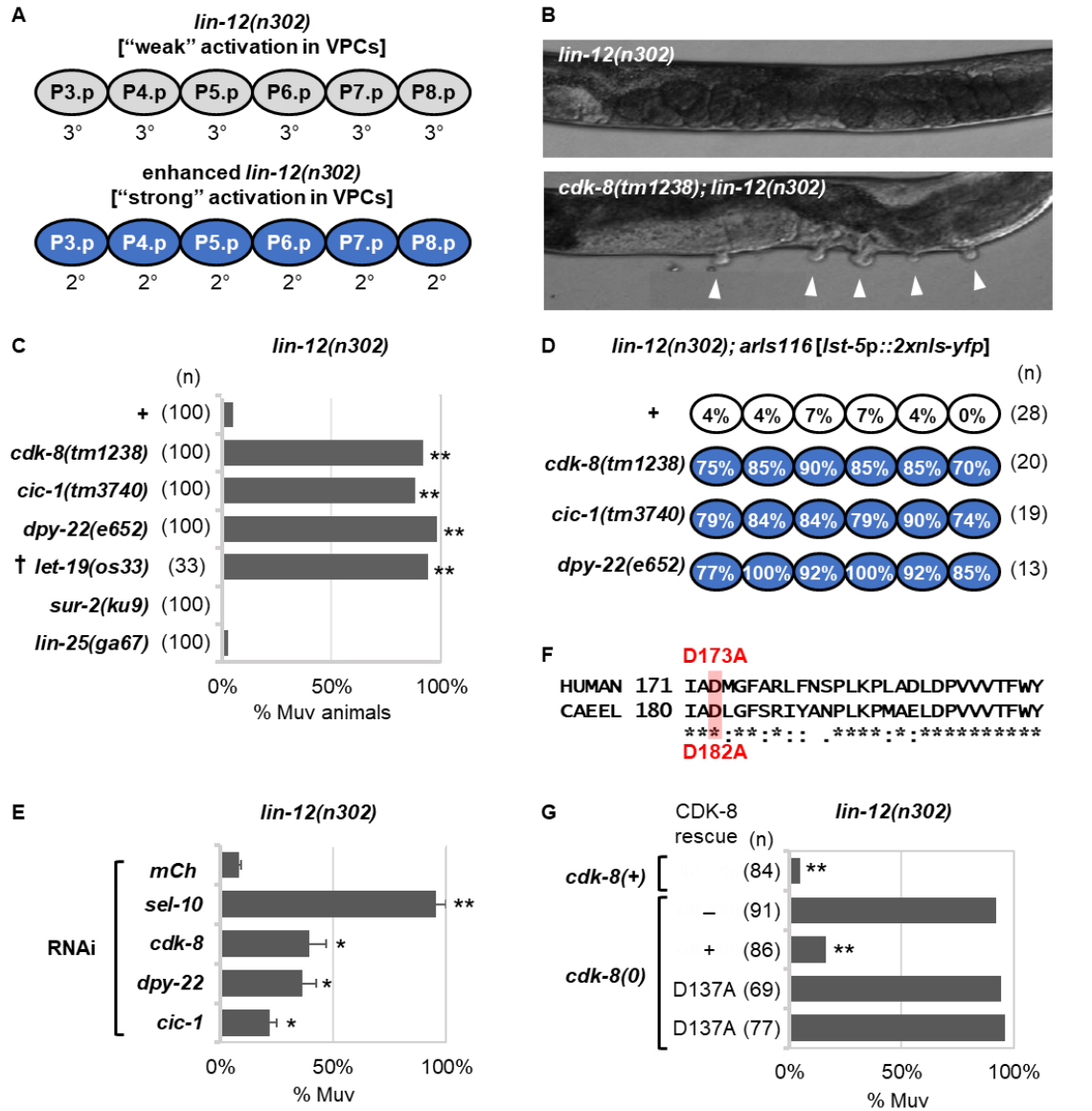
We thank Michelle Attner and Claire de la Cova for valuable discussion and comments on this manuscript, and Dan Shaye, Maria Sallee, and Xantha Karp for their expert opinions and insights during the origins of this project. We are grateful to Gleniza Gomez for technical assistance, and members of the Greenwald lab for their scientific input and feedback. Some of the strains used in this study were provided by the *Caenorhabditis* Genetics Center, which is supported by the NIH Office of Research Infrastructure Programs (P40 OD010440). This work was supported by NIH grants R01GM114140 (to I.G.) and F31CA177168 (to R.S.U.).

## **Chapter 2. Figures**



**Figure 1.** VPC fate specification. (A) Schematic of VPC fate specification. The EGF-like inductive signal produced by the anchor cell (AC) of the gonad activates a canonical EGFR-Ras-ERK cascade in P6.p, causing it to adopt the 1° vulval fate and transcribe lateral signal genes, including the DSL-type ligand *lag-2*. The lateral signal activates LIN-12 in P5.p and P7.p, which adopt the 2° vulval fate. The fates are represented as 1° vulval fate (red), 2° vulval fate (blue), and 3° non-vulval fate (gray). (B) Photomicrographs of VPCs and their descendants in the L3

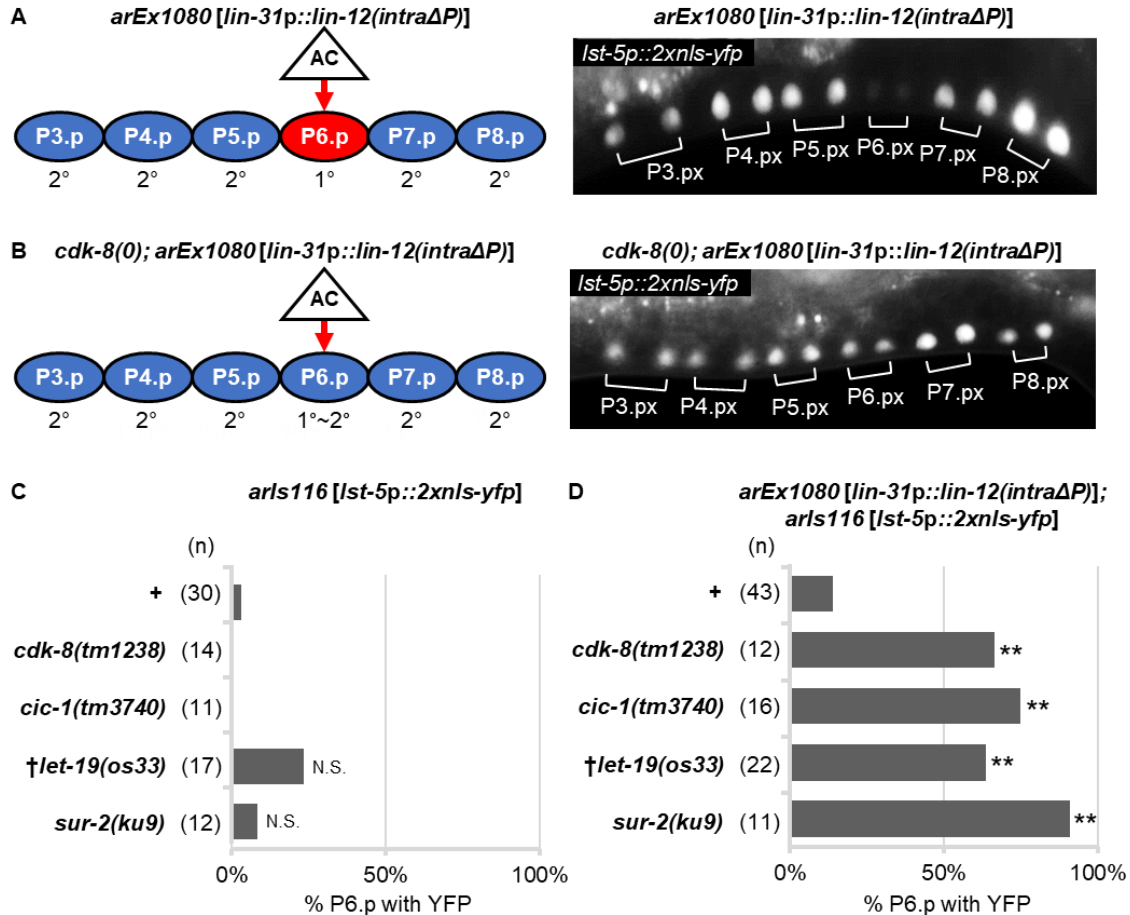
stage. The red 1<sup>o</sup>-fate reporter, *arls222[lag-2p::tagrfp]*, is a direct target of the EGFR-Ras-ERK pathway. The yellow 2<sup>o</sup>-fate reporter, *arls116[lst-5p::2xnlis-yfp]*, is a direct target of LIN-12/Notch. Top, marker expression in VPCs (the “Pn.p” stage); middle, marker expression in the daughters of P5.p-P7.p (the “Pn.px” stage); bottom, marker expression in the granddaughters of P5.p-P7.p (the “Pn.pxx” stage). (C) *cdk-8* null mutants have normal expression of cell fate markers. 14/14 individuals for each genotype, scored in a single experiment, showed normal marker expression. Right, photomicrograph of a *cdk-8(tm1238); arls222[lag-2p::tagrfp]* hermaphrodite at the Pn.px stage, showing normal *lag-2* reporter expression in the anchor cell (arrowhead) and in the two daughters of P6.p (bracket). Left, photomicrograph of a *cdk-8(tm128); arls116[lst-5p::2xnlis-yfp]* hermaphrodite at the Pn.px stage, showing normal 2<sup>o</sup> fate marker expression in the daughters of P5.p and P7.p (brackets).



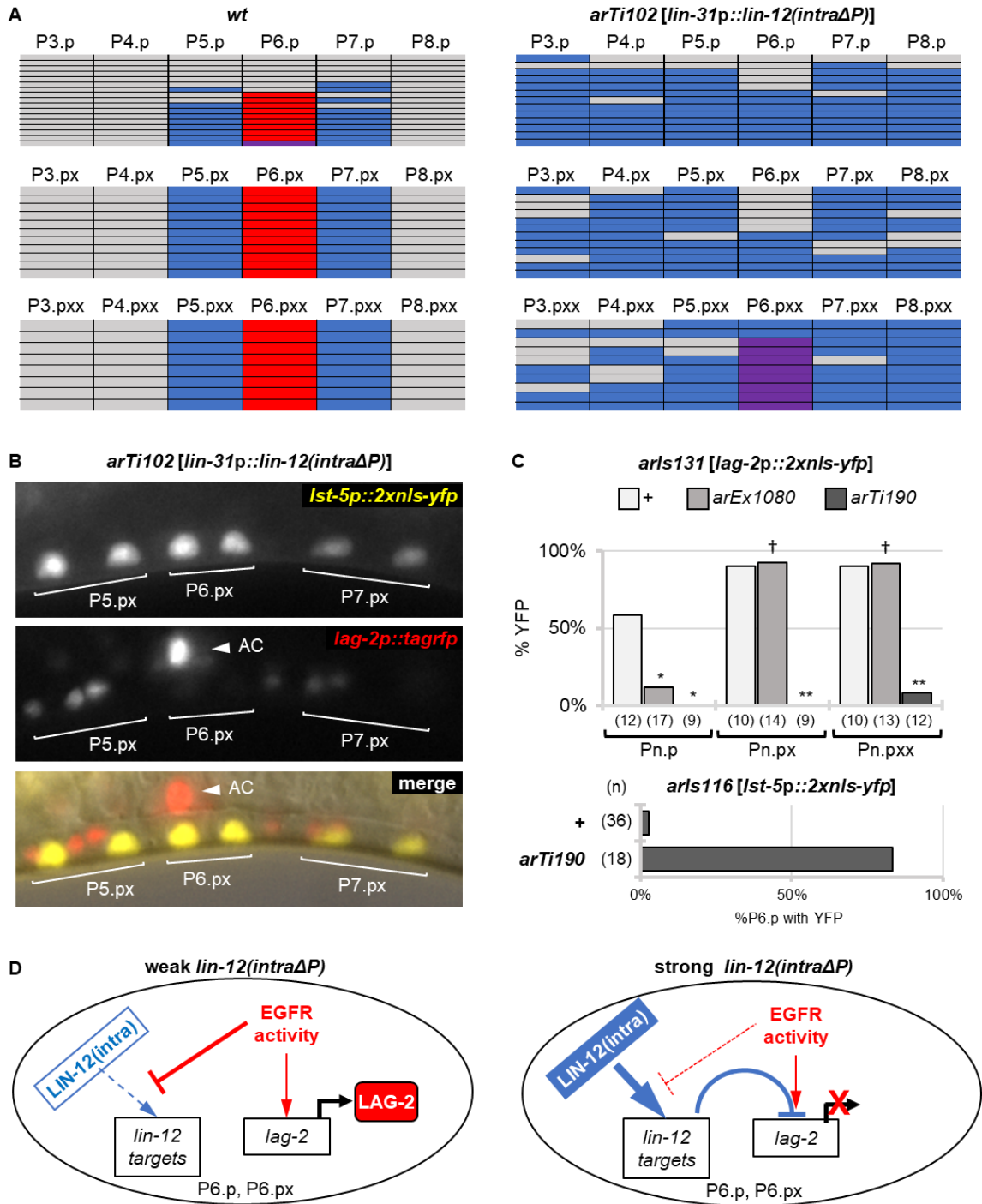
**Figure 2.** The CKM acts in a kinase dependent manner to negatively regulate *lin-12* activity. (A) Schematic showing VPC fates adopted depending on the degree of elevated *lin-12* activity. *lin-12(d)* mutations prevent the development of the anchor cell. In *lin-12(n302)*, a relatively "weak" *lin-12(d)* allele, all VPCs adopt the 3° non-vulval fate, as would wild-type VPCs in the absence of an anchor cell. *lin-12(n302)* activity can be enhanced in VPCs by removal of negative regulators, resulting in "strong" activity and causing all VPCs to adopt the 2° fate. (B) Photomicrographs showing that *cdk-8(0)* enhances *lin-12(n302)* activity to cause the distinctive Multivulva phenotype associated with all VPCs adopting the 2° fate. (C) Loss of individual CKM components, but not the core Mediator components *sur-2* or *lin-25*, enhances *lin-12(n302)* activity, as assessed by the Multivulva (Muv) phenotype. Graph shows percentage of adult hermaphrodites that are Muv. \*\**P* < 0.001 compared to *lin-12(n302)* (Fisher's exact test). † Scored homozygous *let-19(os33)* progeny from heterozygous *let-19(os33)/mln1* mothers. (D) Loss of individual CKM components enhance *lin-12(n302)* activity, as assessed by expression of the LIN-12 target reporter *arls116[lst-5p::2xnl5-yfp]*. Schematic representation of the percentage of individual VPCs that display YFP fluorescence. (E) Reduction of individual CKM components by RNAi enhances *lin-*



*lin-12(n302)* activity. Graph shows percentage of adult hermaphrodites that are Muv.  $**P < 0.001$ ,  $*P < 0.01$  compared to RNAi against mCherry (Fisher's exact test). (F) ClustalW2 alignment (Larkin *et al.* 2007) of human Cdk8 and *C. elegans* CDK-8 showing conservation of the region required for kinase activity. The aspartate residue essential for Cdk8 kinase activity, D182, and the corresponding *C. elegans* residue, D173, mutated to alanine for the analysis in G are highlighted in red. (G) CDK-8 kinase activity is necessary for negative regulation of *lin-12(n302)* activity. Graph shows percentage of adult hermaphrodites that are Muv. Transgene *arTi117* expresses CDK-8(+) in the VPCs, restoring activity and rescuing enhancement of *lin-12(n302)* by *cdk-8(0)*. Two independent transgenes (*arTi120* and *arTi121*) expressing the putative kinase-dead CDK-8(D182A) mutant in the VPCs do not rescue *cdk-8(0)*. All three transgenes express a bicistronic transcript in which CDK-8 fused to T2A-mCherry-H2B in order to confirm transgene expression in VPCs (see Materials and Methods).  $**P < 0.001$  compared to *cdk-8(0); lin-12(n302)* (Fisher's exact test).

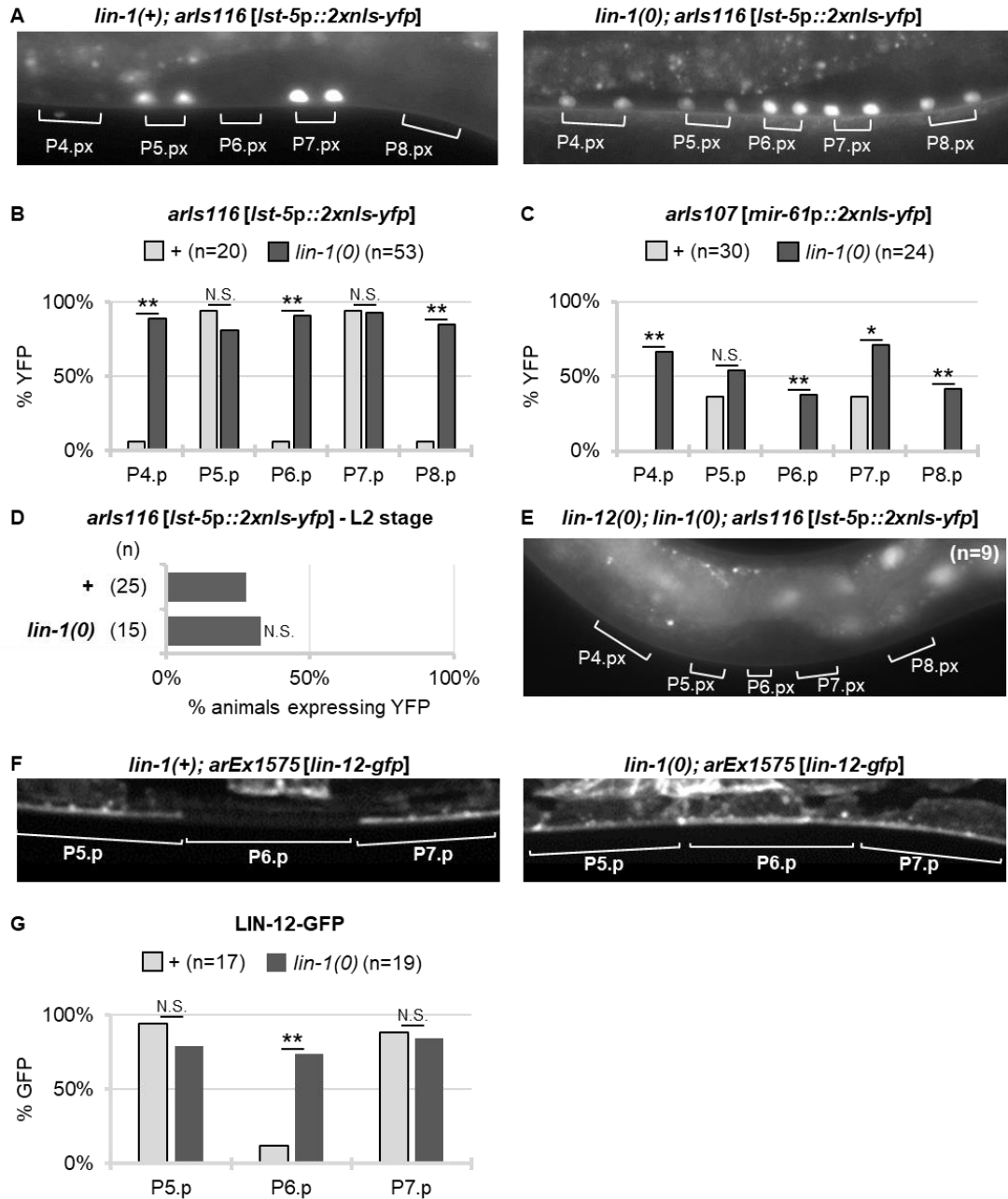


**Figure 3.** Resistance to constitutively active LIN-12 signal transduction in P6.p. (A) Left, schematic representing the resistance to LIN-12 activation in P6.p in the presence of the AC. The *arEx1080* transgene expresses constitutively active LIN-12(*intraΔP*) in all VPCs. However, the LIN-12 target reporter *arls116* is not expressed in P6.p, allowing genes to be assessed for roles in resistance to activated LIN-12 associated with 1° fate. Right, photomicrograph showing expression of the LIN-12 target reporter *arls116[lst-5p::2xnl5-yfp]*; *arEx1080[lin-31p::lin-12(intraΔP)]* in daughters of all VPCs except P6.p, where LIN-12 signal transduction is resisted. (B) Loss of resistance to LIN-12 activation in P6.p in *cdk-8* null mutants. Left, schematic in which P6.p fate is denoted as 1°~2°, since it now expresses *arls116[lst-5p::2xnl5-yfp]* but will form a functional vulva. Figure 4 considers the state of P6.p further. Right, photomicrograph of *cdk-8(tm1238); arls116[lst-5p::2xnl5-yfp]; arEx1080[lin-31p::lin-12(intraΔP)]* showing resistance in P6.p is lost and YFP is present in daughters of all VPCs. (C) Control for D, showing that *arls116[lst-5p::2xnl5-yfp]* is not ectopically expressed in P6.p in the absence of individual CKM components or *sur-2*. Graph shows percentage of animals with YFP fluorescence in P6.p. N.S. denotes not significant compared to wild type (Fisher's exact test). (D) Loss of individual components of the CKM or *sur-2* relieve resistance to expression of *arls116[lst-5p::2xnl5-yfp]* in P6.p in the presence of *arEx1080[lin-31p::lin-12(intraΔP)]*. Graph shows percentage of animals with YFP fluorescence in P6.p. \*\**P* < 0.001 compared to wild type (Fisher's exact test).



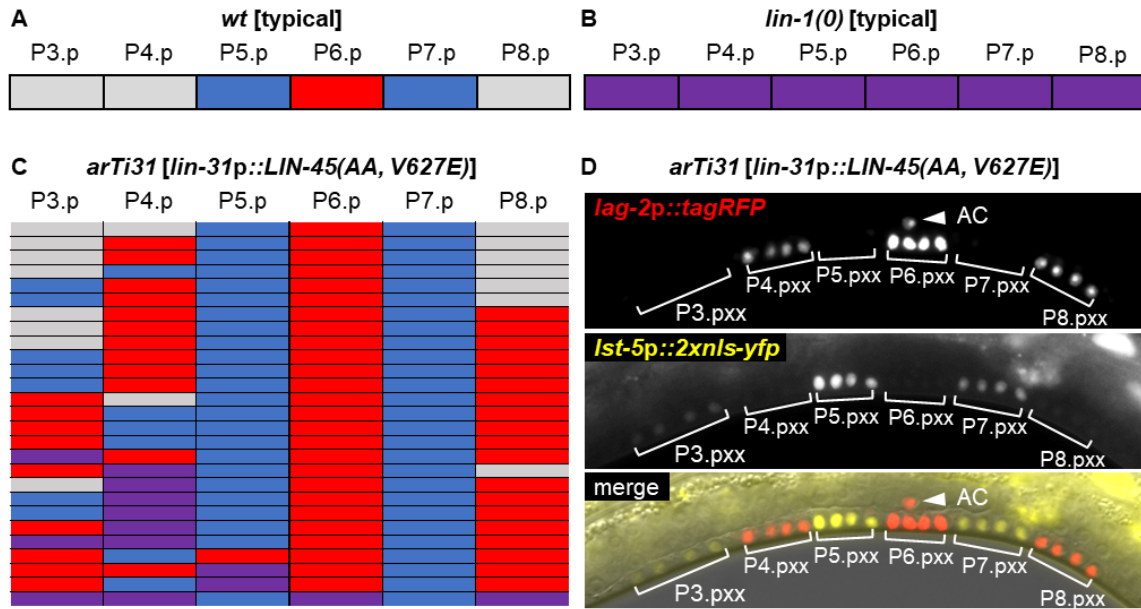
**Figure 4.** Activated LIN-12 expressed from single-copy transgenes overcomes resistance in P6.p and leads to repression of lateral signal gene expression. (A) Constitutive LIN-12 activity provided by *arTi102[lin-31p::lin-12(intraΔP)]* overcomes resistance to *lin-12* activity in P6.p, the 1<sup>o</sup> VPC. Each row in the chart represents an individual with *arls222[lag-2p::tagrfp]* and *arls116[ist-5p::2xnlis-yfp]* reporters. On the left, the reporters are in an otherwise wild-type background; on

the right, they are in the background of *arT1102*, which expresses LIN-12(intra $\Delta$ P). In each hermaphrodite, each marker was scored on a per VPC basis. Red, only tagRFP fluorescence was present; blue, only YFP fluorescence was present; purple, both tagRFP and YFP were present; grey, no fluorescence was observed. (B) *arls131[lag-2p::2xnl5-yfp]* expression is inhibited by LIN-12(intra $\Delta$ P) expressed from *arTi190*. Photomicrographs of a hermaphrodite of genotype *arTi102[lin-31p::lin-12(intra $\Delta$ P)]; arls222[lag-2p::tagrfp]; arls116[lst-5p::2xnl5-yfp]* showing expression of the *lst-5* reporter in daughters of P6.p (top), and, inhibition of the *lag-2* reporter expression in P6.p in the same individual (middle). In the merge (bottom), tagRFP can be seen in the AC (arrowhead) and neurons, but not in Pn.px cells. (C) Constitutive LIN-12 activity from *arTi190[lin-31p::lin-12(intra $\Delta$ P)-mkate2]* overcomes resistance to *lin-12* activity in P6.p, leading to reduced expression of *arls131[lag-2p::2xnl5-yfp]* and to ectopic transcription of *arls116[lst-5p::2xnl5-yfp]*. In this panel, the two markers were scored in separate strains. The graphs shows percentage of animals with fluorescent protein expression in P6.p, its daughters, and granddaughters. At the Pn.p stage, \* $P < 0.015$  and \*\* $P < 0.0005$  when wild-type and transgene-containing strains were compared (Fisher's exact test). When *arEx1080* and *arTi190* are compared in the Pn.px and Pn.pxx stages, † $P < 0.0005$ . In the bottom graph, the "+" value represents the same data shown in A. (D) Model illustrating that resistance to activated LIN-12 in P6.p depends on the relative balance of EGFR and LIN-12 activity. Left, resistance to "weak" activity of LIN-12(intra $\Delta$ P) allows for expression of *lag-2* reporters and lack of expression of LIN-12 target reporters. Right, resistance can be overcome by "strong" activity of LIN-12(intra $\Delta$ P), resulting in expression of LIN-12 target gene reporters and diminished expression of *lag-2* reporters.

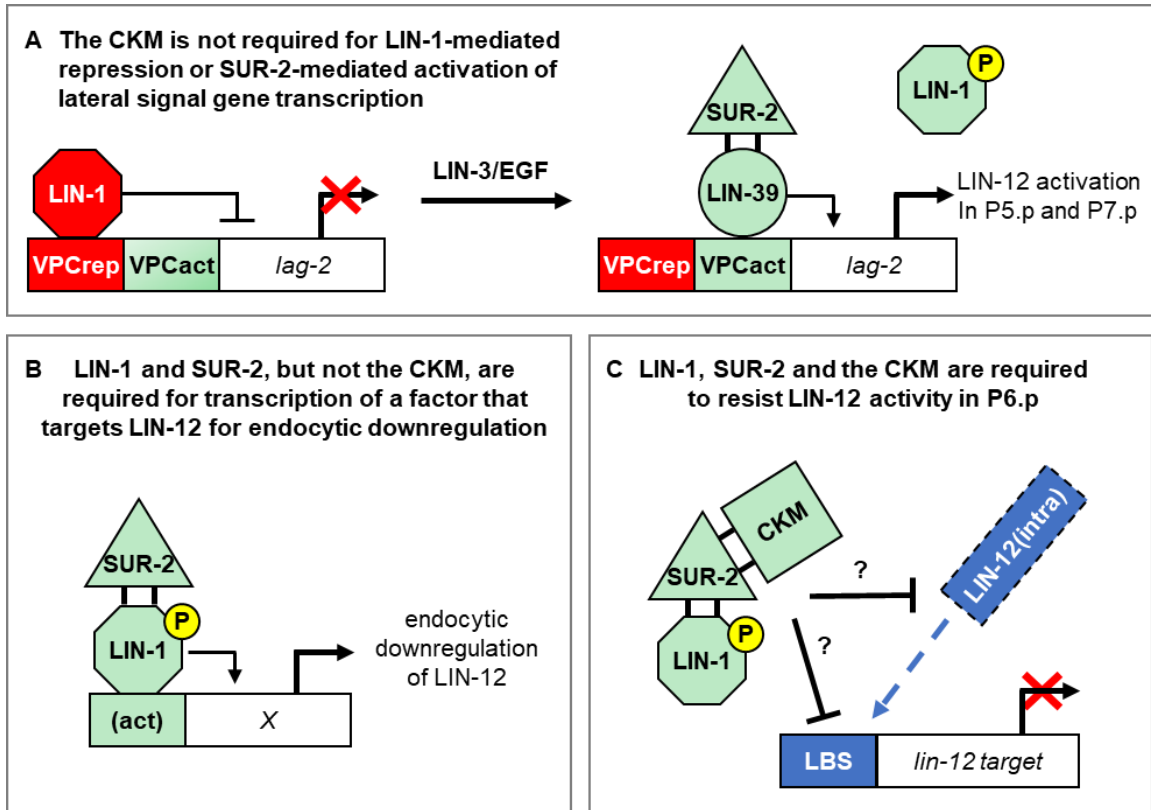


**Figure 5.** Loss of LIN-1 results in ectopic LIN-12 activity in all VPCS, and abrogates LIN-12-GFP endocytic downregulation in P6.p. (A) Photomicrograph of *arls116*[*Ist-5p::2xnl5-yfp*] expression in *lin-1(+)* (left) or *lin-1(n304)* (null, right). (B) Loss of LIN-1 results in ectopic expression of the LIN-12 target gene reporter *arls116*[*Ist-5p::2xnl5-yfp*] in all VPCs. Here and in C, the graph compares percentage of VPCs in *lin-1(+)* to *lin-1(0)* that express YFP. \*\* $P < 0.001$  and \*  $P < 0.016$  for *lin-1(+)* compared to *lin-1(0)* (Fisher's Exact Test). (C) Loss of LIN-1 results in ectopic expression of a different LIN-12 target gene reporter, *arls107*[*mir-61p::2xnl5-yfp*] in all VPCs. (D) Loss of LIN-1 does not cause precocious expression of *arls116*[*Ist-5p::2xnl5-yfp*]. Graph shows percentage of animals having more than one VPC expressing YFP. N.S. denotes not significant compared to

wild type (Fisher's exact test). (E) Photomicrograph of a *lin-12(n941); lin-1(n304); arls116[*lst-5p::2xnl5-yfp*]* hermaphrodite. Expression of YFP is not observed, indicating that ectopic expression of LIN-12 target reporters in *lin-1(0)* requires *lin-12* activity. Animals homozygous for both mutations were isolated from heterozygous strain of genotype *lin-12(n941)/qC1; lin-1(n304)/oxTi915; arls116[*lst-5p::2xnl5-yfp*]*. (F) Photomicrographs showing endocytic downregulation of LIN-12-GFP accumulation in the apical membrane of *lin-1(+)* hermaphrodite (left), and loss of downregulation in a *lin-1(0)* hermaphrodite (right). Each image is a maximum projection of a z-stack taken on a Zeiss spinning disk confocal system. Images were processed using FIJI/ImageJ (Schindelin *et al.* 2012; Schindelin *et al.* 2015). (G) Graphs show percentage of VPCs with GFP evident in the apical membrane of the genotypes shown in F: *pha-1; arEx1575[*lin-12-gfp*]* (left) and *pha-1; lin-1(n304); arEx1575[*lin-12-gfp*]* (right). \*\**P* < 0.001 for *lin-1(+)* compared to *lin-1(0)* (Fisher's Exact Test).



**Figure 6.** Resolution of cell fate in different genotypes. All strains contain *arls222[lag-2p::tagrfp]* and *arls116[Ist-5p::2xnl5-yfp]*, scored simultaneously on a per-VPC basis, except for *lin-1(0)*, which is based on the complete penetrance of *lag-2* expression in Zhang and Greenwald (2011) and data in Figure 5. Red, only the tagRFP marker was observed; blue, only YFP was observed; purple, both markers were observed; grey, neither marker was observed. (A) Typical expression pattern for wild-type hermaphrodites; refer to Figure 1B for images. (B) Typical expression pattern for *lin-1(n304)* hermaphrodites. (C) Chart depicting reporter expression on a per-VPC basis of *arTi31[(lin-31p::lin-45(AA, V627E))]; arls222[lag-2p::tagrfp]; arls116[Ist-5p::2xnl5-yfp]* hermaphrodites. (D) Photomicrograph of *arTi31[(lin-31p::lin-45(AA, V627E))]; arls222[lag-2p::tagrfp]; arls116[Ist-5p::2xnl5-yfp]*. Top, tagRFP channel; middle, YFP channel; bottom, images merged with DIC.



**Figure 7.** Summary and models for the roles of LIN-1, SUR-2, and the CKM in P6.p. Black lines connecting components are hypothetical protein-protein interactions based on known interactions in mammalian cells that are consistent with our genetic data, but more complex models in which the various components act in parallel are also possible. (A) Regulation of *lag-2* transcription in VPCs. We show herein that the CKM is not required for either repression of a *lag-2* reporter in uninduced VPCs or transcriptional activation in P6.p. Prior analysis of a cis-regulatory module in this reporter (Zhang and Greenwald 2011) suggested that LIN-3/EGF activation of EGFR-Ras-ERK leads to phosphorylation of LIN-1 and relief of repression of *lag-2* via VPCrep, allowing a Hox gene, likely LIN-39 (Niu *et al.* 2011), to promote its transcription via VPCact. SUR-2/Med23 is required for *lag-2* transcription even when VPCrep is deleted, consistent with SUR-2 acting in conjunction with LIN-39 to promote *lag-2* transcription through VPCact rather than functioning with LIN-1/Elk1 to promote repression through VPCrep. (B) Endocytic downregulation of LIN-12. We present results herein indicating that *lin-1*, but not the CKM, is required for endocytic downregulation of LIN-12 in P6.p. Since *sur-2* is also required for this process (Shaye and Greenwald 2002), and phosphorylated Elk1 interacts with Med23 in mammalian cells, we propose that a complex between LIN-1 and SUR-2 promotes expression of one or more target genes that promote endocytic downregulation of LIN-12. (C) Resistance to LIN-12 activity in P6.p. Our analysis suggests that P6.p is able to resist constitutively active LIN-12, and that overcoming this resistance by higher constitutive activity has deleterious consequences for the expression of *lag-2*. We also report that LIN-1, SUR-2 and the CKM are required for this resistance. Because all three components have the ability to form a complex in mammalian cells, we propose that they do so for this function. We envisage that resistance could be achieved if the complex acts directly to repress key LIN-12 target gene(s) or indirectly through transcription of a factor that opposes LIN-12 nuclear complex activity, assembly, or stability. We note that the 1 kb regulatory region present in the *arls116[lst-5p::2xnl5-yfp]* reporter does not contain a canonical Elk1 binding site, but there are numerous short GGA sequences that could in principle be Ets factor binding sites.



## **Chapter 2. Supplemental Material**

## Effect of *lin-1(gf)* on 2<sup>o</sup>-fate marker expression

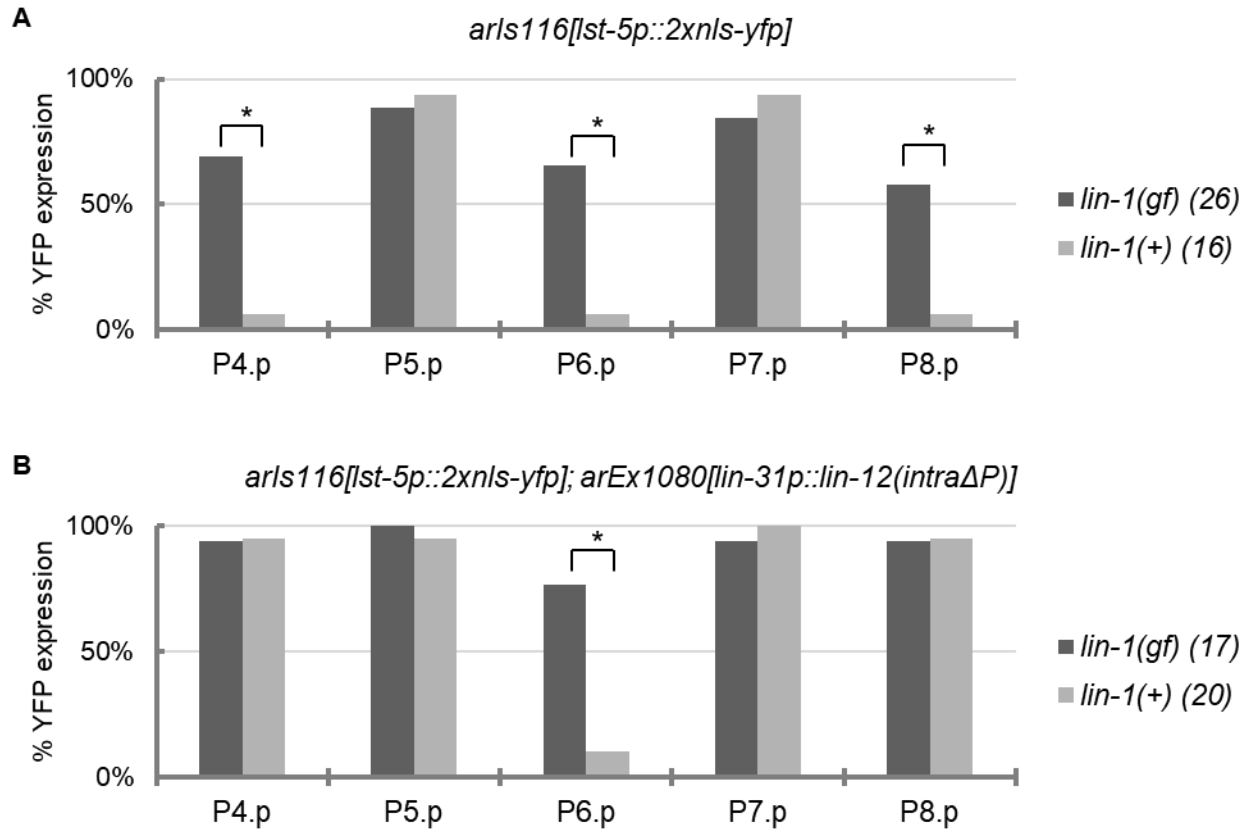
I found that loss of *lin-1* activity results in ectopic 2<sup>o</sup>-fate marker expression in all VPCs (Fig. 5 A-C). In an attempt to gain further insight into the role that LIN-1 was playing in VPC fate adoption, I looked at *arls116[lst-5p::2xnl5-yfp]* expression in a *lin-1* gain-of-function background.

The allele *lin-1(n1790)* contains an early-stop codon and is predicted to encode a mutant LIN-1 protein that lacks the C-terminal 90 amino acids (Jacobs et al 1998). The loss of an ERK docking site within this truncated C-terminal region is predicted to greatly reduce the efficiency of LIN-1 phosphorylation by ERK, a hypothesis supported by *in vitro* biochemical assays (Jacobs et al. 1998)(Jacobs et al. 1999). This suggested that the protein product of *lin-1(n1790)* would be unable to be efficiently phosphorylated by ERK, and thus remain in repressor-mode.

I observed that *arls116[lst-5p::2xnl5-yfp]* is ectopically expressed in all VPCs and their descendants in the *lin-1(n1790)* background (Fig. S1A), similar to the phenotype observed in a *lin-1* null background. Unsurprisingly, when activated LIN-12 is present via the transgene *arEx1080[lin-12(intraΔP)]* YFP expression is greatly elevated in P6.p and descendants compared to wild type (Fig. S1B). These findings are consistent with the hypothesis that LIN-1 activity is required for EGFR-mediated resistance to LIN-12/Notch activity and suggest a positive role for phosphorylated LIN-1 in 1<sup>o</sup>-fate adoption. However, we hypothesized in Chapter 2 that ectopic *arls116[lst-5p::2xnl5-yfp]* expression in a *lin-1* null background is due to VPC-wide derepression of *lag-2* causing ectopic LIN-12 activation. This contradicts the hypothesis that *lin-1(n1790)* produces a constitutively repressive form of LIN-1, which would be expected to inhibit *lag-2* transcription.

One explanation for this contradiction is that *lin-1(n1790)* is not a gain-of-function allele. There is evidence that *lin-1(n1790)* behaves as a loss-of-function mutant due to nonsense-mediated decay of *lin-1(n1790)* transcripts (Jacobs et al. 1998). Thus, I cannot rule out the possibility that the observations discussed here are the result of loss of *lin-1* function rather than a hypermorphic effect of *lin-1(n1790)*.

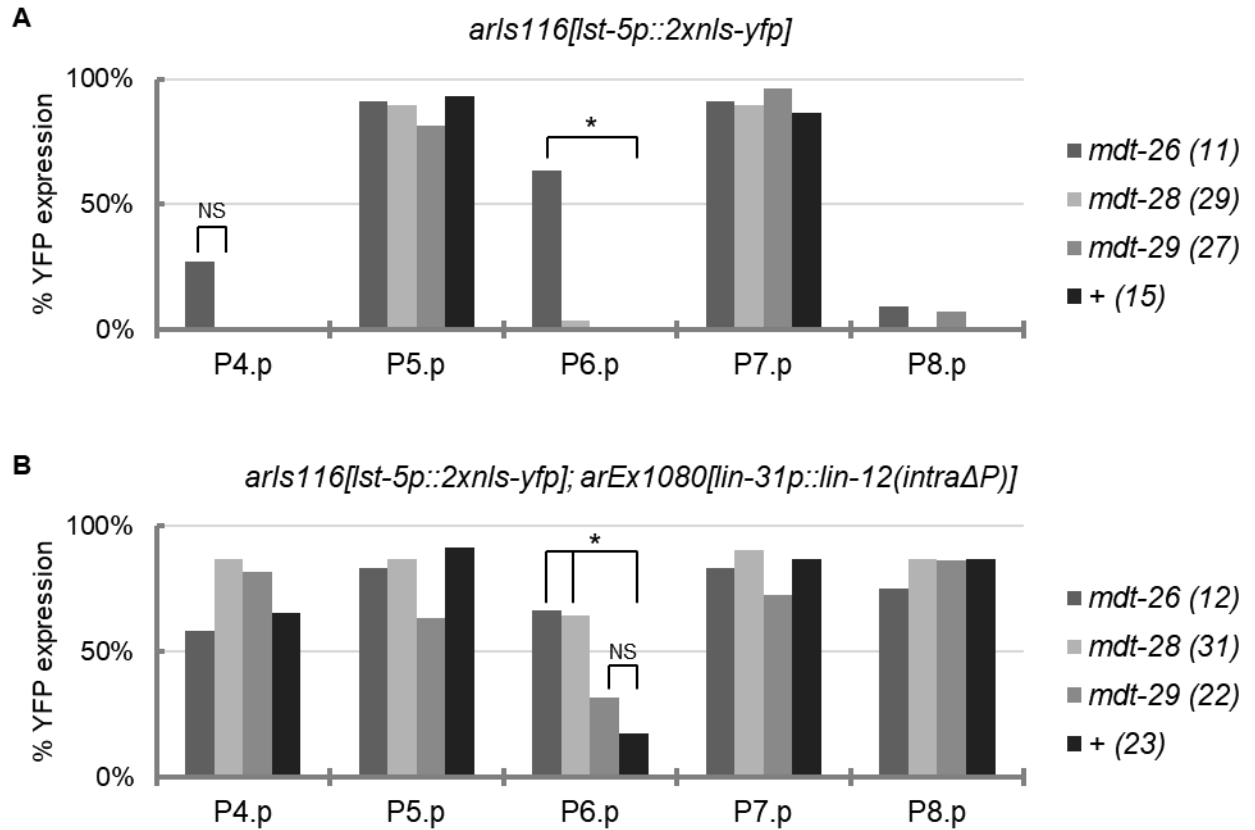
Although there are many experiments that could be done using the *lin-1(n1790)* allele, with the advent of CRISPR it is now possible to generate a “clean” gain-of-function allele which should avoid nonsense mediated decay. Using CRISPR, a researcher could precisely delete the region between the early stop codon present in *lin-1(n1790)* and the endogenous 3' UTR. Alternatively, CRISPR could be used to mutate or delete the FQFP docking site located near the C-terminus.



**Figure S1.** 2<sup>o</sup>-fate marker expression in putative *lin-1* gain-of-function background. A) Graph of YFP fluorescence from *arls116[lst-5p::2xnl5-yfp]* in VPCs and their descendants. (B) Graph of YFP fluorescence from *arls116[lst-5p::2xnl5-yfp]* in VPCs and their descendants in the presence of activated LIN-12. For both graphs, \* $P < 0.001$  and NS denotes “not significant” compared to *lin-1(+)* (Fisher’s exact test). *lin-1(gf)* corresponds to *lin-1(n1790)*.

## **Examination of requirement for additional Mediator components in EGFR-mediated resistance to LIN-12 activity**

I examined additional Mediator components for their requirement in EGFR-mediated resistance to LIN-12/Notch activity. The loss of the MDT-28 and MDT-29 did not impact expression of *arls116[*lst-5p::2xnl5-yfp*]* in an otherwise *wildtype* background, whereas the loss of the metazoan-specific regulatory module *mdt-26* resulted in ectopic YFP expression in P6.p specifically (Fig. S2A). When activated LIN-12/Notch is provide via *arEx1080[*lin-12(intraΔP)*]*, activity from *mdt-28*, but not *mdt-29*, is required for EGFR-mediated resistance to LIN-12 activity in P6.p (Fig. S2B). Although these results are intriguing, I ultimately decided not to explore them further due to time constraints and the inherent complexity of the Mediator complex.

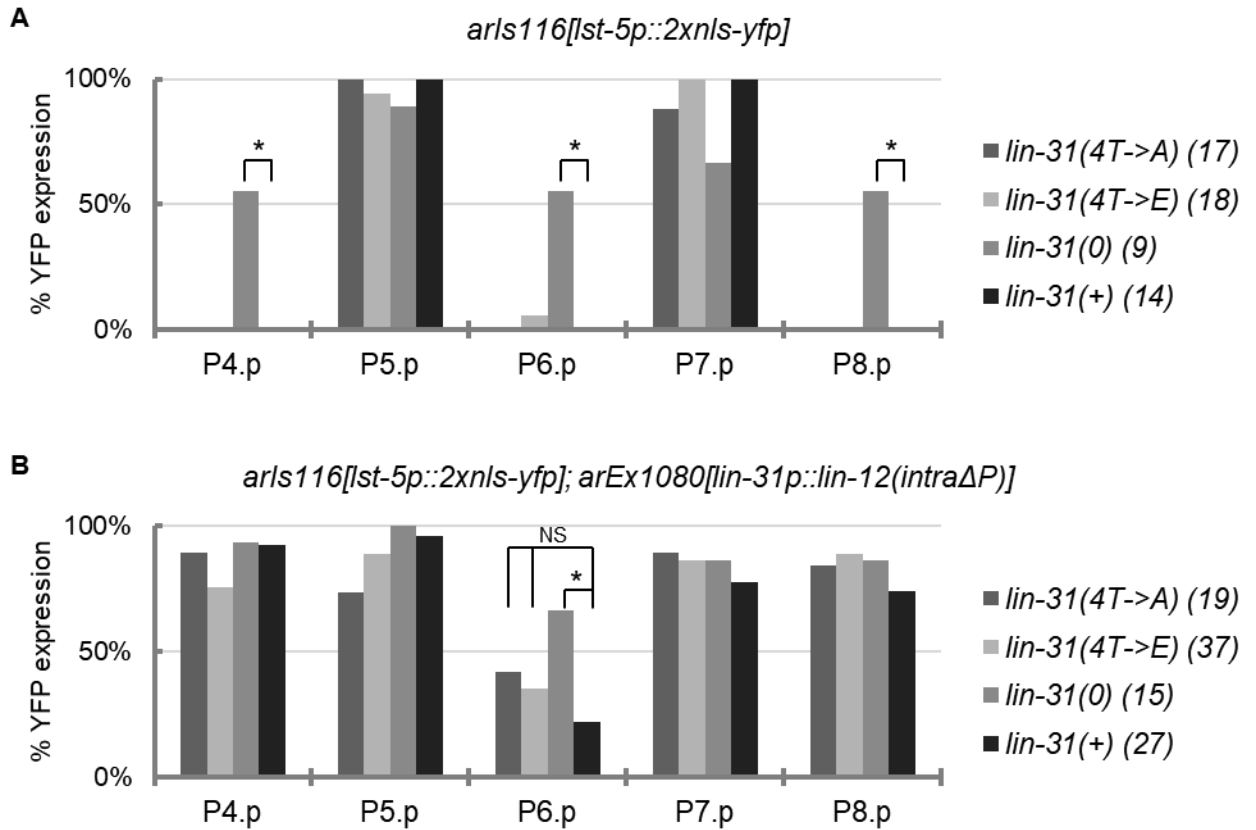


**Figure S2.** 2<sup>o</sup>-fate marker expression in Mediator component loss-of-function mutants. (A) Graph of YFP fluorescence from *arls116[lst-5p::2xnls-yfp]* in VPCs and their descendants. (B) Graph of YFP fluorescence from *arls116[lst-5p::2xnls-yfp]* in VPCs and their descendants in the presence of activated LIN-12. For both graphs, \* $P < 0.0075$  and NS denotes “not significant” compared to wild type (Fisher’s exact test). The following alleles were used: *mdt-26(tm6272)*, *mdt-28(tm1704)*, *mdt-29(tm2893)*. *mdt-26(tm6272)* animals were maintained using a derivative of *mIn1* containing a GFP marker; *mdt-26(tm6272)* homozygotes were selected by loss of GFP marker.

## Characterization of *lin-31* mutants on 2<sup>o</sup>-fate marker expression

*lin-31* encodes an HNF-3/*fork head* family transcription factor (Miller et al. 1993), and has been proposed to function as a repressor of vulval fate in complex with LIN-1 (Tan et al. 1998). When I examined *arls116[lst-5p::2xnl5-yfp]* expression in a *lin-31* null background, I observed ectopic expression in all VPCs (Fig. S3A). As expected, when activated LIN-12 is present via the transgene *arEx1080[lin-12(intraΔP)]* YFP expression is elevated in P6.p and descendants compared to *lin-31(+)* (Fig. S3B). Curiously, it was observed that loss of *lin-31* did not result in transcriptional derepression of *lag-2* in the VPCs (Zhang and Greenwald 2010). Thus, it is unclear what is causing the ectopic expression from *arEx1080[lin-12(intraΔP)]*. The priority to understanding this is to determine the requirement for *lin-12*, similar to Figure 5E.

Additionally, I investigated two CRISPR-engineered *lin-31* mutants. Four threonine residues in LIN-31, predicted to be phosphorylated by ERK (Tan et al. 1998), were targeted for mutagenesis. These were mutated to alanine in *lin-31(4T->A)* or glutamic acid in *lin-31(4T->E)* (Dickinson et al. 2013). These mutations were reported to cause abnormal vulval phenotypes in L4 and adult animals. I combined these alleles with *arls116[lst-5p::2xnl5-yfp]* and scored for YFP expression in VPCs. In the absence of activated LIN-12, *arls116[lst-5p::2xnl5-yfp]* expression was indistinguishable from *lin-31(+)* (Fig. S3A). When activated LIN-12 was added via the transgene *arEx1080[lin-12(intraΔP)]*, I observed no significant increase in YFP expression in P6.p and its descendants (Fig. S3B). It is difficult to draw conclusions from these experiments, and the role of *lin-31* in vulval development remains unresolved.



**Figure S3.** 2<sup>o</sup>-fate marker expression in *lin-31* mutant backgrounds. (A) Graph of YFP fluorescence from *arls116[lst-5p::2xnlis-yfp]* in VPCs and their descendants. (B) Graph of YFP fluorescence from *arls116[lst-5p::2xnlis-yfp]* in VPCs and their descendants in the presence of activated LIN-12. For both graphs, \* $P < 0.008$  and NS denotes “not significant” compared to *lin-31(+)* (Fisher’s exact test). *lin-31(4T->A)* corresponds to *lin-31(cp1)*; *lin-31(4T->E)* corresponds to *lin-31(cp3)*; *lin-31(0)* corresponds to *lin-31(n301)*.



## **Chapter 3. Characterization of expression and patterning of LAG-1**

## Abstract

LIN-12/Notch signaling is a conserved mechanism of cell-cell communication that mediates many cell-fate decisions. The conserved class of proteins known as CSL (CBF1/Su(H)/LAG-1) function to both activate and repress transcription of LIN-12/Notch target genes, and the regulation of CSL proteins, both transcriptionally and post-translationally, is important for normal specification of many cell types. Although LIN-12/Notch activity has been extensively studied in *C. elegans*, little is known about the expression and regulation of the CSL protein, LAG-1. Here I used CRISPR techniques to engineer endogenous, fluorescently-tagged LAG-1 fusion proteins and characterized their expression in the VPCs and during the AC/VU decision. I find that low levels of LAG-1 expression are independent of *lin-12* activity, and that LAG-1 accumulation increases later in development due to LIN-12/Notch activity. The characterization of LAG-1 I describe here is a to understanding the regulatory mechanisms of LAG-1 and what affect these mechanisms have on LIN-12/Notch activity in vulval induction and the AC/VU decision.

## Introduction

Notch signaling mediates the specification of many cell fates and normal development of many tissues [reviewed in Andersson *et al.* (2011)]. Abnormal activation of Notch has been attributed to a number of human diseases in various tissues (Mašek and Andersson 2017). For instance, in a majority of samples tested, genetic tests of T-cell acute lymphoblastic leukemia (T-ALL) samples revealed hyperactive mutations in Notch1 (Koch and Radtke 2011). Thus, understanding the regulation of Notch signaling and activation of Notch target genes is critical for understanding development and certain diseases.

The development of the *C. elegans* vulva is an exceptional paradigm to study the regulation of LIN-12/Notch signaling. Vulval development begins with six vulval precursor cells (VPCs), numbered P3.p-P8.p, are born during the L1 stage and made competent to adopt one of three fates. VPC fate specification begins during the L2 stage with the production of an epidermal growth factor (EGF)-like protein LIN-3 by the anchor cell (AC), termed the “inductive signal.”

EGF/LIN-3 ligand activates EGF receptor (EGFR)-Ras-ERK initiating a canonical Ras-Raf-ERK phosphorylation expressed in the nearest VPC, P6.p. Phosphorylation of downstream effector proteins by ERK in P6.p, such as the Elk-1 family protein LIN-1 (Beitel *et al.* 1995; Jacobs *et al.* 1998), results in adoption of 1° fate and transcriptional activation of LIN-12/Notch ligand genes (Chen and Greenwald 2004; Zhang and Greenwald 2011). The ligands comprise the “lateral signal” and activate LIN-12/Notch on the membranes of the neighboring cells, P5.p and P7.p, leading to transcription of *lin-12* target genes and adoption of the 2° fate. The remaining cells, P3.p, P4.p and P8.p, receive neither the inductive nor lateral signal and adopt the 3° fate [reviewed by Sternberg (2005)].

The precise spatial and temporal pattern of VPC specification requires the input and integration of several signaling pathways. During the L2 stage, the heterochronic gene *lin-14* was found to block constitutive *lin-12* activity, suggesting a mechanism to block premature LIN-12 activation (Li and Greenwald 2010). As described in Chapter 2, a characteristic of EGFR-Ras-ERK activation in VPCs is a mechanism that resists activity of constitutively activated LIN-12, including forms that resemble the activating mutations found in a subset of T-ALL (Greenwald and Seydoux 1990; Weng *et al.* 2004). The molecular mechanisms behind these forms of negative regulation to activated LIN-12 remain unknown.

The LIN-12/Notch receptor proteins are a single-pass transmembrane protein that functions as an extracellular receptor. Activation of Notch by a Delta/Serrate/LAG-2 (DSL) ligand results in two proteolytic cleavage events that release the Notch intracellular domain from the plasma membrane. The freed Notch intracellular domain is then translocated to the nucleus where it interacts with a member of the CBF1/Suppressor of Hairless/LAG-1 (CSL) class of transcription factors. The Notch-CSL complex associates with an accessory protein, SEL-8 in *C. elegans*, Mastermind in *Drosophila* and Mastermind-Like (MAML) in mammals, to form a ternary core transcriptional activation complex that recruits co-activators and promotes target gene expression [reviewed by Greenwald and Kovall (2013)].

The CSL class of DNA binding proteins are essential components of Notch signaling. Presence of the sole CSL protein LAG-1 is required for development in *C. elegans* (Lambie and Kimble 1991; Christensen *et al.* 1996), *Drosophila* (Schweisguth and Posakony 1992), and mammals (Oka *et al.* 1995) alike. In general, CSL proteins form repressor complexes with co-repressors in the absence of activated Notch, and upon translocation of the Notch intracellular domain to the nucleus, CSL proteins link the Notch intracellular domain to DNA and other co-activators to promote target gene expression. Several co-repressors have been identified in *Drosophila*, such as Hairless (Schweisguth and Posakony 1994), and in mammals, such as MINT/SHARP (Oswald *et al.* 2002; Kuroda *et al.* 2003) and Kyot2 (Taniguchi *et al.* 1998). A repressor function for LAG-1 has been described in the developing gland cells (Ghai and Gaudet 2008), and although *C. elegans* have orthologs of some of these co-repressors, currently no LAG-1-associated co-repressors has been identified.

CSL is the main effector of Notch-mediated cellular specification, and thus a focal point for regulation. The positive autoregulation of transcription factors is a widely utilized method of controlling and maintaining responses to signaling events [reviewed by Hobert (2011)], and the positive autoregulation of Su(H) has been shown to be required for formation of the socket cell in *Drosophila* (Liu and Posakony 2014). In *C. elegans*, LIN-12/Notch positively regulates itself during specification of the ventral uterine precursor cell (Wilkinson *et al.* 1994). Post-translational regulation and modifications of CSL proteins have been shown to be mechanisms to attenuate Notch signaling as well. In mammalian cells, the RBP-J interacting and tubulin associated (RITA) protein was shown to negatively regulate Notch1 activity by physically binding to RBP-J/CBF1 and exporting it from the nucleus (Wacker *et al.* 2011). In *Drosophila* cell culture, structural and biochemical studies suggest that Notch signal transduction may be reduced via the phosphorylation of Su(H) (Nagel *et al.* 2017), and indicated that Su(H) may be phosphorylated directly by mitogen activated protein kinase (MAPK) (Auer *et al.* 2015).

Here I characterize the expression of LAG-1 protein in the VPCs and during another LIN-12/Notch mediated fate-specification event, the AC/VU decision in the somatic gonad. Initial

experiments using fosmid-based translational reporters indicated that LAG-1 was present in P5.p, P6.p, and P7.p at equivalent levels; however, I later used CRISPR techniques to engineer endogenously-tagged *lag-1* alleles and found that accumulation of LAG-1 had a dynamic pattern VPCs and in the somatic gonad. I found that LAG-1 levels are established at a low basal level independent of *lin-12* activity, and that LAG-1 levels appeared to be elevated in cells known to have *lin-12* activity as development continues. Further analyses of LAG-1 levels in these cellular contexts in different genetic and transgenic backgrounds show that LAG-1 levels are increased in the presence of activated LIN-12.

## Materials and Methods

### C. elegans genetics

See Table S1 for complete strain information. All strains were raised according to standard practices at 20° (Brenner 1974). The following alleles were used in this section: LGI: *cdk-8(tm1238)*, *sur-2(ku9)*. LGIII: *lin-12(n137)*, *lin-12(n302)*, *lin-12(n941)*, *unc-119(ed3)*, *pha-1(e2123)*. LGIV: *lin-1(n304)*, *DnT1(IV:V)*, *lag-1(q418)*. LGV: *DnT1(IV:V)*, *sel-10(ok1632)*.

*DnT1* is modified version of the *nT1* translocation and contains a dominant *unc* mutation, *unc-?(n754)*, and an unknown recessive *let* allele.

The following transgenes were used: *oxTi414* (Frøkjær-Jensen et al. 2014) was used to mark the *lag-1* locus during crosses; *arTi22[hlh-2(prox)p::gfp-h2b]* (Michelle Attner), the *hlh-2(prox)* promoter is described in (Sallee and Greenwald 2015), *arTi43[lin-31p::lin-12(intra)]* and *arTi113[lin-31p::lin-12(intraΔP)]* (Deng 2016).

### mCherry-LAG-1 fosmid transgenesis

To make the *arEx1680* and *arEx1681* transgenes pRSU11 was linearized and injected into *pha-1(e2123)* animals at 15ng/uL with, pBX (*pha-1(+)*) at 1ng/uL, pCW2.1 (*ceh-22p::gfp*) at 1 ng/uL, and N2 genomic DNA linearized with PVUII at 50 ng/uL. Injected P0 animals were kept at 15° for 4 days and then shifted to 25°. F2 progeny were singled from P0 plates stable lines to generate

stable lines with a maximum of one array per injection plate to ensure independent arrays.

Animals were maintained at 25°.

### **LAG-1-GFP fosmid transgenesis**

To make the *arEx1893* and *arEx1894* transgenes, the LAG-1-GFP fosmid reporter from the TransgeneOme project (Sarov *et al.* 2012) was linearized and injected into *unc-119(ed3)* animals at 15ng/uL, with a *lin-44p::yfp* (Nikos-Hobert lab) at 3ng/uL, and sheared OP50 genomic DNA at 100ng/uL. Non-unc F1 animals were isolated, and those that produced non-unc F2 progeny were used to establish lines.

### ***lag-1(0)* rescue assay**

The *lag-1(q418)* allele was maintained over the balancer *DnT1* which contains a dominant *unc* allele. To score for rescue of the *lag-1(0)* larval lethal phenotype, array positive animals were placed on fresh plates and allowed to lay eggs for 24 hours. 2-3 days later, array-positive animals were assayed for Unc phenotype. Array-positive non-Unc animals were scored as “rescued”.

### **Plasmid construction**

pRSU11: mCherry-LAG-1 fosmid was constructed as described in (Tursun *et al.* 2009) using pBALU8 as PCR template and recombineering into the *lag-1*-containing fosmid WRM625aC01.

pRSU100: repair template for LAG-1-GFP was cloned into the pBS vector using sequential cloning steps. The final product was a repair template containing: *lag-1 5' homology::gfp::lag-1 3'UTR::reverse orientation[LoxP::rps-27p::hygr::unc-54 3'UTR::LoxP]::lag-1 3' homology*.

pRSU78: LAG-1-mKate2 repair template was made using Self-Excising Cassette (SEC) reagents and protocols described by (Dickinson *et al.* 2015). Homology arms of 656bp (5') and 616bp (3') were generated by PCR using pRSU100 as the template. The SEC plasmid pDD285 was digested with *SpeI* and *AvrII*. pRSU78 was generated from these reagents using HiFi Assembly Mix (NEB).

pRSU101: Contains *lag-1* targeting sequence: GATGGTGTCGTCTACTCGTC. Target sequence was identified by searching for sequences that conformed to the pattern: GN<sub>19</sub>NGG (Dickinson *et*

*al.* 2013; Kim *et al.* 2014), and were near the 3' end of the *lag-1*. A fusion PCR product containing the inserted target sequence was generated and restriction cloned into pDD162 using SpeI and NdeI.

pRSU82: Contains the *lag-1* targeting sequence: CGAGAGTGGGAATCTAGTAAT, which was designed using [crispr.mit.edu](http://crispr.mit.edu). The RF-Cloning web app (<http://www.rf-cloning.org/>) (Bond and Naus 2012) was used to generate the primers and the protocol was followed as described to introduce target sequence into the pU6::*unc-119* sgRNA vector described by Friedland *et al.* (2013)

### **CRISPR allele generation**

*lag-1::gfp*: To generate *lag-1(ar611[lag-1::gfp + loxP HygR loxP])*, N2 animals were injected with pRSU100 at 50 ng/μL, pRSU101 at 50 ng/μL along with pCCM935 50ng/μL, and pRF4 at 50 ng/μL. After 3-4 days plates were examined for twitching progeny. Plates positive for twitching progeny were assayed for insertion of GFP by scanning on a fluorescent compound microscope and confirmed using PCR (Kim *et al.* 2014).

*lag-1::mkate2*: To generate *lag-1(ar613[lag-1::mKate2])*, all plasmids were purified with midi-prep columns (Qiagen) or ethanol precipitation. N2 animals were injected with pRSU78 at 10 ng/μL, pRSU82 at 80 ng/μL, "P<sub>eft-3</sub>::Cas9-SV40 NLS::*tbb-2* 3'UTR" (Friedland *et al.* 2013) at 50ng/μL, p705(*dpy-7p::2xnl5-yfp*) at 10ng/μL, *rab-3p::yfp* plasmid (Hobert lab) at 5 ng/μL, and pCW2.1 (*ceh-22p::gfp*) at 10 ng/μL. Successful integrant was isolated and self-excising cassette removed according to protocol described by Dickinson *et al.* (2015).

### **Scoring fluorescent LAG-1 expression**

To score expression in the VPCs and AC/VU, approximately 20 gravid adult animals were placed on a fresh plate and allowed to lay eggs at 25°. To score VPC expression, adults were removed after 12 hours, and L3 progeny was scored approximately 36 hours later. To score AC/VU expression, egg laying was restricted to 2 hours and progeny were scored the following day. *lin-1(n304)* mutants were kept at 20° and synchronization via timed egg-lays was not attempted.

All animals were scored on Zeiss Axio Imager Z1 with a Hamamatsu Orca-ER camera and an X-Cite 120Q light source (EXFO photonics solutions) at 100% power. All images were processed using FIJI/ImageJ (Schindelin *et al.* 2012; Schindelin *et al.* 2015)

LAG-1-mKate2 fluorescence in VPCs was imaged at 40X with an 500ms exposure and camera set to 2x2 binning mode. GFP fluorescence from *arTi43* or *arTi113* was simultaneously imaged at 800ms. mKate2 fluorescence during the AC/VU decision was scored at 63X by taking a z-stack through the entire animal with 1  $\mu$ m step, an 800ms exposure and GFP fluorescence from *arTi22* was simultaneously imaged at 500ms exposure with the camera set to 2x2 binning mode. The *ar611(lag-1::gfp)* strain, LAG-1-GFP was scored at 40x with camera set to 1x1 with exposure time of 800ms. LAG-1-GFP from *arEx1893* and *arEx1894* transgenes were scored at 40x with camera set to 1x1 with exposure time of 500ms.

## Results

### **An N-terminally tagged LAG-1-mCherry translational fosmid reporter rescued *lag-1(0)* lethality, but did not produce visible expression**

During the L2 stage, the heterochronic gene *lin-14* blocks expression of LIN-12 target gene reporters in the presence of constitutively active *lin-12* (Li and Greenwald 2010). A similar phenomenon occurs during the L3 in 1<sup>o</sup> VPCs due to EGFR activation (Shaye and Greenwald 2005)(Chapter 2). An early hypothesis was that negative regulation of LIN-12 by was achieved downregulation of LAG-1 or sequestering LAG-1 from the nucleus.

Before the development of CRISPR based gene-editing techniques for *C. elegans*, fosmid-based reporters were the gold-standard due to the relatively large amount of genomic context, *i.e.* regulatory information, they provided compared to alternative methods of reporter construction. Additional benefits were the existence of a fosmid library that covered a majority of *C. elegans* genes ([wormbase](#)), and the development of protocols and reagents that allowed for fast and efficient generation of fluorescent gene reporters (Tursun *et al.* 2009; Sarov *et al.* 2012).



To analyze the expression of LAG-1 in the VPCs, I made an N-terminal mCherry-LAG-1 translational fusion reporter by recombineering the coding sequence for mCherry in-frame immediately following the start codon of *lag-1* (Fig. 2B). I generated two independent extrachromosomal transgenic arrays and observed dim fluorescence in random VPCs at a low penetrance. This observation, along with occasional dim fluorescence in some head neurons, indicated that mCherry-LAG-1 was possibly being expressed at low levels below my detection limit. Antibody staining did not increase the visibility of mCherry-LAG-1 in the VPCs. I used an antibody which recognizes the apical junction marker, AJM-1, to identify VPCs and serve as a positive control (Koppen *et al.* 2001; Shaye and Greenwald 2005). I combined these arrays with the null allele, *lag-1(q418)*, to determine if these reporters could rescue LAG-1 function. Null alleles of *lag-1* are sterile and *lag-1(0)* segregants from heterozygous mothers typically arrest during the L1 larval stage (Christensen *et al.* 1996). I found that both arrays provided some rescue of the L1 lethality of *lag-1(0)* homozygotes (Fig. 2C), indicating that these fosmid arrays produced functional LAG-1 protein.

Fluorescent expression data obtained from these transgenes were therefore not useful for determining regulation or patterning of LAG-1. Two possible explanations for these results are that mCherry-LAG-1 may not be stable in the VPCs or a transgenic artifact. A more recent suggestion is the prediction of an additional LAG-1 isoform. These possibilities were not investigated further.

### **C-terminally tagged LAG-1-GFP translational fosmid reporters were visible and not patterned during VPC specification**

I used an available C-terminally tagged GFP-fusion fosmid reporter (Sarov *et al.* 2012) to generate two independent extrachromosomal transgenic arrays. I observed LAG-1-GFP levels to be generally equivalent and nuclear in P5.p, P6.p, and P7.p, and in the descendants of these VPCs (Fig. 3B-C). As described below, I later determined this result to be a transgenic artifact (Fig. 3B, D); however, this observation led me to assume that regulation of LAG-1 levels or subcellular localization was not a likely mechanism for resistance to LIN-12 activation in P6.p and

to pursue alternative hypotheses, which are addressed in Chapter 4. Additionally, this result highlights a potential pitfall of multi-copy arrays and will be discussed in more detail later.

### **Endogenous CRISPR-engineered translational reporters of LAG-1 display a dynamic expression pattern in the VPCs**

CRISPR-Cas9 allows for precise editing of the *C. elegans* genome by taking advantage of homologous recombination machinery [reviewed by Dickinson and Goldstein (2016)]. This method provides a number of advantages compared to older transgenic-based reporters, including: endogenous regulation, minimal disruption of the genome compared to irradiation-based integration methods, and does not use multi-copy arrays, which can vary in copy number and be silenced due to their repetitive nature over time.

I used CRISPR techniques to engineer the insertion of the coding sequences of two different fluorescent proteins in-frame at the C-terminus of the endogenous *lag-1* locus. Both alleles produced visible fluorescence and had a similar dynamic expression pattern in the VPCs (Fig. 3B, 3D, 4A). In otherwise *wild-type* L2 animals, I saw LAG-1-mKate2 or LAG-1-GFP accumulation in all the VPCs. When compared on a VPC-by-VPC basis, these levels appeared to be equivalent, and I could not qualitatively identify a pattern at this stage. These levels remained constant and uniform in the VPCs until approximately the L2 molt. At approximately the beginning of the L3 stage, I observed that accumulation of LAG-1-GFP or LAG-1-mKate2 in P5.p and P7.p was higher in comparison to the other VPCs, and appeared to rise relative to the starting level prior to that time. This pattern was most pronounced after the first division of the VPCs and was maintained into the Pn.pxx stage. My qualitative assessment could not determine whether LAG-1 levels in P3.p, P4.p, P6.p, or P8.p had risen compared to their levels during the L2 stage, nor could I determine whether LAG-1 levels in P5.p and P7.p had continued to rise or had plateaued.

The observation that tagged LAG-1 fluorescence is higher in 2° VPCs compared to 1° and 3° VPCs is reminiscent of the pattern of 2°-fate adoption in the VPCs due to *lin-12* activity. I consider these observations to strongly suggest that *lin-12* activity positively regulates LAG-1 in

2° VPCs. This positive regulation could be direct or indirect, and if it were direct, then this might indicate the positive autoregulation of *lag-1* transcription. Another possibility is that LAG-1 may be negatively regulated in non-2°-fate cells, possibly via protein degradation although other modes of regulation are possible.

To explore these possibilities, I generated several strains containing *lag-1::mkate2* to examine the effect that removing or enhancing *lin-12* activity had on LAG-1-mKate2 levels. I imaged animals using similar setting, including exposure times, to allow me to compare the relative brightness of mKate2 fluorescence from animal to animal.

### **LAG-1-mKate2 levels and patterning in the VPCs are dependent on *lin-12* signaling**

If the elevated levels of fluorescently tagged LAG-1 seen in P5.p and P7.p are dependent on *lin-12* activity, then loss of *lin-12* should result in reduced LAG-1-mKate2 levels in all VPCs and loss of a LAG-1-mKate2 pattern. Similarly, providing constitutively activate LIN-12, either genetically or via transgene, would be expected to result in increased LAG-1-mKate2 levels in all VPCs, and again result in the loss of a LAG-1-mKate2 pattern.

I first assayed LAG-1-mKate2 accumulation in two backgrounds that abrogate *lin-12* activity in the VPCs. In hermaphrodites of a *lin-12(0)* background VPCs do not adopt the 2° fate (Greenwald *et al.* 1983a). I combined *lag-1::mkate2* with *lin-12(n941)*, a null allele. During the L2 stage, I observed that LAG-1-mKate2 was present in all VPCs at levels similar to those seen in *wild-type* L2 animals. During the L3 stage, LAG-1-mKate2 levels did not become elevated in P5.p or P7.p or their descendants during compared to the other VPCs. Instead, LAG-1-mKate2 levels appeared to remain constant in all VPCs relative to their starting levels (Fig. 5A). This result supports the idea that LAG-1 levels in the VPCs are dependent on *lin-12* activity; however, hermaphrodites lacking *lin-12* produce two anchor cells and result in additional induction of the 1° fate which could affect *lag-1* expression.

To test this possibility, I used a mutant that produces a normal AC, but fails to activate LIN-12 in the VPCs. *sur-2* is the *C. elegans* ortholog of the Mediator component Med23 and is required in P6.p for transcriptional activation of *lin-12* ligand (Zhang and Greenwald 2011). *sur-*

2(0) hermaphrodites develop an anchor cell and P6.p receives the inductive signal like normal; however, LIN-12 is not activated in P5.p and P7.p due to loss of the lateral signal (Singh and Han 1995). I combined *lag-1::mkate2* with *sur-2(ku9)*, a null allele, and examined LAG-1-mKate2 levels in the VPCs. Again, during the L2 stage, LAG-1-mKate2 levels were uniform in all VPCs at levels roughly equivalent to *wild-type* L2 VPCs. During the L3 stage, LAG-1-mKate2 levels remained uniform at levels similar to their starting levels (Fig. 5A), consistent with the prediction that LAG-1 is positively regulated by LIN-12 activity.

### **Strong constitutive LIN-12 activity elevates LAG-1-mKate levels in all VPCs**

I next investigated the effect that enhancement of *lin-12* activity had on LAG-1-mKate2 levels in the VPCs. Many mutations that cause ligand-independent activation have been characterized and are collectively known as *lin-12(d)* alleles (Greenwald *et al.* 1983a; Seydoux *et al.* 1990). While all *lin-12(d)* alleles fail to produce an anchor cell, they generally can be categorized into two classes based on their vulval phenotype, “strong” and “weak”. A strong *lin-12(d)* allele cause VPCs to adopt the 2° fate, and adult hermaphrodites develop a Multivulva phenotype; a weak *lin-12(d)* allele fails to induce 2° fate in VPCs, and adult hermaphrodites are Vulvaless. I used the strong *lin-12(d)* allele, *lin-12(n137)*, to observe the effect that strong constitutively-activated LIN-12 had on LAG-1-mKate2 levels. During the L2 stage, I observed LAG-1-mKate2 levels to be uniform in all VPCs at approximately the same level as *wild-type* L2 hermaphrodites. LAG-1-mKate2 levels then increased during the L3 in all VPCs in a uniform manner (Fig. 5B), consistent with LAG-1 being positively regulated in 2° VPCs by constitutive *lin-12* activity. The uniform level of LAG-1-mKate2 in all of the VPCs seemed similar to the levels of LAG-1-mKate2 in P5.p and P7.p in *wild-type* animals.

Because *lin-12(d)* hermaphrodites lack anchor cells, I combined *lag-1::mkate2* with a transgene that expresses constitutively activated LIN-12 in a VPC specific manner to investigate LAG-1-mKate2 levels in hermaphrodites that still receive the inductive signal. *arTi113[lin-31p::lin-12(intraΔP)-gfp]* is a single-copy array that uses regulatory sequences from the *lin-31* gene to specifically express in the VPCs (Tan *et al.* 1998). Expression of the intracellular domain of LIN-

12 [LIN-12(intra)] mimics the activation of LIN-12 (Struhl *et al.* 1993). LIN-12(intra $\Delta$ P) is a further truncation of the protein and removes a region containing a Cdc4 phosphodegron (CPD), resulting in a stable and highly active form of LIN-12 (Li and Greenwald 2010; de la Cova and Greenwald 2012; Deng and Greenwald 2016). When combined with *lag-1::mkate2*, I observed that accumulation of LAG-1-mKate2 was uniform in all VPCs during the L2 stage at levels comparable to *wild-type* L2 hermaphrodites. LAG-1-mKate2 levels then rose in all VPC uniformly as development continued during the L3 stage (Fig. 5B). Again, the elevated levels of LAG-1-mKate2 seen in all VPCs was comparable to the levels seen in P5.p and P7.p of *wild-type* L3 animals. These observations are consistent with the those made using *lin-12(n137)*, and suggests that EGFR activation in P6.p does not result in lower accumulation of LAG-1-mKate2. However, as discussed in Chapter 2, high levels of LIN-12 activity in P6.p can inhibit certain 1<sup>o</sup> characteristics, and therefore this result does not rule out the possibility that EGFR activation may negatively regulate levels of LAG-1.

In sum, these observations suggest that prior to vulval induction, LAG-1 is present in all VPCs at a low basal level and that *lin-12* is not required to establish this initial baseline. It appears that the presence of activated LIN-12 during the L2 does not result in increased LAG-1 accumulation. This would be consistent with previous observations of a block to constitutive *lin-12* activity, mediated by *lin-14*, during the L2 stage. During the L3, the presence of LIN-12 activity results in an accumulation of LAG-1 uniformly in all VPCs to a level comparable to that of P5.p and P7.p in *wild-type* L3 animals. The experiments performed, however, did not allow me to separate LIN-12 activity from 2<sup>o</sup>-fate adoption, and it remains possible that LAG-1 is degraded in non-2<sup>o</sup>. I attempt to address this in the following sections by examining if removal of negative regulators, or the presence of weaker forms of constitutively active LIN-12 affect accumulation of LAG-1.

### **LAG-1-mKate2 levels are not affected by removal of *sel-10* or *cdk-8***

Removing negative regulators of *lin-12* could potentially affect LAG-1 accumulation in two different ways. Their removal may directly stabilize LAG-1 or may result in higher observed LAG-1 levels due to mild enhancement of increased *lin-12* activity.

The Fbw7 ortholog SEL-10 targets the LIN-12 intracellular domain for ubiquitination and eventual degradation by the proteasome (Sundaram and Greenwald 1993; Hubbard *et al.* 1997), and there is evidence to suggest that formation of the nuclear complex with LAG-1 is required for this process (Deng and Greenwald 2016). Null mutants of *sel-10* are viable, and hermaphrodites that lack *sel-10*, but are otherwise wild type, generally produce a normal vulva. When I assayed *lag-1::mkate2* in a *sel-10(0)* background, I did not observe a significant change in LAG-1-mKate2 levels compared to wild type during any stage.

In mammalian cells, the mediator-associated kinase Cdk8 phosphorylates the intracellular domain of Notch to promote targeting by Fbw7 (Fryer *et al.* 2004). While phosphorylation of LIN-12 by the ortholog CDK-8 has not been demonstrated in *C. elegans*, it has been shown that CDK-8 negatively regulates *lin-12* in the VPCs (Chapter 2). Hermaphrodites that are homozygous for a null allele of *cdk-8* are viable and generally produce a normal vulva. The absence of CDK-8 did not result in a change of LAG-1-mKate2 accumulation compared to wild type in any stage. These results suggest that LAG-1 is not negatively regulated by either of these proteins, although there may be factors that work redundantly with SEL-10 or CDK-8. These observations show that a mild enhancement of *lin-12* activity due to removal of *sel-10* or *cdk-8* is not sufficient to effect LAG-1-mKate2 accumulation.

### **Weak forms of constitutively active LIN-12 influence LAG-1 accumulation**

As described above, strong constitutive LIN-12 activity elevates LAG-1-mKate2 levels in all VPCs and causes all VPCs to adopt the 2° fate. I attempted to analyze LAG-1-mKate2 levels in backgrounds that have constitutive LIN-12 activity, but do not induce the VPCs to adopt 2° fate.

The weak *lin-12(d)* activity from *lin-12(n302)* is sufficient to produce a cell-fate change in the somatic gonad, resulting in a 0 AC phenotype based on lineage analysis and a failure to

induce a vulva (Greenwald *et al.* 1983a). *lin-12(n302)* activity is not sufficient, however, to cause formation of pseudovulvae (Greenwald *et al.* 1983a) or to activate expression of a 2<sup>o</sup>-fate reporter (Chapter 2) in the VPCs. By these criteria I viewed VPCs to remain uninduced in *lin-12(n302)* animals, thus I predicted that LAG-1-mKate2 levels would remain uniform in the VPCs at low levels, similar to my previous observations of uninduced VPCs in a *lin-12(0)* or *sur-2(0)* background. However, my examination suggests that *lin-12(n302)* is active in the VPCs during the L3 stage. Many animals I examined appeared to have uniformly higher LAG-1-mKate2 levels in all VPCs relative to their prior levels or to uninduced VPCs of *lin-12(0)*, consistent with constitutive activation of *lin-12* in all VPCs (Fig. 6A). Contrary to a strong *lin-12(d)* background, this was seen in a much lower percentage of L3 animals (11/29 for *lin-12(n302)*) versus (25/28 for *lin-12(n137)*). In addition to penetrance, the increase of LAG-1-mKate2 accumulation generally appeared to be less than what was observed in the strong *lin-12(d)*; however, a more quantitative measurement of fluorescence is required to accurately make this comparison.

I observed a subset of *lin-12(n302); lag-1::mkate2* animals that appeared to have *wild-type* VPC pattern based on LAG-1-mKate2 fluorescence in adjacent VPCs. Similar to the pattern seen in *wild-type* L3 animals, LAG-1-mKate2 accumulation was higher in P5.p and P7.p relative to the other VPCs in small number (3/14) of Pn.p-staged animals. The penetrance of this pattern increased following the first round of VPC divisions, during the Pn.px and Pn.pxx stages, where I observed this pattern in (8/14) animals (Fig. 6A). These observations suggest that LAG-1-mKate2 levels are sensitive to the weak constitutive activation of *lin-12(n302)* in VPCs, as well as a few other implications discussed further below.

Providing LIN-12(intra)-GFP via a transgene does not produce a Multivulva phenotype nor visible GFP fluorescence as it is efficiently turned over in the VPCs (de la Cova and Greenwald 2012; Deng and Greenwald 2016). I used the single-copy *arTi43[lin-31p::lin-12(intra)-gfp]* to further test the effect that weak constitutive LIN-12 activity has on LAG-1-mKate2 accumulation. Loss of *sel-10* in hermaphrodites carrying *arTi43[lin-31p::lin-12(intra)-gfp]* leads to a Multivulva phenotype similar to *arTi113[lin-31p::lin-12(intra $\Delta$ P)-gfp]*.

I simultaneously assessed *arTi43[lin-31p::lin-12(intra)-gfp]; lag-1::mkate2* animals for mKate2 and GFP fluorescence. GFP fluorescence was only rarely visible in the VPCs, indicating that LIN-12(intra)-GFP was being degraded as expected. When I analyzed mKate2 fluorescence in Pn.p-staged animals, LAG-1-mKate2 accumulation was uniform in all VPCs. These LAG-1-mKate2 levels were higher than the levels seen in non-2° VPCs of *wild-type* Pn.p-staged animals. I observed this pattern in (17/17) animals (Fig. 6B), whereas in *wild-type* Pn.p-staged animals, no animal had similarly uniform elevated LAG-1-mKate2, and (14/21) had the wild-type-like 2°-fate pattern. Following the first VPC division, the LAG-1-mKate2 accumulation in the presence of LIN-12(intra)-GFP returned to being elevated in 2° VPCs, and was observed to be higher in daughters and granddaughters of P5.p and P7.p in 15/17 animals (Fig. 6B).

I stabilized LIN-12(intra)-GFP combining *sel-10(0)* with *arTi43[lin-31p::lin-12(intra)-gfp]; lag-1::mkate2*. LAG-1-mKate2 accumulation was seen to be elevated in all VPCs, as well as VPC daughters and granddaughters, similar to my observations of LAG-1-mKate2 using the *arTi113[lin-31p::lin-12(intraΔP)-gfp]* transgene.

It is possible that an interaction between GFP and mKate2 led to artificially high levels of LAG-1-mKate2 in all VPCs. This explanation seems unlikely because such an interaction should stabilize LIN-12(intra)-GFP as well, which was not observed by GFP fluorescence.

In sum, I combined *lag-1::mkate2* into two different backgrounds that produce constitutive weak LIN-12 activity in the VPCs. Neither of these forms are known to ectopically induce 2° fate by our typical criteria, *i.e.* cell lineage, Multivulva phenotype, or transgenic 2°-fate reporters. The levels of LAG-1-mKate2 accumulation that I observed in these two backgrounds, however, are consistent with ectopic LIN-12 activity. These results suggest that LAG-1 levels are elevated even due to weak LIN-12 activity.

### **LAG-1-mKate2 is regulated in a *lin-12* dependent manner during the AC/VU decision**

The AC/VU decision provides another paradigm in *C. elegans* to study *lin-12* and its role in fate specification. The somatic cells Z1.pp and Z4.aa divide during the L1 stage to produce two pairs of sister cells. The proximal members of each pair, Z1.ppp and Z4.aaa, termed “α cells”, are



equally competent to adopt either the anchor cell (AC) fate or the ventral uterine precursor cell (VU) fate (Kimble and Hirsh 1979). In one of the few variable cell-fate decisions in *C. elegans*, these cells adopt fates in a stochastic manner, such that in *wild-type* hermaphrodites 50% of the time Z1.ppp becomes the AC, and 50% of the time Z4.aaa will become the AC. VU fate is due to cell-autonomous *lin-12* activity (Seydoux and Greenwald 1989), and in *lin-12(0)* animals, both cells adopt the AC fate (Greenwald *et al.* 1983a). Both  $\alpha$  cells initially express *lin-12*, and a positive feedback loop leads to an increase of *lin-12* expression in the presumptive VU (Wilkinson *et al.* 1994) (Fig. 7A) and *lin-12* expression is reduced in the presumptive AC by an unknown mechanism. The distal cells, Z1.ppa and Z4.aap, termed “ $\beta$  cells”, are born with the potential to adopt the AC fate or the VU fate. In *wild-type* development, this competence is lost sooner than the  $\alpha$  cells and they adopt the VU fate in a *lin-12* independent manner (Seydoux *et al.* 1990).

To mark the  $\alpha$  and  $\beta$  cells in the somatic gonad, I used the transcriptional reporter *arTi22[hlh-2(prox)p::gfp-h2b]*, and used Nomarski microscopy to identify the presumptive AC by morphology. Expression of this reporter begins in Z1.pp and Z4.aa, the two parental cells, and remains restricted to the four  $\alpha$  and  $\beta$  cells through fate specification into the L3 stage (Fig. 7B).

The observations described above suggest that LAG-1 levels are increased in cells with *lin-12* activity, thus, if LAG-1 is similarly regulated in the  $\alpha$  and  $\beta$  cells during the AC/VU decision, I expect to see LAG-1-mKate2 levels elevate in the  $\alpha$  VU. This may not be true in the  $\beta$  VUs, since this cell-fate decision is largely independent of *lin-12* activity, although LIN-12 is present in these cells (Wilkinson *et al.* 1994; Levitan and Greenwald 1998b), and in *lin-12(0)*, a  $\beta$  cell becomes an AC at low-penetrance (Greenwald *et al.* 1983a; Seydoux and Greenwald 1989; Sallee *et al.* 2015). I examined LAG-1-mKate2 accumulation in the somatic gonad of hermaphrodites carrying the *arTi22[hlh-2(prox)p::gfp-h2b]* transgene. LAG-1-mKate2 was not present at detectable levels in Z1.pp and Z4.aa. Following division of Z1.pp and Z4.aa, but before AC specification, I observed a mix of patterns LAG-1-mKate accumulation. In (2/10) animals LAG-1-mKate2 was not detectable in any cell; in (4/10) animals LAG-1-mKate2 was present at low levels in three cells and higher in one cell; and in (4/10) animals LAG-1-mKate2 was elevated

and equivalent in all four cells (Fig. 7C). Following specification of the AC, LAG-1-mKate2 was clearly patterned, and levels in the three VUs were higher than the presumptive AC in (10/10) hermaphrodites (Fig. 7D). These results suggest that LAG-1 is positively regulated by *lin-12* activity during the AC/VU decision.

I combined *lag-1::mkate2; arTi22[hlh-2(prox)p::gfp-h2b]* with the null allele *lin-12(n941)*. The two  $\alpha$  cells both adopt the AC fate, and LAG-1-mKate2 levels were low, as expected to be low in these cells. The  $\beta$  cells usually adopt the VU fate even in the absence of *lin-12*; in these cells, LAG-1-mKate2 levels were also low. This observation suggests that elevated levels of LAG-1-mKate2 is not an aspect of VU fate specification but is dependent on *lin-12* activity.

In sum, these results suggest that LAG-1 accumulation increases due to *lin-12* activity in the somatic gonad, similar to what I observed in the VPCs. Although not detectable by fluorescence, I would predict that LAG-1-mKate2 is present at a low basal level in Z1.pp and Z4.aa to prevent ectopic activation of *lin-12* target genes and potentially to promote transcription following LIN-12 activation, but I cannot exclude the possibility that LAG-1 entirely absent in these cells. Following division of Z1.pp and Z4.aa, LAG-1 levels increase in all cells until becoming uniform in the  $\alpha$  and  $\beta$  cells. LIN-12 activation in the presumptive VUs promotes maintenance of LAG-1 levels and possibly increases LAG-1 accumulation, although my analysis was insufficient to determine between these possibilities. The presumptive AC which lacks *lin-12* activity and LAG-1 levels are dramatically reduced in this cell.

## Discussion

The CSL family of proteins are core components of the Notch signaling pathway. Generally, CSL proteins function as a transcriptional repressor in the absence of Notch signaling, and as a transcriptional activator in the presence of Notch signaling. In *Drosophila* and mammals, regulation of CSL protein levels or subcellular localization have been shown to affect the transcriptional response to Notch activation (Barolo *et al.* 2000; Wacker *et al.* 2011; Liu and

Posakony 2014). Little has been described about the regulation of the *C. elegans* CSL protein, LAG-1. Here, I investigated the regulation of LAG-1 during VPC specification and the AC/VU decision. My characterization of endogenously tagged LAG-1 suggest that LAG-1 is initially present in these cells at a low basal level prior to specification, and activation of LIN-12 produces an increase of LAG-1 accumulation; the nature of this regulation, e.g. transcriptional or post-translational, remains unknown.

### **Implications of LAG-1 fosmid reporter results**

I used two different fosmid-based translational reporters to determine the pattern of LAG-1 in the VPCs. I observed only rare expression from the *mcherry-lag-1* reporter, and I observed LAG-1-GFP fluorescence from the C-terminal GFP-tagged fosmid reporter at roughly equivalent levels in P5.p, P6.p, and P7.p and their descendants. These results were later contradicted by the dynamic pattern of GFP fluorescence in the *lag-1::gfp* CRISPR knock-in.

The low levels of fluorescence from the N-terminal mCherry fosmid reporter has many possible explanations, some of which are discussed further below. An intriguing possibility emerged when the *lag-1* gene structure was updated, and a new isoform was identified. The *mcherry* sequence was inserted immediately upstream of the *lag-1a* isoform (Fig. 2A), and this led to the formation of several hypotheses. This is discussed in further detail in Chapter 5. Another possibility though is that, in general, N-terminally tagged forms of LAG-1 are not stable in the VPCs, unlike C-terminally tagged LAG-1.

The C-terminal GFP tag in both the fosmid reporter and the CRISPR knock-in are predicted to be identical, and therefore are not likely sources of the discrepancies. I based the *lag-1::gfp* knock-in template on the fosmid reporter sequence, and the two changes I introduced to the nucleotide sequence are not expected to affect the primary sequence of the LAG-1-GFP fusion protein product, and thus, are not likely to be the source of the discrepancy. First, I introduced a silent mutation in the final exon of the *lag-1::gfp* repair template to prevent endonuclease activity from Cas9, and this mutation exists in *lag-1::mkate2* as well. While the possibility that this alternative codon led to a dramatic difference of observed LAG-1 levels is

hypothetically possible, there are more likely explanations. The second alteration to the *lag-1::gfp* repair template was the inclusion of a large Hygromycin selection cassette immediately downstream of the predicted *lag-1* 3' UTR. This was initially a cause for concern; however, *lag-1::mkate2* does not contain such a cassette, and the fact that the fluorescence pattern observed in both strains is in general agreement suggests that the presence of this Hygromycin resistance cassette does not affect the patterning of LAG-1-GFP. This was only carefully examined in the VPCs and expression of *lag-1::gfp* could be affected in other tissues.

One possibility is that the difference is an artifact of genetic background. The *lag-1::gfp* and *lag-1::mkate2* alleles were both made in the *wild-type* N2 strain background. The LAG-1-GFP fosmid reporter contains an *unc-119(+)* selection marker, and transgenic lines were generated, maintained, and analyzed in a *unc-119* mutant background. The *unc-119(-)* phenotype was completely rescued by the fosmid array, suggesting that loss of *unc-119* activity is not the cause of the observed differences. Although the parental *unc-119(-)* strain was backcrossed several times, it remains possible that some other background mutation influenced LAG-1-GFP accumulation from the fosmid.

Many other possibilities exist that would explain the differences of fluorescently-tagged LAG-1 accumulation in these different constructs. A critical concern is that important cis-regulatory elements are missing in fosmid reporters. Although the *lag-1* fosmid is large and contains the entire gene-to-gene region in excess, there may be cis-regulatory sequences that exist outside the fosmid. The multi-copy extrachromosomal arrays are highly repetitive and contain a variable number of repeats from array to array. It is unknown how this might affect transcription of tagged *lag-1* from a reporter transgene. A caveat of transgenes that may explain the pattern from the LAG-1-GFP reporter, is that transgenic protein is in addition to the endogenous already present. This "extra" transgenic LAG-1-GFP may affect its own regulation if *lag-1* is positively autoregulated and is discussed in more detail in Chapter 5. The ability to create endogenous fusion proteins, like those described here, provides a way to address many of

these caveats associated with transgenes, which, as I learned first-hand during this project, can lead to erroneous conclusions.

### **Use of endogenously-encoded reporters of LIN-12 activity**

The weak *lin-12(d)* allele, *lin-12(n302)*, does not form an anchor cell and does not induce VPCs to adopt the 2° fate based on failure to form psuedovulvae (Greenwald *et al.* 1983a) and failure to activate transcription of the *lin-12* target reporter *arls116[*lst-5p::2xnl-s-yfp*]* (Chapter 2). In a *lin-12(n302)* background, I observed a number of animals in which LAG-1-mKate2 accumulation appeared to be higher in P5.p and P7.p, and their descendants compared to other VPCs in a number of animals similar the the LAG-1-mKate2 pattern seen in *wild-type* animals. This observation has two implications: there is continued production of the LIN-3/EGF inductive signal from one or both of the  $\alpha$  cells, and that the protein encoded by *lin-12(n302)* can be activated through interaction with ligand. In other animals, LAG-1-mKate2 appeared to be uniformly increased in all VPCs relative to uninduced VPCs, indicative of *lin-12(n302)* activity.

Similarly, LIN-12(intra) does not induce VPCs to adopt the 2° fate when expressed transgenically, unless enhanced by loss of a negative regulator (de la Cova and Greenwald 2012; Deng and Greenwald 2016). However, when I provided LIN-12(intra)-GFP transgenically, I observed that accumulation of LAG-1-mKate2 did not display the 2° pattern typically observed in *wild-type* animals during the Pn.p stage, but rather accumulation increased in all VPCs (Fig. 6B). This observation is an indication that LIN-12(intra)-GFP is active in all the VPCs during the Pn.p stge.

LAG-1-mKate2 accumulation is sensitive to weak LIN-12 activation in the VPCs. It is unknown if LIN-12 activity is promoting transcription of *lag-1::mkate2*, or if the presence of LIN-12(intra) is stabilizing LAG-1-mKate2; I discuss the regulation of LAG-1 in the next section. These observations are consistent with previously published results, and with the idea that VPCs require *lin-12* activity above a certain threshold to adopt 2° fate. Certain aspects, like transcriptional activation of *arls116[*lst-5p::2xnl-s-yfp*]* (Choi 2009) and formation of psuedovulvae (Greenwald *et*

*al.* 1983a), require strong *lin-12(d)* activity or the enhancement of weak *lin-12(d)* activity (Sundaram and Greenwald 1993)(Chapter 2). LIN-12(intra) activity is not sufficient to induce a Muv phenotype unless stabilized by the removal of negative regulators (de la Cova and Greenwald 2012; Deng and Greenwald 2016). LAG-1-mKate2 levels appear to be an indicator of low levels of LIN-12 activation, rather than reporting 2<sup>o</sup> fate. As discussed in Chapter 4, finding reporters for LIN-12 activity in the VPCs has been challenging, and endogenously tagged LAG-1 may represent a useful reporter. There is room for improvement, as mKate2 has, in my hands, proven to be a relatively dim fluorescent protein in the VPCs. Using the *lag-1::gfp* strain or making new endogenously tagged versions of LAG-1, discussed below, would be beneficial. If *lag-1* is determined to be a transcriptional target of LIN-12, then an endogenous transcriptional reporter may be advantageous. The use of quantitative fluorescent microscopy would greatly improve precision and is discussed below.

### **Regulating LIN-12 activity in the VPCs through control of LAG-1 levels or subcellular localization**

A key motivator for the construction and characterization of the LAG-1 translational reporters and endogenously tagged LAG-1 described above was to determine if resistance to activated LIN-12 in the VPCs during the L2 stage (Li and Greenwald 2010), and in P6.p during the L3 stage (Shaye and Greenwald 2005; Li and Greenwald 2010)(Chapter 2) was mediated by regulation of LAG-1 proteins levels or its subcellular localization.

In mammalian cells, it has been proposed that the RITA protein may attenuate Notch activity via the removal of Cbf1 from the nucleus (Wacker *et al.* 2011). I never observed LAG-1-mKate2 or LAG-1-GFP to be localized anywhere in the VPCs but the nuclei. It could be that low cytoplasmic LAG-1-GFP or LAG-1-mKate2 fluorescence was obscured by background fluorescence and therefore not detectable. Still, my observations provide no evidence that exclusion or export of LAG-1 from the nucleus is a mechanism by which LIN-12 activity is regulated in the VPCs.

My characterization of LAG-1-mKate2 and LAG-1-GFP during the L2 and L3 stage do not allow me to form a conclusion about whether LAG-1 levels are important for regulating LIN-12 activity. During the L2 stage, my assessment is that constitutive LIN-12 activity did not produce a substantial increase of LAG-1-mKate2 levels; however, I cannot reliably make this claim without a more quantitative approach like that discussed above. Furthermore, even if this claim is true, I do not know whether this would be a cause or a consequence of resistance to constitutive LIN-12 activity in L2 VPCs.

During the L3 stage I faced a similar chicken-or-egg problem. My observations indicate that LAG-1 levels are positively regulated by LIN-12 activity, but I could not investigate whether this increase of LAG-1 accumulation is a requirement for LIN-12 activity. To properly address these hypotheses, I would require new reagents that allow me to control LAG-1 levels independently of LIN-12 activity. I discuss these ideas further in Chapter 5.

#### **Further investigation of LAG-1 regulation**

My colleague Katherine Luo will be continuing this investigation into the regulatory mechanisms of LAG-1 and how regulation of LAG-1 relates to *lin-12* signaling in the VPCs. She has begun quantifying the fluorescence of LAG-1-GFP in the VPCs as discussed above. This approach will allow for more precise comparisons of LAG-1 levels between the VPCs in the same animal, and between animals of different genotypes. My qualitative approach was not able to accurately determine if constitutive LIN-12 activity raised the baseline levels of LAG-1 in VPCs during the L2 stage, or if constitutive LIN-12 activity increased LAG-1 levels equivalently across all cells during the L3 stage. Her preliminary results thus far indicate that this quantitative approach will be able to answer these questions.

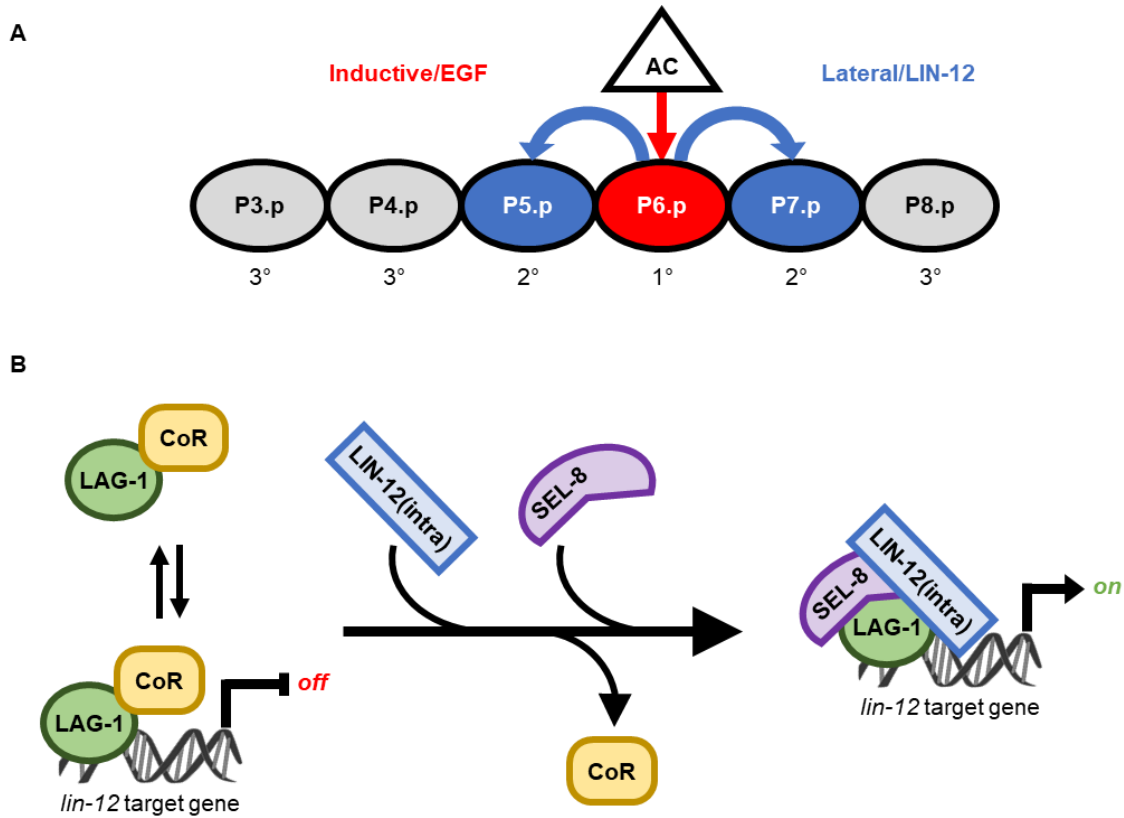
Together we designed experiments that utilize CRISPR/Cas9 techniques to generate two new tagged *lag-1* alleles to determine the level of regulation of LAG-1. First, a *lag-1::gfp-t2a-tdtomato-nls* allele to investigate whether the level of regulation is post-translational. The viral T2A peptide sequence induces ribosome skipping (Ahier and Jarriault 2014), leading to the translation of two separate proteins, in this instance LAG-1-GFP along with tdTomato-NLS. Since

both proteins are translated from the same mRNA, they will be controlled by the same 5' and 3' cis-acting regulatory sequences. Differences between the LAG-1-GFP and tdTomato-NLS patterns would be indicative of post-translational regulation. The second experiment is to make a *lag-1::gfp-sl2-tdtomato-nls* allele in order to investigate regulation of the *lag-1* transcript. In this case the coding sequences for the two fluorescent proteins are separated by an SL2 acceptor sequence [reviewed by Blumenthal (2005)], which produces a bicistronic primary transcript. Trans-splicing of this bicistronic primary transcript will produce two separate mRNA molecules: one that encodes LAG-1-GFP and the other that encodes tdTomato-NLS. The SL2 trans-splicing means that the *tdtomato-nls* mRNA will have the endogenous 3' cis-acting regulatory sequence, while the *lag-1::gfp* mRNA will have the unregulated Ur element at the 3' end. A difference between the LAG-1-GFP and tdTomato-NLS patterns here would be indicative of regulation at the level of mRNA as well as post-translational regulation. Comparing results of these two alleles will allow us to determine between regulation at the levels of transcription, post-transcription, and post-translation.

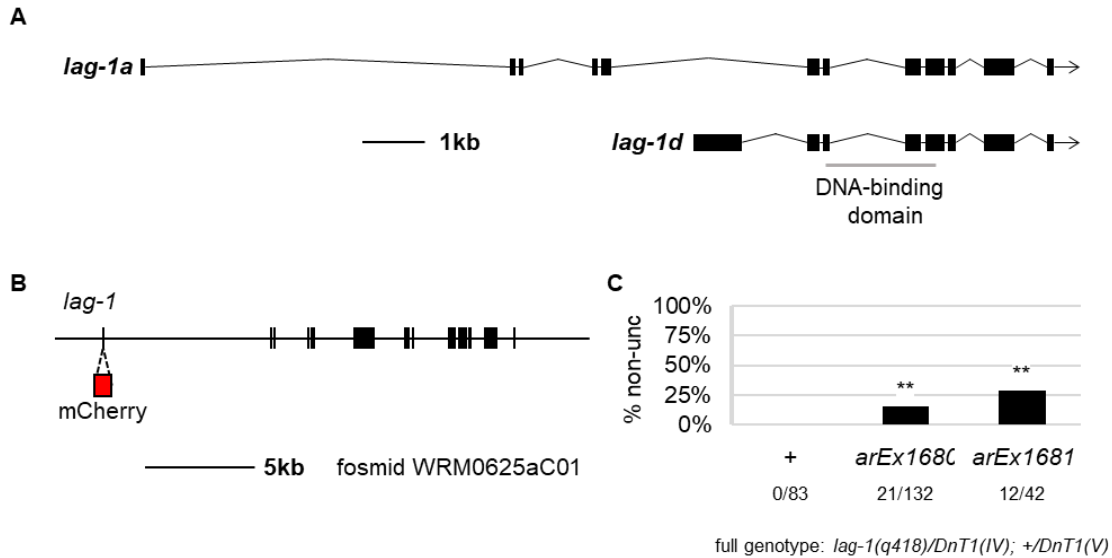
The dauer stage is an alternative developmental pathway induced by “harsh” conditions, such as overcrowding or lack of food [reviewed by Hu (2007)]. Constitutive LIN-12 activity is blocked in the VPCs by an unknown mechanism during the dauer larval stage (Karp and Greenwald 2013). Katherine is extending this investigation of LAG-1 regulation into the context of VPC quiescence during the dauer stage.



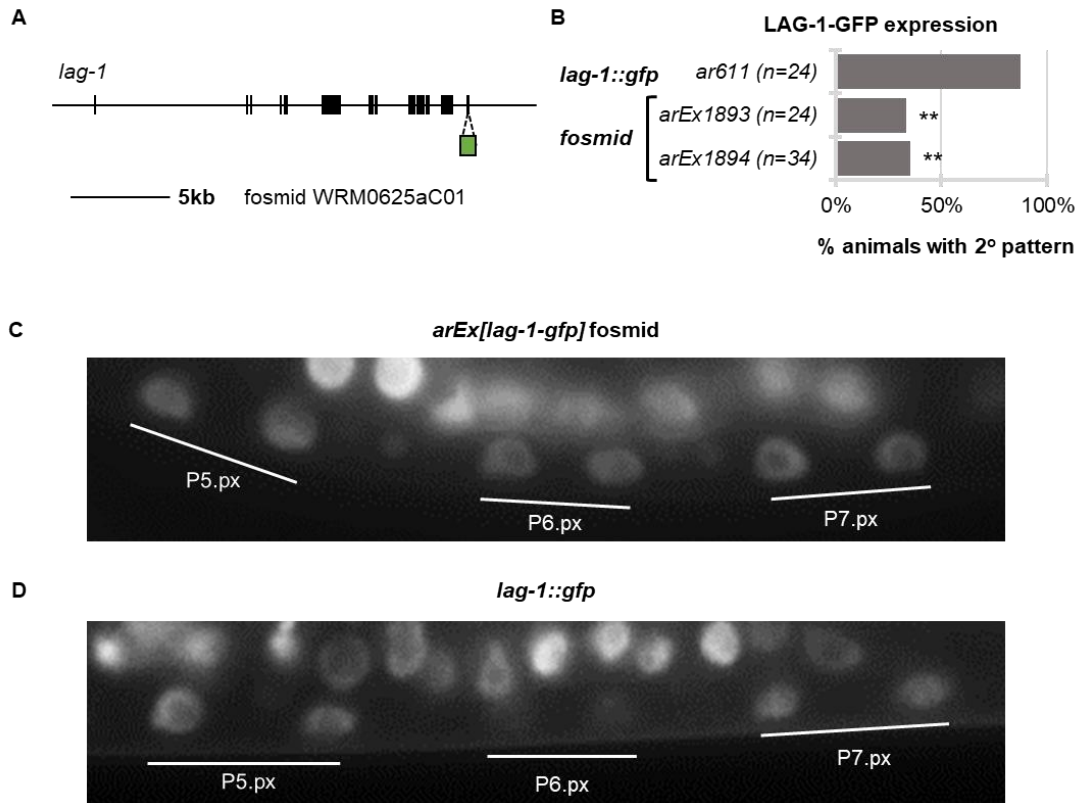
## **Chapter 3. Figures**



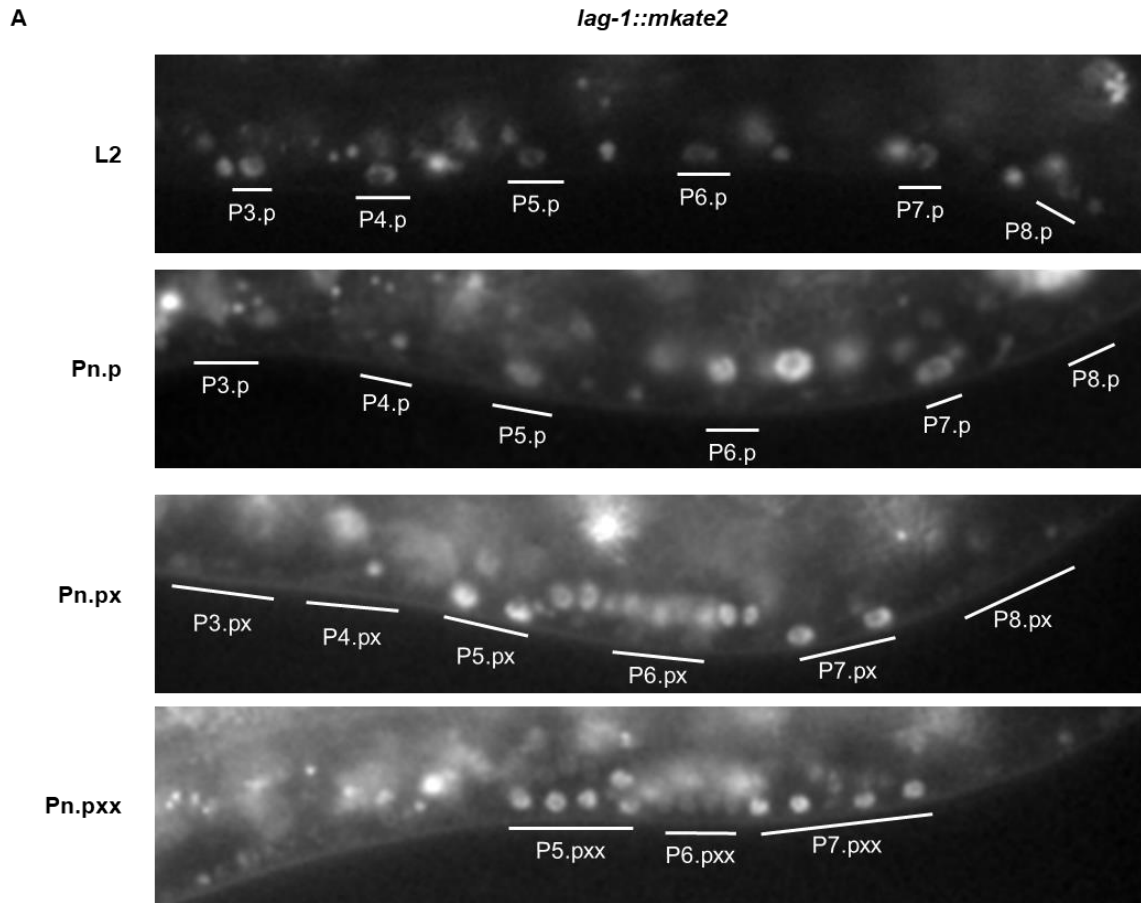
**Figure 1.** Schematics of VPC specification and formation of LIN-12 transcriptional activation complex. (A) The EGF-like inductive signal from the AC activates EGFR in the nearest VPC, P6.p. EGFR activation leads to adoption of the 1° cell fate and expression of LIN-12 ligand genes. Ligands form a lateral signal and activate LIN-12 in the neighboring VPCS, P5.p and P7.p, leading to transcriptional activation of *lin-12* target genes and adoption of the 2° fate. The outer VPCs, P3.p, P4.p and P8.p do not receive either signal and remain uninduced, eventually fusing with the hypodermis. (B) The CSL class transcription factor LAG-1 is a repressor of *lin-12* target gene in the absence of activated LIN-12. Biochemical and structural studies indicate that LAG-1 and other CSL proteins are dynamically associated with DNA while in repressor mode. Upon activation of LIN-12, the LIN-12 intracellular domain, LIN-12(intra), is translocated to the nucleus and forms a active transcriptional complex with LAG-1 and SEL-8, a protein analogous to Mastermind. The dynamics of the LAG-1-LIN-12 activation complex with DNA are not well known; however, evidence from several studies suggest that the LAG-1-LIN-12 activation complex is more stably associated with DNA than LAG-1 repressor complexes [reviewed by Kovall *et al.* (2017)]



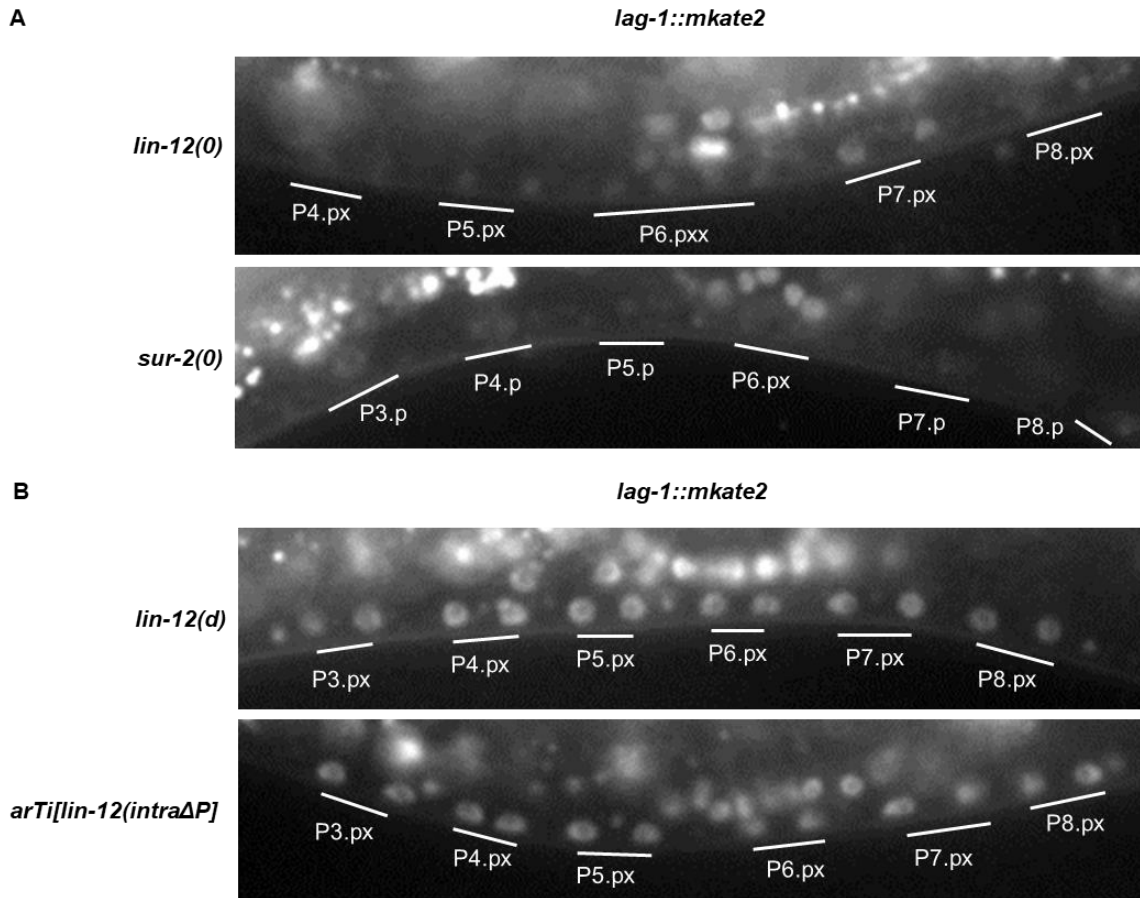
**Figure 2.** Diagram of *lag-1* genomic locus and mCherry-LAG-1 fosmid reporter. (A) Schematic of the predicted structure of the *lag-1* genomic locus. Coding sequences are depicted as black boxes and spliced introns as angled black lines. Structure of the *lag-1a* isoform on top and the more recently predicted *lag-1d* isoform on bottom. The core domain, including the DNA-binding domain, is encoded by the distal exons of *lag-1* which are common between the two isoforms. (B) Schematic showing mCherry-LAG-1 fosmid reporter. The sequence of an *mcherry* cassette was recombineered into the fosmid WRM0625aC01 immediately following the start codon of the *lag-1a* isoform. (C) Larval lethality of *lag-1(0)* can be rescued by two transgenes containing mCherry-LAG-1. Fosmid transgenes were combined with *lag-1(0)/DnT1*. *DnT1* is a modified version of the translocation *nT1* containing *unc(n754)*, which causes a dominant Unc phenotype. I picked array-positive progeny of *lag-1(0)/DnT1* and scored for the Unc phenotype. Chart shows percentage of non-Unc animals assayed. \*\* $P < 0.0001$  by Fisher's exact test.



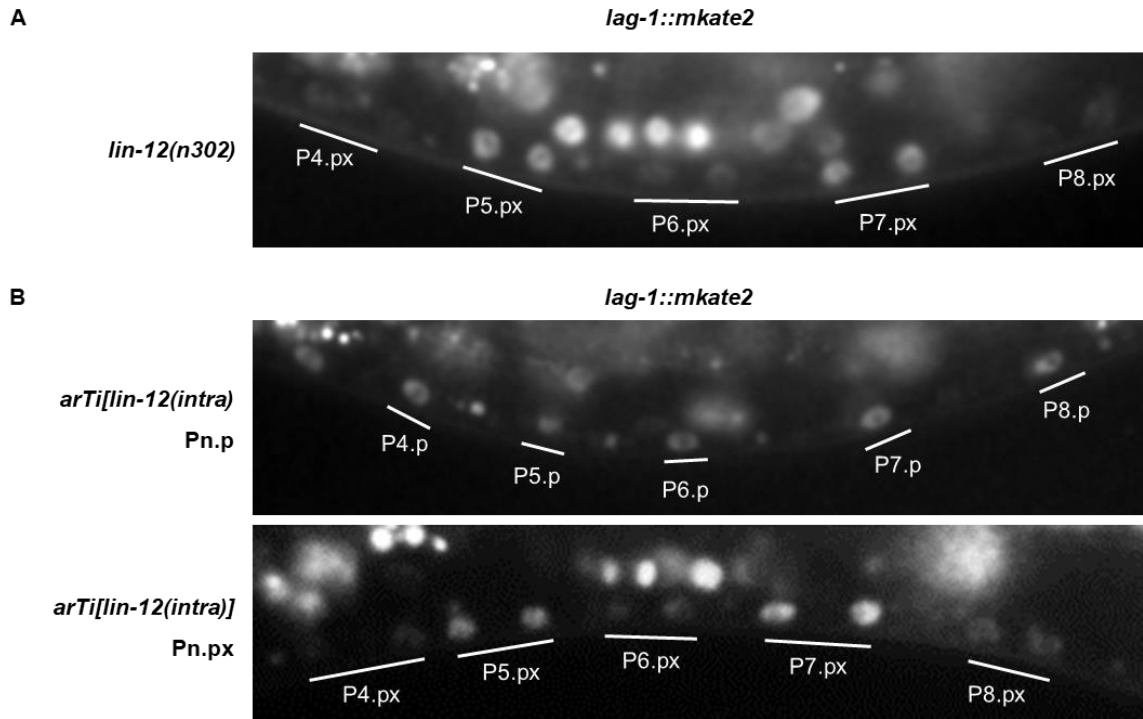
**Figure 3.** LAG-1-GFP from transgenic and endogenous sources. (A) Schematic showing LAG-1-GFP fosmid reporter. The sequence of a *gfp* cassette was recombined into the fosmid WRM0625aC01 immediately following the stop codon of all predicted *lag-1* isoforms. (B) LAG-1-GFP levels from transgenes containing fosmid reporter are equivalent in P5.p, P6.p, and P7.p. LAG-1-GFP levels from the *lag-1::gfp* allele are higher in the 2° VPCs, P5.p and P7.p, relative to the other VPCs. Graph showing percentage of animals with LAG-1-GFP levels in a 2°-fate pattern. \* $P < 0.0003$  Fishers's Exact Test. (C) Image *unc-119(ed3); arEx1860[lag-1-gfp<sup>fos</sup>]* Pn.px-staged animal. LAG-1-GFP levels are equivalent in descendants of P5.p, P6.p, and P7.p. Image obtained at exposure time of 500ms. (D) Image of *lag-1(ar611[lag-1::gfp])* Pn.px-staged animal. LAG-1-GFP levels are lower in descendants of P6.p than descendants of P5.p, and P7.p. Images in C and D were both obtained at exposure time of 800ms.



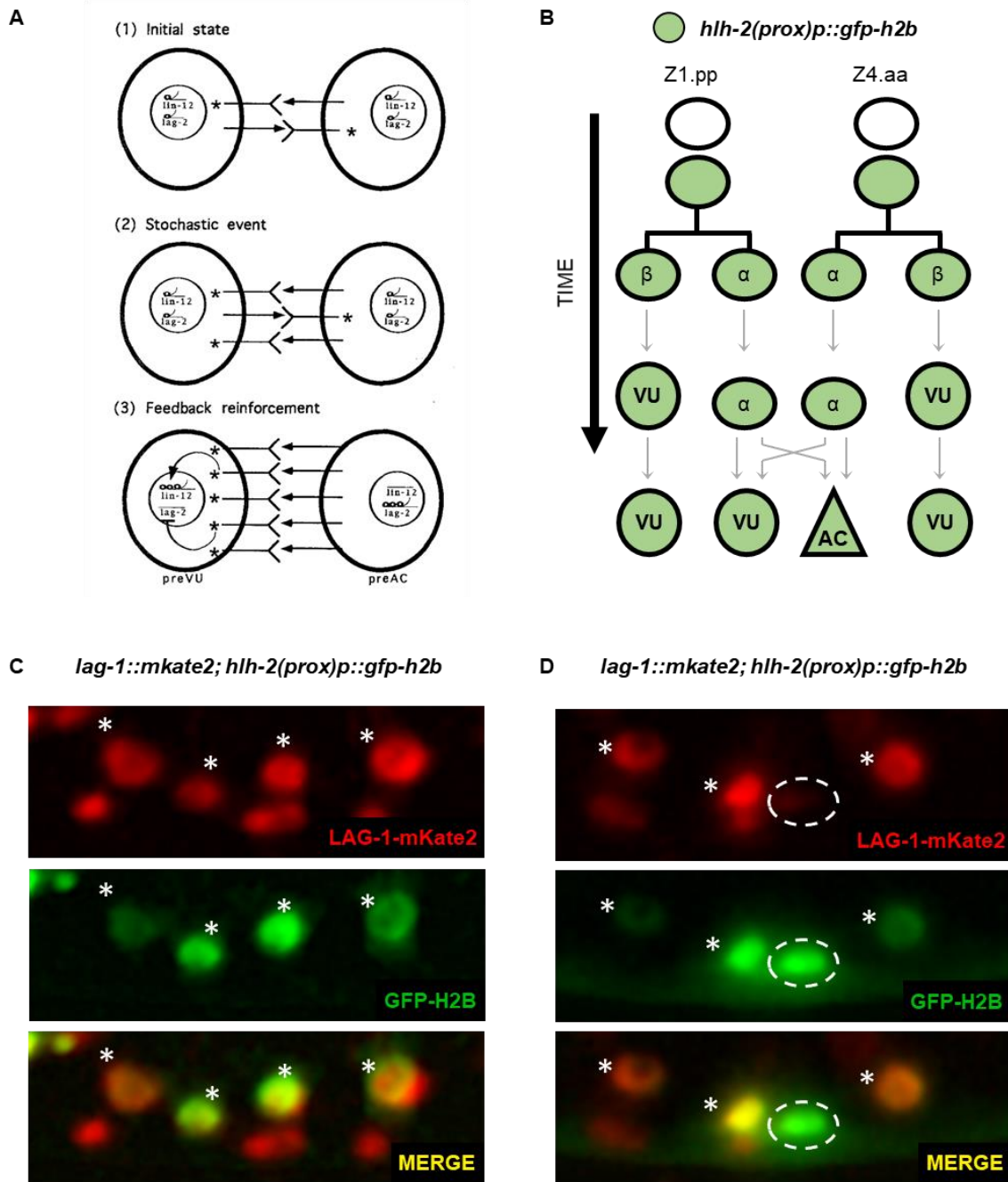
**Figure 4.** LAG-1-mKate2 accumulation in the VPCs from L2 stage to Pn.pxx stage. (A) Images of *lag-1(ar613 [lag-1::mkate2])*. During the L2 stage, LAG-1-mKate2 is in all VPCs at a basal level. As development continues, the LAG-1-mKate2 levels increase in P5.p and P7.p relative to the other VPCs. This pattern of LAG-1-mKate2 accumulation remains higher in the descendants of P5.p and P7.p, during the Pn.px and Pn.pxx stages. All images in Figures 4, 5, and 6 were taken on the same microscope using the same settings, including exposure times.



**Figure 5.** LAG-1-mKate2 accumulation in the VPCs is dependent on *lin-12* activity. (A) Images of *lin-12(n941); lag-1(ar613[lag-1::mkate2])*, top, and *sur-2(ku9); lag-1(ar613[lag-1::mkate2])*, bottom. Loss of *lin-12* activation results in LAG-1-Kate2 levels remaining uniform in all VPCs at low levels comparable to non-2° VPCs in *wild-type* animals. (B) Images of *lin-12(n137); lag-1(ar613[lag-1::mkate2])*, top, and *arTi113[lin-31p::lin-12(intraΔP)-gfp]; lag-1(ar613[lag-1::mkate2])*, bottom. Constitutive LIN-12 activity results in increased LAG-1-mKate2 levels uniformly in all VPCs. All images in Figures 4, 5, and 6 were taken on the same microscope using the same settings, including exposure times.



**Figure 6.** LAG-1-mKate2 accumulation is sensitive to the presence of weak LIN-12. (A) Images of *lin-12(n302); lag-1(ar613 [lag-1::mkate2])* showing LAG-1-mKate2 levels higher in descendants of P5.p and P7.p relative to other VPC descendants, this pattern was observed in (11/29). (B) Images of *arTi43[lin-31p::lin-12(intra)-gfp]; lag-1(ar613[lag-1::mkate2])* showing differences in LAG-1-mKate2 accumulation between Pn.p- and Pn.px-staged animals. Top image shows a Pn.p-staged animal in which LAG-1-mKate2 levels are uniform in all VPCs and comparable to 2° VPCs in *wild-type* animals, this pattern was seen in (17/17) Pn.p-staged animals. Bottom image shows a Pn.px-staged animal in which LAG-1-mKate2 levels are higher in descendants of P5.p and P7.p relative to the other VPC descendants, this is the typical 2°-fate pattern seen in *wild-type* animals and was observed in (15/17) Pn.px- or Pn.pxx-staged animals. All images in Figures 4, 5, and 6 were taken on the same microscope using the same settings, including exposure times.



**Figure 7.** LAG-1-mKate2 accumulation increases in somatic gonadal cells that receive *lin-12* signaling during the AC/VU. (A) Diagram of AC/VU decision in the two  $\alpha$  Z1.ppp and Z4.aaa taken from Wilkinson *et al.* (1994). In panel (1) the two cells are initially competent to adopt the anchor cell (AC) or ventral uterine (VU) precursor cell fate. Both cells express *lin-12* and the DSL ligand gene *lag-2*. In panel (2), a small stochastic variation in LIN-12 activation between the two cells initiates positive feedback loops that amplify this difference. In panel (3), these feedback loops, including positive autoregulation of *lin-12* in the presumptive VU, drive cell-fate commitment. (B) Lineage of  $\alpha$  and  $\beta$  cells beginning from Z1.pp and Z4.aa. Horizontal lines



represent cell divisions and vertical lines represent lineage through development and are not to scale. Expression of *arTi22[hlh-2(prox)p::gfp-h2b]* is indicated in green. (C) Images from *lag-1(ar613[lag-1::mkate2]); arTi22[hlh-2(prox)p::gfp-h2b]* animal depicting the four  $\alpha$  and  $\beta$  cells (denoted by asterisks) during the AC/VU decision. Top, LAG-1-mKate2 levels are equal in the four cells. Middle, GFP-H2B. Bottom, channels merged. Images in C and D are maximum z-projections. (D) Images from *lag-1(ar613[lag-1::mkate2]); arTi22[hlh-2(prox)p::gfp-h2b]* animal following commitment of the AC (denoted by dashed circle) and the VUs (denoted by asterisks). Top, LAG-1-mKate2 levels are elevated in the VUs and not visible in the AC. Middle, GFP-H2B. Bottom, channels merged.

**Chapter 4: Characterization of cis-regulatory sequences of the LIN-12 target gene *lst-5* and *in vivo* analysis of LAG-1 target binding in the VPCs: successes and complications**

## Abstract

The specification of the vulval precursor cells (VPCs) provides a powerful paradigm to study the regulation of LIN-12/Notch. Here I describe attempts to investigate the molecular mechanism behind a resistance to LIN-12 activity in P6.p due to EGFR-Ras-ERK activity. I attempted mutational and deletion analysis on the regulatory sequence of *lst-5*, a direct transcriptional target of LIN-12. I identified a 354 bp cis-regulatory region required for repression of *lst-5* in P6.p during the L3 stage; however, the multi-copy arrays used at that time made follow-up experiments difficult to interpret. I found that a single-copy *lst-5* transcriptional reporter was expressed in all VPCs rather than in P5.p and P7.p, the pattern expected for LIN-12-dependent transcriptional reporter. I attempted to visualize the LIN-12-LAG-1 transcriptional activation complex *in vivo* to determine if negative regulation of *lin-12* targets was achieved through post-translational regulation of this complex. Ultimately, these attempts were unsuccessful, but the experiments described here led to the production of useful reagents.

## Introduction

The development of the adult *C. elegans* vulva provides an excellent system to study cell specification and the regulation of LIN-12/Notch. Six vulval precursor cells (VPCs) are initially equally competent to adopt one of three fates, until an EGF-like “inductive signal” is produced by a cell in the somatic gonad. The inductive signal triggers activation of a canonical EGFR-Ras-ERK signaling pathway in P6.p, the nearest VPC, causing it to adopt the 1<sup>o</sup> fate and activates transcription of LIN-12 ligand genes. These ligands comprise a “lateral signal” which activates LIN-12 in the flanking VPCs, P5.p and P7.p, causing these cells to adopt the 2<sup>o</sup>-cell fate.

Activation of LIN-12 is achieved through two sequential proteolytic cleavage events, which release the intracellular domain of LIN-12 from its transmembrane tether. This “intra” domain is translocated to the nucleus where it will activate target gene transcription; transcriptional activation is achieved through a protein-protein interaction between LIN-12(intra)

and the DNA-binding protein LAG-1. LAG-1 is a well-conserved protein of the CSL class, so named for orthologs in other organisms, CBF1 in mammals and Suppressor of Hairless (Su(H)) in *Drosophila*. Generally, in the absence of LIN-12(intra), LAG-1 functions as a co-repressor, but when complexed with LIN-12(intra), the LAG-1-LIN-12(intra) complex functions as a transcriptional activator.

In Chapter 2, I describe resistance to a form of LIN-12 that is constitutively active and stable, LIN-12(intra $\Delta$ P), in P6.p due to EGFR-Ras-ERK activation. Observations indicated that the genes *lin-1*, *sur-2*, and *cdk-8* are all required for this resistance, but the molecular mechanisms that mediate this form of *lin-12* negative regulation remain unknown. In chapter 3 I describe my observations of LAG-1-GFP translational fosmid reporter. Briefly, this reporter indicated that LAG-1-GFP was not patterned in VPCs and was present in P5.p, P6.p, and P7.p at uniform levels. This observation suggested that resistance to LIN-12 activity may be at the level of the LIN-12-LAG-1 transcriptional activation complex.

To investigate this possibility, I decided upon two strategies that would be done in parallel and could share reagents. I would perform deletion and mutational analysis using a LIN-12 transcriptional target to identify cis-acting regulatory sequences that mediate these forms of regulation. Additionally, I designed a variation of the “Nuclear Spot Assay” (NSA) to visualize whether trans-acting factors, such as LAG-1, were bound to regulatory sequences of LIN-12 target transgenes. NSAs have been utilized and described in many publications, e.g. (Carmi et al. 1998; Fakhouri et al. 2010; Meister et al. 2011; Cochella and Hobert 2012; Patel and Hobert 2017), and I discuss this in further detail below. I generated a suite of fluorescent transcriptional reporter transgenes designed to identify *cis*- and *trans*- acting factors that mediate these blocks to LIN-12 activity. I identified cis-regulatory elements required for these forms of negative regulation, including evidence of a region that is required for transcriptional repression in P6.p. Unfortunately, these lines of experiments could not be continued due to technical issues; however, during my attempts to perform these experiments I produced reagents useful for other projects, such as the endogenously-tagged LAG-1 protein fusions described in Chapter 3. I describe these efforts here.

## Materials and methods

### C. elegans genetics

All strains were raised according to standard practices at 20° or 25° degrees (Brenner 1974).

The following transgenes were used in this section: *arEx1080[lin-31p::lin-12(intraΔP)]* (Li and Greenwald 2010); *oxTi414* (Frøkjær-Jensen et al. 2014) was used to mark the *lag-1* locus during crosses; *arTi207[lin-31p::scfv-sfgfp]* (Justin Shaffer).

The recipient strain making transgenes described below was GE24 *pha-1(e2123)* unless otherwise noted. Strains carrying *pha-1(+)* transgenes were maintained at 25°.

### Transgenic arrays

The following transgenes were generated by injecting PCR products or fusion PCR products using the plasmids as templates p766 or p767 (Choi 2009). PCR products were injected at 10ng/ul with linearized pBX (*pha-1(+)*) at 1ng/uL, pCW21 (*ceh-22p::gfp*) at 1ng/uL and OP50 genomic DNA at 50ng/uL.

*arEx1709-1713 [Ist-5(566)p::2xnls-yfp::unc-54 3'UTR]*

*arEx1767-1771 [Ist-5(566 ΔLBS)p::2xnls-yfp::unc-54 3'UTR]*

The following transgenes were generated by injecting PCR products at 10ng/ul with linearized pBX (*pha-1(+)*) at 3ng/uL, *ttx-3p::gfp* at 5ng/uL and OP50 genomic DNA at 50ng/uL.

*arEx1865-1868 [Ist-5(535)p::2xnls-yfp::unc-54 3'UTR]*

*arEx1868-1872 [Ist-5(535ΔLBS)p::2xnls-yfp::unc-54 3'UTR]*

*arEx1887-1889 [Ist-5(181)p::2xnls-yfp::unc-54 3'UTR]*

The following transgenes were generated by injecting PCR products at 10ng/ul with pBX (*pha-1(+)*) at 20ng/uL, *ttx-3p::gfp* at 20ng/uL and pBS KS(+) at 40ng/uL.

*arEx1865-1868 [Ist-5(535)p::2xnls-yfp::unc-54 3'UTR]*

*arEx2161 [Ist-5(181)p::2xnls-yfp::unc-54 3'UTR]*

*arEx2096-2097 [Ist-5(535Δ194...144)p::2xnls-yfp::unc-54 3'UTR]*

*arEx2102-2104 [Ist-5(535...112)p::2xnls-yfp::unc-54 3'UTR]*

*arEx2105-2106 [Ist-5(535...243)p::2xnls-yfp::unc-54 3'UTR]*

*arEx2108-2107 [Ist-5(425...354)p::2xnls-yfp::unc-54 3'UTR]*

*arEx2109-2110 [Ist-5(461...354)p::2xnls-yfp::unc-54 3'UTR]*

The following transgenes were generated by injecting PCR products at 10ng/ul with pBX (*pha-1(+)*) at 20ng/uL, *ttx-3p::gfp* at 20ng/uL and LacO repeats (SphI-KpnI fragment from pSV2-DHFR-8.32 (Robinett *et al.* 1996)) at 40ng/uL.

*arEx2490-2492 [Ist-5(535)p::2xnls-yfp::unc-54 3'UTR]*

*arEx2493-2495 [Ist-5(181)p::2xnls-yfp::unc-54 3'UTR]*

### **Generation of miniMos based transgenes**

The *arT153*, *arTi154* and *arTi155* transgenes were made by injecting pRSU79. Single-copy transgenes were generated by germline injection into N2 animals and insertions were isolated as described by Frøkjær-Jensen *et al.* (2014).

### **Plasmid construction**

pRSU79: *eft-3p::tagBFP-LacI-tbb2 3'UTR* was made using Gibson assembly. The *eft-3p* regulatory region was amplified from the pCFJ1209 vector (Frøkjær-Jensen *et al.* 2014); *lacI* sequence from bSEM669 (Updike and Mango 2006).

### **Reporter scoring**

All *Ist-5* reporters were scored on Zeiss Axio Imager Z1 with a Hamamatsu Orca-ER camera and an X-Cite 120Q light source (EXFO photonics solutions) at 100% power. YFP expression was scored at an exposure time of 800 ms. Individual VPCs were scored for expression and rated “on”

or “off”. For experiments with *arEx1080*, *myo-3p::mcherry* was simultaneously imaged using an exposure time of 50 ms.

The nuclear spot assay experiments were performed using a Zeiss spinning disk confocal microscope system. Red and Blue fluorescence was taken simultaneously using a dual camera set-up. Images were processed using Fiji distribution of ImageJ.

## Results and Discussion

### The regulatory sequence of *lst-5* as a tool to study regulation of *lin-12* signaling

LAG-1 binding sites (LBSs) can be predicted computationally using consensus binding motifs derived from known targets of Su(H) (Yu *et al.* 2004). This approach led to the identification of a set of lateral signal target (*lst*) genes (Yoo *et al.* 2004; Yoo and Greenwald 2005), and additional genes, including *lst-5* and *lst-6* (Choi 2009). Initially, three LBSs were predicted in the approximately 1 kb sequence upstream of *lst-5* and *lst-6* (Fig. 1A; Choi 2009). The predicted gene structure of *lst-5* was updated during validation of *lst-5* transcriptional reporters. A new 5' exon of *lst-5* was predicted to exist in the 1 kb upstream region, and this prediction was validated by RT-PCR experiments which provided evidence for the existence of at least two isoforms of *lst-5* (Choi 2009). Transcriptional reporters containing the “new” upstream region (*lst-5p “new”*) were tested, and expression in the 2° VPCs and their descendants was not observed (Fig. 1B). It was concluded that regulatory information critical for expression in 2° VPCs was contained in the sequences of the 5' exon and first intron of *lst-5* (Choi 2009).

Transcriptional reporters of the 1 kb upstream sequence of the “old” *lst-5* prediction (*lst-5(FL)p*), were found to be expressed in 2° VPCs and their descendants (Fig. 1B). When combined with a *lin-12(d)* allele, expression was observed in all VPCs (Choi 2009). This expression was lost when the three LBSs were mutated (*lst-5(FLΔ3xLBS)p*) (Fig. 1B). These observations suggested that *lst-5* was a *bona fide* *lin-12* target. Additionally, it was observed that *lst-5* transcriptional reporters had a relatively “clean” expression pattern in comparison to

transcriptional reporters of other *Ist* genes. For example, *Ist-3* transcriptional reporters are expressed in all VPCs during the L2 stage and expression resolves to P5.p and P7.p during VPC specification (Yoo *et al.* 2004), whereas *Ist-5* transcriptional reporters are typically only expressed in P5.p and P7.p and their descendants in the L3 stage. An integrated *Ist-5* reporter, *arls116*, has since been used extensively to mark 2° VPCs (Choi 2009; Li and Greenwald 2010; Li 2011; Karp and Greenwald 2013; Keil *et al.* 2017), and appeared to be regulated during the L2 and L3 stages in the expected manner. These reasons led me to decide that *Ist-5(FL)p* was ideal for use as a LIN-12 target sequence.

### **The first exon and first intron of *Ist-5* are sufficient to drive expression in 2° VPCs**

Since the 5' exon and first intron of *Ist-5* were required to drive expression in P5.p and P7.p, I asked if these regions were sufficient to drive expression in 2° VPCs. I generated transcriptional reporters containing a 566 bp fragment that contained the entirety of the 5' exon and first intron of *Ist-5*, and a small portion of the upstream region (*Ist-5(566)p*) (Fig. 2 A-B). Analysis of reporters made from this construct showed expression in P5.p and P7.p and their descendants, indicating that the sequences of the 5' exon and first intron were sufficient to be transcriptionally activated by LIN-12. Mutating the sole LBS lead to decreased expression in P5.p and P7.p and their descendants (Fig. 2A, C).

The *Ist-5(566)p::2xnlis-yfp* reporter contained the start codon of the 5' exon and 29 bps of the flanking 5' region, including the entire 5'UTR of *Ist-5a*. This indicated that this region may contain cis-regulatory sequences important of expression in 2° VPCs. To determine this, I generated a new set of transcriptional reporters that truncated the upstream region further and eliminated the "AT" of the start codon to generate *Ist-5(535)p*. Analysis of this reporter showed expression in P5.p and P7.p and their descendants (Fig. 3A-B). Mutating the sole LBS in this construct produced diminished expression in P5.p and P7.p and their descendants (Fig. 3A-C). These observations are consistent with the conclusion that the 5' exon and first intron of *Ist-5* contains the necessary regulatory information required for activation by LIN-12 in VPCs.



### Deletion analysis of *Ist-5p* transcriptional reporters

The transgene *arEx1080[lin-31p::lin-12(intraΔP)]* expresses a constitutively active form of LIN-12(intra) that has been stabilized by the removal of the PEST domain (see Chapter 2). Adult hermaphrodites carrying this transgene possess an anchor cell and are Multivulva. When the integrated reporter array *arls116[Ist-5(FL)p::2xnl5-yfp]* is combined with *arEx1080[lin-31p::lin-12(intraΔP)]*, YFP expression is seen in all VPCs with the exception of P6.p, which is resistant to LIN-12 activity (Chapter 2).

To identify cis-acting regions required for resistance to LIN-12 activity during the L3 stage I performed deletion analysis of the *Ist-5* regulatory region (Fig.4). I generated transgenic reporter arrays of containing truncations or deletions of the *Ist-5* regulatory sequence, and combined them with *arEx1080[lin-31p::lin-12(intraΔP)]*. Expression of YFP in P6.p in the presence of *arEx1080[lin-31p::lin-12(intraΔP)]* suggests that a cis-acting sequence contained in the deleted region may be required for transcriptional repression of *Ist-5* reporters in P6.p.

My observations indicate that a 354 bp region in the distal element of *Ist-5(535)p* is required to repress transcription in P6.p and descendants. The *Ist-5(181)p::2xnl5-yfp* reporters (Fig. 4G) showed the highest penetrance of YFP fluorescence in P6.p of any truncated *Ist-5* reporter tested. The two transgenic arrays shown in Fig. 4G were made at different times using different transgenic conditions, indicating that this result is reproducible. Truncations at the 5' end of *Ist-5(181)p::2xnl5-yfp*, in the coding region, resulted in ectopic reporter transcription in P6.p, without the requirement for *arEx1080[lin-31p::lin-12(intraΔP)]* (Fig. 4 H-I).

Other reporters with truncations in the 3' region showed relief of transcriptional repression in P6.p as well (Fig. 4 D-E); however, expression from these transgenes was generally much dimmer and much more variable in all VPCs than the expression from *Ist-5(181)p::2xnl5-yfp* transgenes. The low and variable levels of fluorescence made scoring animals challenging and led me to question the reproducibility of these observations. I therefore attempted to generate new transgenes that had more consistent expression.

Two single-copy miniMos random-insertion transgenes of *Ist-5(535)p::2xnl5-yfp* and three of *Ist-5(181)p::2xnl5-yfp* produced either no expression or dim expression. A site-directed single-copy insertion of *Ist-5(FL)p::2xnl5-yfp* into a characterized site on LG1 did not produce visible expression. I attempt to amplify the signal using a protein multimerization system known as “SunTag” (Tanenbaum *et al.* 2014). An LG1 site-directed single-copy insertion *Ist-5(FL)p::2xnl5-yfp-suntag* reporter into the enabled visualization of expression from a (Fig. 5A-B); however, this reporter was expressed in P6.p as well as P5.p and P7.p, indicating that it was not useful as a 2<sup>o</sup>-fate marker. I discuss this further in Chapter 5.

### **Nuclear Spot Assay**

In Chapter 3, I observed that a LAG-1-GFP fosmid reporter was expressed in the nuclei of all VPCs during the L2 stage and in the nucleus of P6.p during the L3 stage. Thus, I concluded that resistance to LIN-12 signaling in these contexts was not due to the absence of nuclear LAG-1, although was discovered to be incorrect after beginning the following experiment. At that time, an alternative hypothesis was that the LAG-1-LIN-12 activation complex was prevented from forming or prevented from binding to DNA.

The Nuclear Spot Assay (NSA) is a versatile method that has been used in *C. elegans* to visualize compaction states of transgenic arrays (Yuzyuk *et al.* 2009; Meister *et al.* 2010; Cochella and Hobert 2012) and the binding-states of transcription factors on target sequences (Carmi *et al.* 1998; Fakhouri *et al.* 2010). My strategy was to perform an NSA that was entirely modular to permit components to be swapped out one at a time and used in different combinations, allowing for greater consistency and better comparisons between the different experiments. I required three reagents to perform the initial experiment: first, an extrachromosomal array containing a *lin-12* target gene reporter and LacO repeats; second, a transgenic source of fluorescently tagged LacI; third, a fluorescently labeled transcription factor. Generating these reagents proved challenging with a major obstacle being the desire to use three fluorophores simultaneously. I discuss my efforts in assembling these reagents here.

The *lst-5(535)p::2xnl-yfp* reporter described above was an ideal candidate for use as a LIN-12 target sequence. The expression pattern suggested that it was transcribed only in response to activated LIN-12 and it was regulated in P6.p and descendants as expected. Since I could visualize a green LAG-1 fosmid translational fusion reporter but not a red one (Chapter 3), I constructed new *lst-5(535)p* reporters that drove expression of red fluorescent proteins. At the time, I considered this more expedient than making a red LAG-1 C-terminal translational fusion. I generated extrachromosomal arrays containing *lst-5(535)p::2xnl-mcherry* and LacO repeats using a variety of injection conditions, but I did not observe mCherry expression in the VPCs.

I attempted to remedy this by using two alternative red-spectrum proteins. Again, I generated extrachromosomal arrays containing LacO repeats and either *lst-5(535)p::2xnl-tagrfp* or *lst-5(535)p::2xnl-mkate2* using different transgenic conditions. I established many new transgenic arrays, but none consistently expressed in 2° VPCs, and none were useable for the NSA. A possible explanation for these negative results is that a cryptic splice site or some other regulatory sequence was introduced at the new junctions; an analysis of the sequences used for these arrays did not reveal anything informative. I made new arrays containing *lst-5(535)p::2xnl-yfp* and LacO repeats and established three independent transgenic lines that had YFP expression in 2° VPCs and their descendants as expected. The use of *lst-5p(535)p::2xnl-yfp* as a LIN-12 target precluded the use of the LAG-1-GFP fosmid reporter. I generated the red *lag-1::mkate2* “knock-in” allele *ar613* discussed in Chapter 3.

For this strategy, it was necessary to tag LacI with a blue-spectrum protein. Initially I attempted to use CFP::LacI (Updike and Mango 2006; Fakhouri *et al.* 2010), but these attempts were unsuccessful for a variety of reasons. Ultimately, I generated single-copy insertions of *tagbfp-lacI* driven by the strong ubiquitous promoter *eft-3p*. These transgenes produced nuclear tagBFP-LacI in all cells including the VPCs.

Expression from *eft-3p::tagbfp-lacI* transgenes was dim and diffuse in nuclei in the absence of a LacO containing target array. When combined with the transgenes containing *lst-5(535)p::2xnl-yfp* and LacO repeats, tagBFP-LacI condensed into puncta, or “dots”, along the

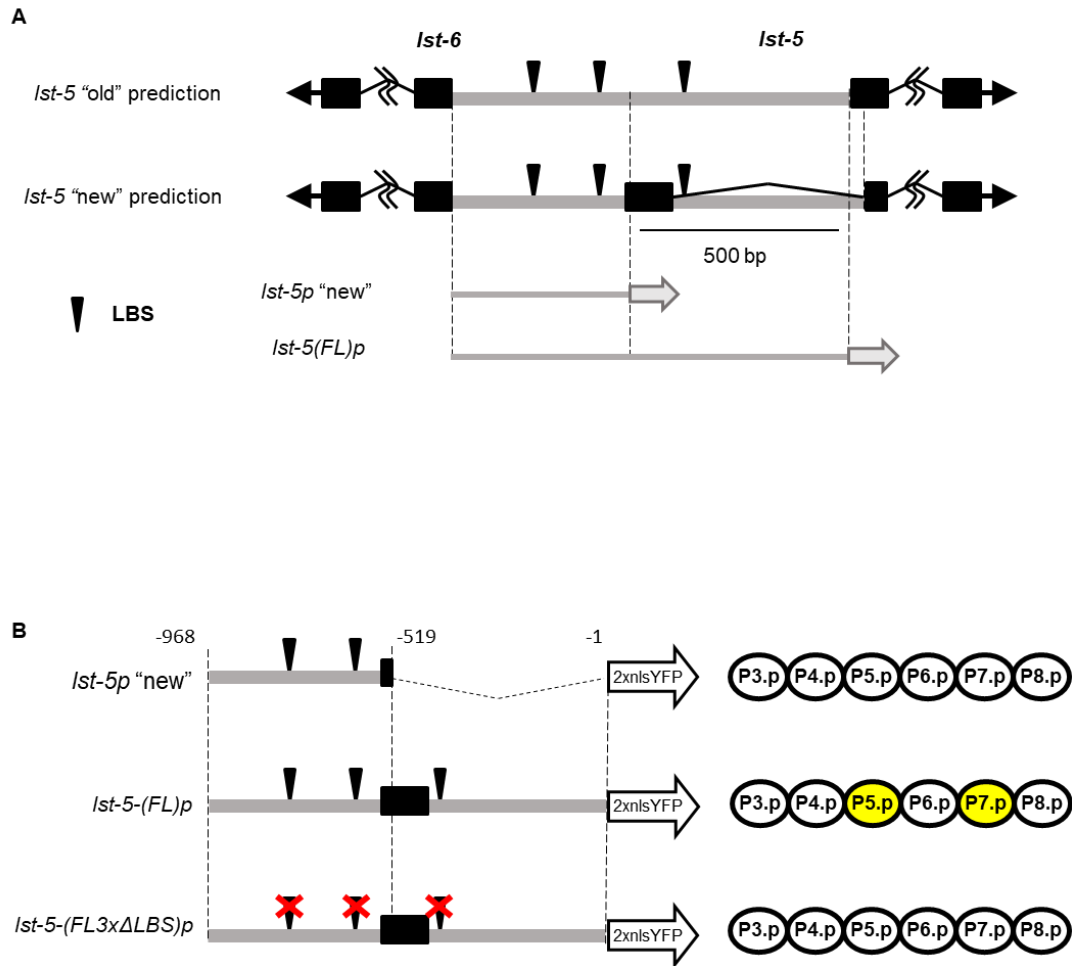
periphery of the VPC nuclei, generally one dot per VPC, indicating that tagBFP-LacI was binding to the LacO repeats contained in the target transgene.

I then combined the *eft-3p::tagbfp-lacI*, *lst-5(535)p::2xnl5-yfp* and LacO repeats, and *lag-1::mkate2*. When I simultaneously imaged tagBFP-LacI and LAG-1-mKate2, I observed they formed overlapping dots in the VPCs, suggesting that both fusion proteins were binding to the target arrays. However, when I removed *eft-3p::tagbfp-lacI* from this strain and imaged animals containing just *lst-5(535)p::2xnl5-yfp* and LacO repeats, and *lag-1::mkate2*, the LAG-1-mKate2 protein no longer condensed into dots, and instead remained diffuse in VPC nuclei, suggesting that association with tagBFP-LacI was responsible for formation of LAG-1-mKate2 dots. I hypothesize this is because mKate2 and tagBFP are derivatives of the same wild-type red fluorescent protein (Subach *et al.* 2008; Shcherbo *et al.* 2009), which is naturally multimerized.

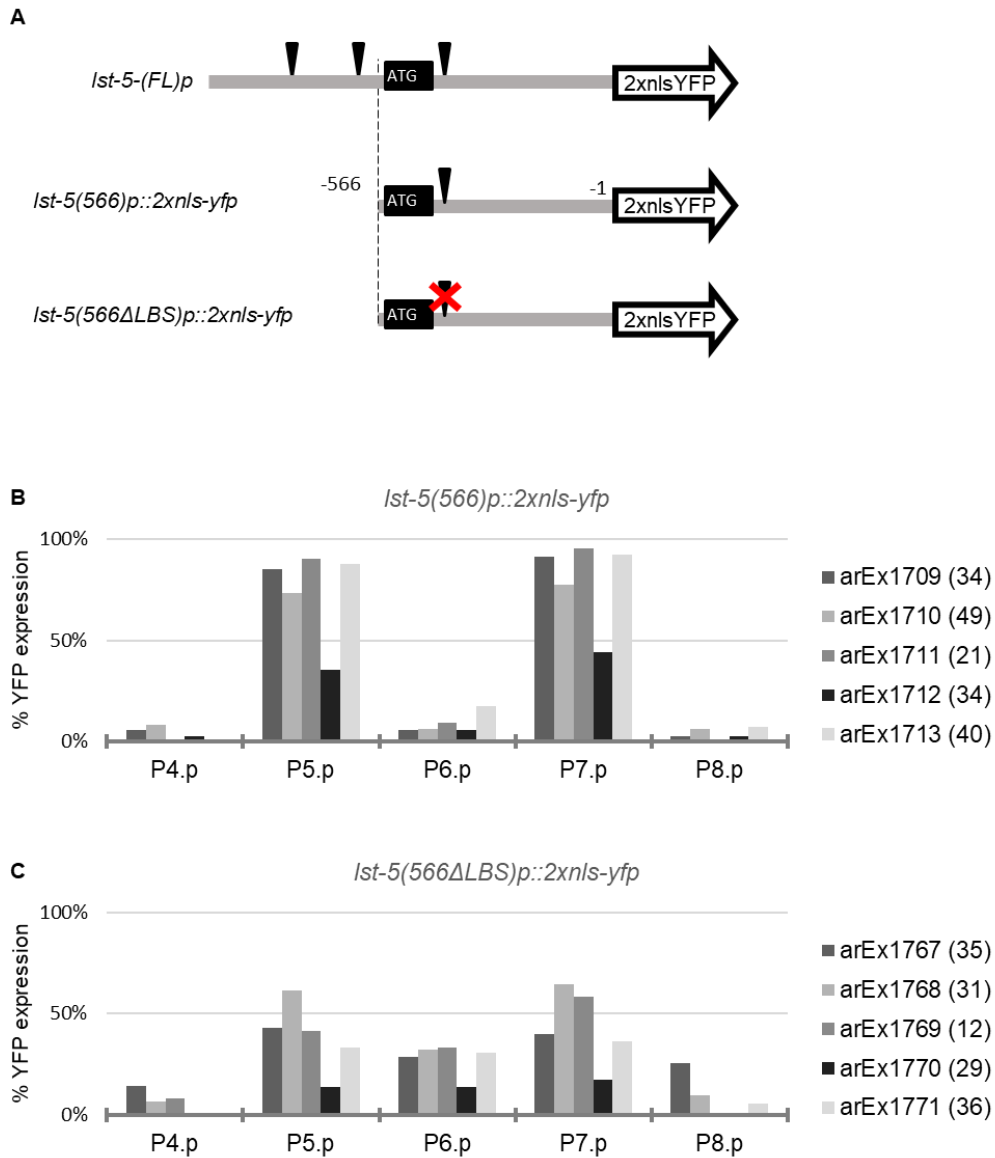
I attempted to troubleshoot this experiment by generating new LacO target transgenes that contain LIN-12 target sequences that do not drive fluorescent protein expression. I combined these new transgenes with *eft-3p::tagbfp-lacI* and the *lag-1::gfp* allele. When I imaged tagBFP-LacI and LAG-1-GFP simultaneously, I observed tagBFP dots, but did not observe LAG-1-GFP dots. This indicated that LacI was able to bind to the LacO repeats in the transgene, but LAG-1-GFP did not bind at sufficient concentration to produce a visible dot. It is consistent with my prediction that tagBFP and mKate2 interact due to their common ancestry, as GFP has a distinct lineage.

The foundational assumption of these experiments, that LAG-1 was present in all VPCs at uniform levels, was invalidated by observations made using the *lag-1(ar613)* allele, described in Chapter 3. These experiments were not pursued further as a result.

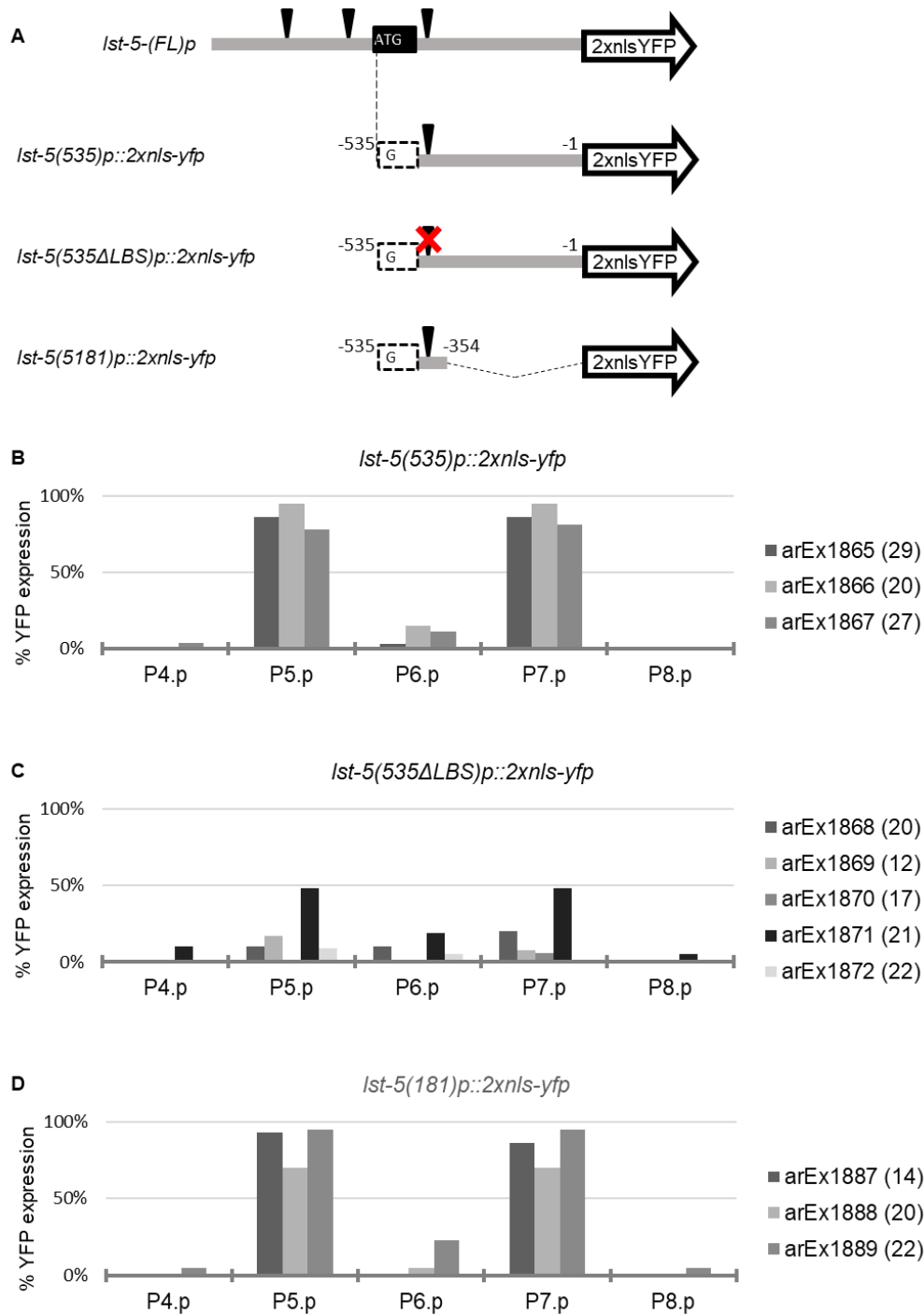
## **Chapter 4. Figures**



**Figure 1.** The gene *Ist-5* is a direct target of LIN-12. (A) Schematic of the upstream region of *Ist-5* and *Ist-6*. Top shows the original gene prediction, *Ist-5* "old", with a roughly 1 kb intergenic region (denoted by gray line) that contained three predicted LAG-1 binding sites (denoted by black triangles)(Choi 2009). Middle shows the updated prediction of the *Ist-5* gene structure, *Ist-5* "new" that included a new 5' exon (exons denoted by black boxes), and RT-PCR experiments revealed at least two different isoforms (angled lines denote spliced introns) (Choi 2009). Below, transcriptional reporters corresponding to the *Ist-5* genomic loci. The 1 kb upstream sequence corresponding to the old *Ist-5* prediction is called *Ist-5(FL)p*. (B) Top, transcriptional reporters of *Ist-5p* "new" did not express in P5.p and P7.p or their descendants. Middle, *Ist-5p(FL)p* transcriptional reporters express in P5.p and P7.p and their descendants. Bottom, expression in P5.p and P7.p is lost when the three LBSs in *Ist-5(FL)p* are mutated (denoted by X over LBS) (Choi 2009).

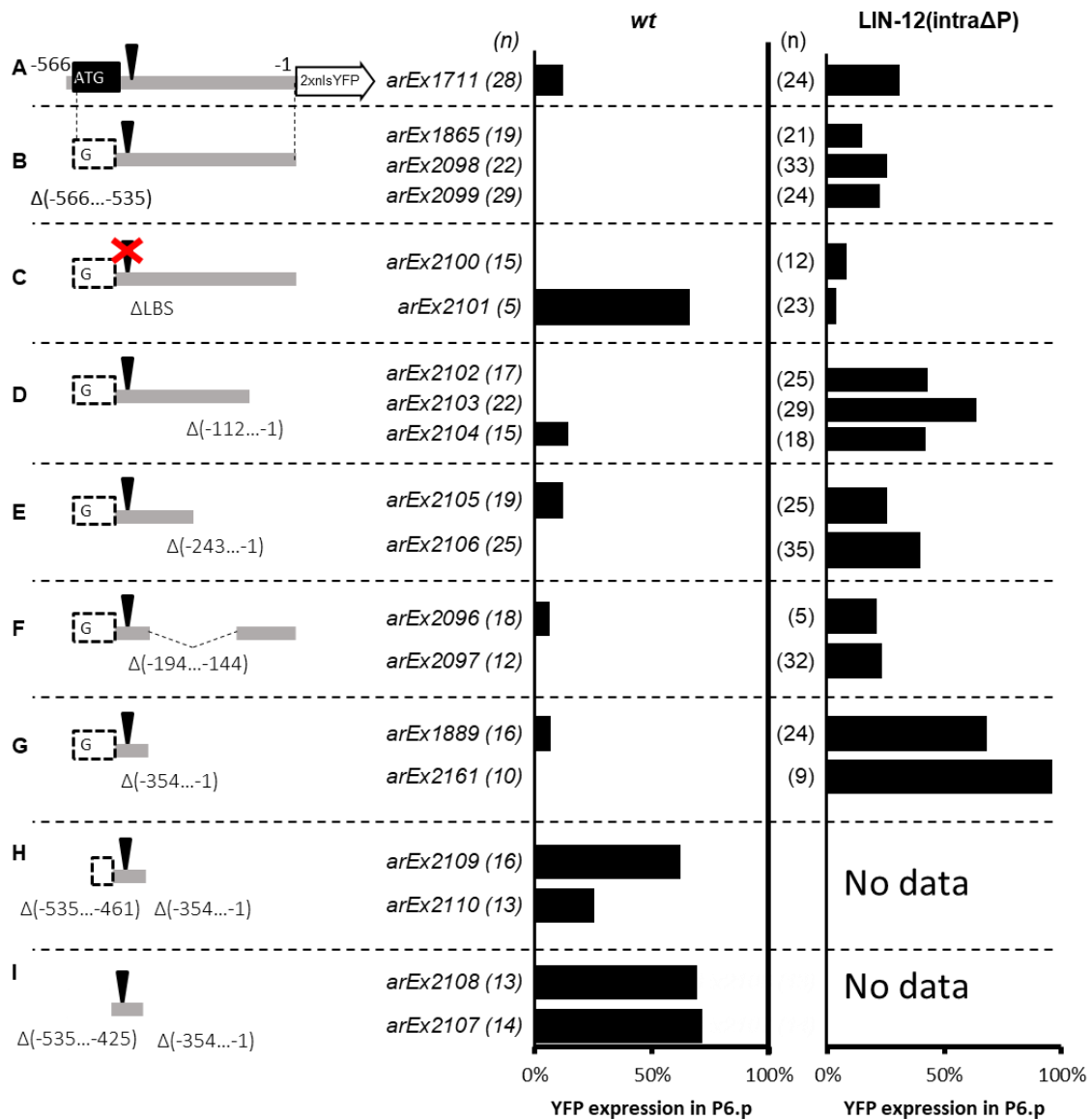


**Figure 2.** 5' exon and first intron of *Ist-5* are sufficient to drive expression in P5.p and P7.p. (A) Top, schematic showing *Ist-5(FL)p::2xnl::yfp* transcriptional reporter. Middle and bottom show truncations of the *Ist-5(FL)p*. "ATG" in black exon indicate that the start codon and ORF of this exon are still intact. Bottom shows mutation of single LBS (B) Graph of YFP fluorescence from *Ist-5(566)p::2xnl::yfp* in VPCs and their descendants. (C) Graph of YFP fluorescence from *Ist-5(566ΔLBS)p::2xnl::yfp* in VPCs and their descendants.

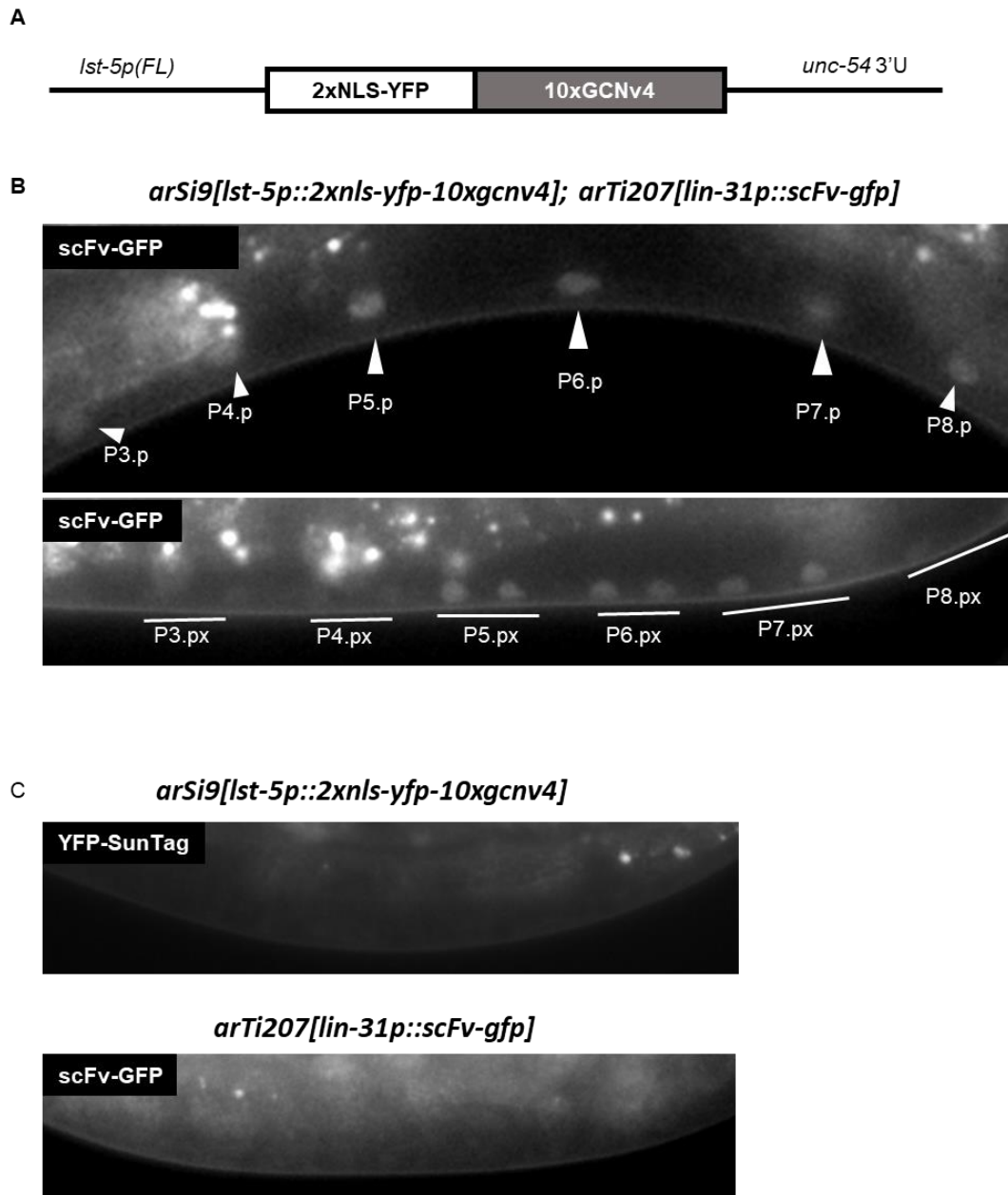


**Figure 3.** Deletions analysis of *Ist-5* 5' exon and first intron. (A) Top, schematic showing *Ist-5(FL)p::2xnlis-yfp* transcriptional reporter and truncations of the *Ist-5(FL)p*. "ATG" in black exon indicate that the start codon and ORF of this exon are still intact. The "AT" of the start codon in the 5' exon were deleted, indicated by the "G" and dashed white box. Middle shows mutation of single LBS. Bottom shows deletion of 354 distal bps. (B) Graph of YFP fluorescence from *Ist-5(535)p::2xnlis-yfp* in VPCs and their descendants. (C) Graph of YFP fluorescence from *Ist-5(535ΔLBS)p::2xnlis-yfp* in VPCs and their descendants. (D) Graph of YFP fluorescence from *Ist-5(181)p::2xnlis-yfp* in VPCs and their descendants.

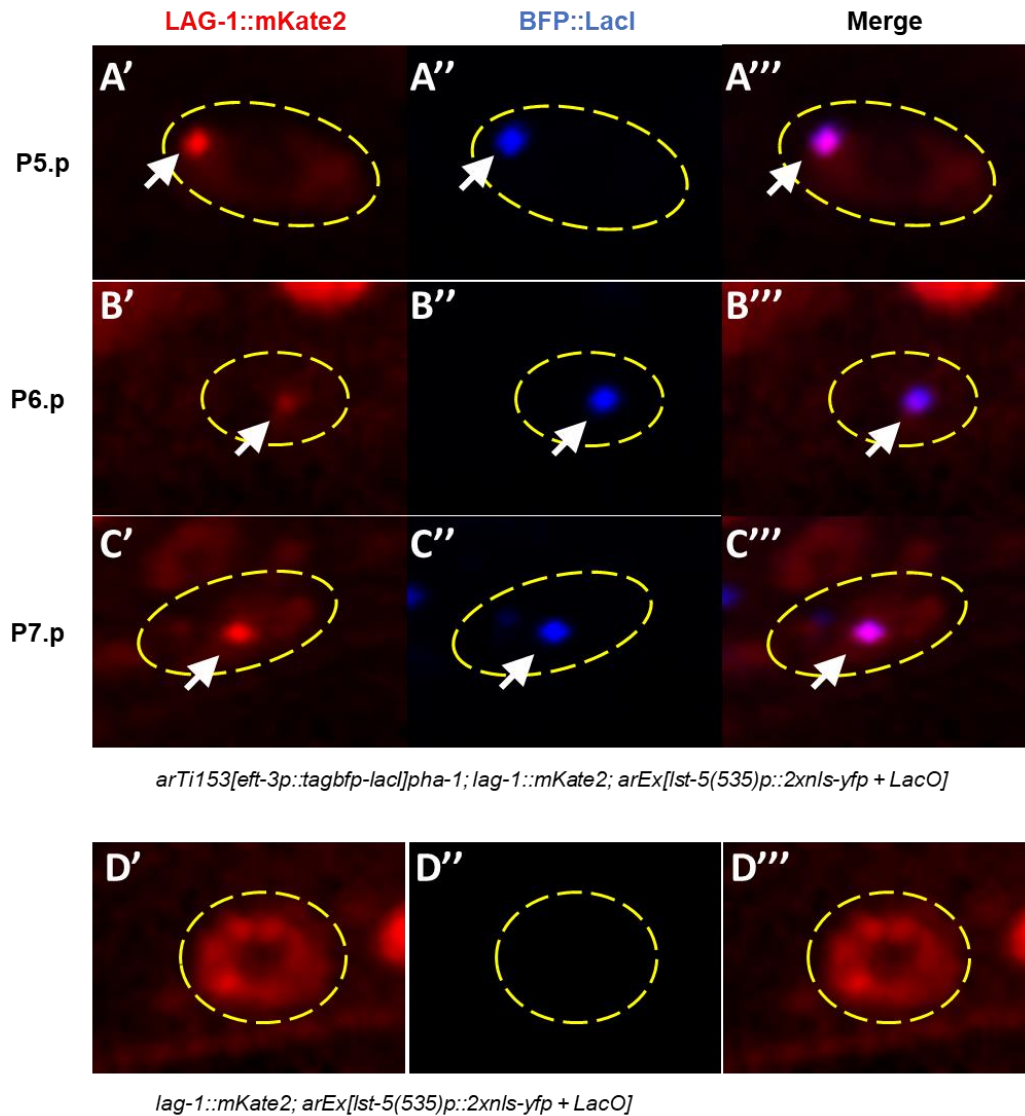




**Figure 4.** Deletion analysis of *Ist-5* 5' exon and first intron in the presence of LIN-12(intraΔP). (A-I) Left column contains schematics of the *Ist-5* regulatory fragment being test. The left-hand graphs show YFP expression in P6.p and descendants in otherwise wild-type animals. The right-hand graphs show YFP expression in P6.p and descendants in the presence of *arEx1080[lin-31p::lin12(intra)ΔP]*. The parental strain for all animals was *pha-1(e2123); arEx1080; arEx[Ist-5yfp]*. I scored progeny for *Ist-5yfp* expression and for presence of arEx1080.



**Figure 5.** *Ist-5p* transcriptional reporter with SunTag. (A) Top, schematic of *Ist-5(FL)p* reporter driving 2xnls-YFP fused to 10xGCNv4 repeats (Tanenbaum *et al.* 2014). (B) Images showing *arSi9[Ist-5p::2xnls-yfp-10xgcnv4]; arTi207[lin-31p::scFv-gfp]* expression in P5.p and P7.p (top) and descendants (bottom). (C) Images showing *arSi9[Ist-5p::2xnls-yfp-10xgcnv4]* expression (top) and *arTi207[lin-31p::scFv-gfp]* expression (bottom). Neither transgene produces visible expression on their own.



**Figure 6.** Nuclear Spot Assay. (A-C) Images of *arTi153[eft-3p::tagbfp-lacI]pha-1; lag-1::mKate2; arEx[lst-5p::yfp + LacO]* in P5.p, P6.p and P7.p (A'-C') Shows LAG-mKate2 expression. (A''-C'') Shows tagBFP-LacI expression. (A'''-C''') Shows merged image. Dots are indicated by arrow. Nucleus is shown by dashed circle. (D) Representative VPC of *lag-1::mKate2; arEx[lst-5p::yfp + LacO]*. No LAG-1-mKate2 dots are formed in the absence of tagBFP-LacI. Images were taken as z-stacks with a spinning disc confocal microscope using similar settings. Images shown are z-projections.

**Table 1.** Summary of target arrays used in dot experiments and results.

LIN-12 target	arrays analyzed	LacI dot	LAG-1 dot
<i>lst-5(535)p::2xnl5-yfp</i>	3	yes	LAG-1-mKate2 and LIN-12(intra $\Delta$ P)-mKate2 formed dots w/ tagBFP-LacI. LAG-1-mKate2 did not form dots on without tagBFP-LacI being present
<i>lst-5(181)p::2xnl5-yfp</i>	3	yes	One array showed LAG-1-mKate2 dots in the presence of tagBFP-LacI Other arrays were not analyzed.
<i>lst-1</i> 1.5 kb 5' region	4	yes	LAG-1-GFP – no dot formation
<i>mir-61</i> 1 kb 5' region	2	yes	LAG-1-GFP – no dot formation
<i>lst-5(FL)p</i>	2	yes	LAG-1-GFP – no dot formation
<i>lst-5(FL3x<math>\Delta</math>LBS)p</i> 1kb 5' region	2	yes	LAG-1-GFP – no dot formation

## **Chapter 5. Discussion**

## Summary

In this thesis, I have described my investigation into the regulatory mechanisms that help integrate signaling events in the VPCs. The six VPCs receive many intercellular signals during their lifetime which cause them to be specified in an invariable spatial pattern. Two important signaling events are the activation of a canonical EGFR pathway to specify 1° fate and activation of LIN-12/Notch to specify the 2° fate. Several forms of crosstalk between EGFR and LIN-12/Notch have been previously observed in *C. elegans*. EGFR activation can inhibit LIN-12/Notch signaling by endocytic downregulation of LIN-12 (Levitan and Greenwald 1998b; Shaye and Greenwald 2002), and LIN-12/Notch activity can antagonize the EGFR-Ras-ERK pathway (Berset *et al.* 2001; Yoo and Greenwald 2005). My investigation adds to this body of work.

In Chapter 2, I investigated an EGFR-mediated mechanism that inhibits LIN-12/Notch activity in P6.p (Shaye and Greenwald 2005; Li and Greenwald 2010). I showed that this inhibition was not absolute, and that strong constitutive activation of LIN-12 produced by transgenes could inhibit transcriptional output of EGFR. I found that the resistance to comparatively weaker transgenic LIN-12/Notch activity required the combined activity of three factors: LIN-1, an Elk1-like Ets transcription factor; the Mediator subunit Med23 ortholog SUR-2, and the Mediator-regulatory module, the CKM (Fig. 1). I show that loss of *lin-1* results in expression of 1° and 2° reporters in all VPCs.

In Chapter 3, I investigated the regulation of the CSL protein, LAG-1. Endogenous CRISPR-engineered LAG-1 fusions were observed in a dynamic pattern in VPCs during specification (Fig. 2). During the L2 stage I observed that LAG-1 protein is present at a basal level uniformly in all VPCs. LAG-1 accumulation increases in P5.p and P7.p relative to the other VPCs, a pattern that I propose to be due to activation of LIN-12.

In Chapter 4, I attempted two different experimental techniques to determine the molecular mechanism of the EGFR-mediated resistance of LIN-12 activity in P6.p. I performed a deletion analysis of the 5' cis-regulatory region of *Ist-5*, a direct LIN-12 target, and identified a portion required for transcriptional repression in P6.p. I attempted to directly visualize the

formation and DNA-binding activity of the LIN-12-LAG-1 transcriptional activation complex *in vivo*. Ultimately, both approaches were stymied by technical issues; however, the single-copy transgenes *arTi102[lin-31p::lin-12(intraΔP)]* and *arTi190[lin-31p::lin-12(intraΔP)-mkate2]* used in Chapter 2, and the *lag-1(611[lag-1::gfp])* and *lag-1(ar613[lag-1::mkate2])* alleles used in Chapter 3 were originally generated for use in these experiments.

## **EGFR-mediated resistance to LIN-12 activity in P6.p**

Previous studies have reported that activation of EGFR-Ras causes P6.p to be refractory to constitutive LIN-12/Notch activity (Greenwald *et al.* 1983a; Sternberg and Horvitz 1989; Shaye and Greenwald 2005; Li and Greenwald 2010). These include observations that the 1<sup>o</sup>-fate reporter, *ayls4[egl-17p::gfp]*, continued to be expressed in the presence of constitutive LIN-12/Notch activity (Shaye and Greenwald 2005). These data suggested that a block to LIN-12 activity was established in P6.p by EGFR activity.

In Chapter 2, we characterized this phenomenon further using three different transgenes to provide constitutively active LIN-12(*intraΔP*) to the VPCs. When we used the multi-copy transgene *arEx1080[lin-31p::lin-12(intraΔP)]* we saw expression of a 1<sup>o</sup>-fate marker, while a 2<sup>o</sup>-fate marker was not expressed in P6.p. These observations were consistent with the previous reports of an EGFR-mediated block of LIN-12 activity. However, when we used the single-copy transgenes *arTi102[lin-31p::lin-12(intraΔP)]*, and *arTi190[lin-31p::lin-12(intraΔP)-mkate2]*, we saw that 1<sup>o</sup>-fate marker expression was inhibited, while a 2<sup>o</sup>-fate marker was expressed in P6.p. These results suggested that the EGFR-mediated block had been overwhelmed and led us to recharacterize the phenomenon as “resistance” to LIN-12 activity to better describe our observations. It also suggested that resistance in P6.p is part of a mechanism for ensuring robust lateral signaling.

We interpreted these observations as indicating that overwhelming of the resistance in P6.p by the single-copy transgene was due to higher LIN-12(*intraΔP*) activity. It would be interesting to compare “activity” of LIN-12(*intraΔP*) to levels of LIN-12(*intraΔP*) protein. Typically in our hands, single-copy transgenes express at lower levels than multi-copy extrachromosomal

arrays do--for examples see (Deng 2016) or (Chapter 4)--and it could be possible that *arEx1080* represents a “sweet spot” of LIN-12(intra $\Delta$ P) levels. The *lin-12(d)* alleles are dosage dependent (Greenwald *et al.* 1983a), and we could test the resistance to LIN-12 activity in P6.p using *arTi102/+* or *arTi190/+*, to see if the LIN-12 activity decreases when these transgenes are heterozygous, although it is not clear that this would necessarily result in lower expression from the transgene, and a negative result would provide much information. The timing of LIN-12 expression is also potentially relevant, and it could be that the single-copy transgenes express LIN-12(intra $\Delta$ P) sooner and more consistently than the multi-copy transgene, *arEx1080*, which allows LIN-12-dependent negative EGFR-Ras-ERK regulators to activate before resistance to LIN-12 is able to be established.

These are difficult questions to answer with our current complement of transgenes. An ideal way to address this would be to generate new transgenes, or endogenously tag the *lin-12* locus, with an auxin-inducible degradation (AID) tag (Zhang *et al.* 2015). This system allows for inducible and efficient removal of tagged proteins in a tissue specific manner. Using this system, we could better understand how absolute levels and timing of activated LIN-12 affects VPC fate specification.

## **Interactions of EGFR and LIN-12/Notch signaling in other contexts**

EGFR and LIN-12/Notch signaling are repeatedly used in developmental processes. It is unsurprising then that these two signaling mechanisms intersect in a variety of developmental contexts. Elucidating the mechanisms behind these interactions has been challenging because they are highly context dependent. Ultimately, we would like to understand the factors that govern the outcome of an interaction between EGFR and LIN-12/Notch. Below, I discuss several contexts in which EGFR and Notch signaling interact.

EGFR and Notch signaling often interact in series, where EGFR or Notch signaling in one cell leads to activation of the other pathway in a neighboring cell. In the VPCs, the LIN-3/EGF signal received by P6.p alleviates transcriptional repression of LIN-12/Notch ligands, thus activating LIN-12 in neighboring cells (Chen and Greenwald 2004; Zhang and Greenwald 2010).



The reverse interaction occurs during *C. elegans* excretory tube development: LIN-12/GLP-1/Notch signaling is required to specify the canal cell which subsequently produces LIN-3/EGF ligand leading to specification of the excretory duct cell via EGFR-Ras activation (Abdus-Saboor *et al.* 2011).

It is unknown whether *lin-3* is a direct target of LIN-12/GLP-1/Notch activity in the canal cell; however, it is informative to contrast this interaction with AC/VU development. Expression from the transcriptional reporter *syIs107*, containing a *lin-3* enhancer element driving *gfp*, is upregulated in the canal cell (Abdus-Saboor *et al.* 2011) and the AC, but not seen in the VUs (Hwang and Sternberg 2004). The simplest explanation for these observations is that *syIs107* is not transcriptionally regulated via direct binding of LAG-1, and therefore suggests that *lin-3* is not a direct target of LIN-12 or GLP-1 in the canal cell. Further testing is required to determine whether *syIs107* accurately reports *lin-3* expression and to validate this hypothesis.

The developing *Drosophila* eye ommatidia is another paradigm for studying the intersection of Notch and EGF signaling. Ommatidia develop within clusters of evenly spaced precursor cells. A mature ommatidium consists of eight photoreceptors (R1-R8), four cone cells, several pigment cells, and a mechanosensory complex [reviewed in Kumar 2012]. Prior to differentiation, Notch signaling in uncommitted cells inhibits expression of proneuronal genes, such as the bHLH gene *atonal* (*ato*), until a single cell is specified to become R8 via Notch lateral inhibition. Expression of *ato* in R8 leads to the transcriptional activation of genes that allow for the secretion of the EGF-Ligand Spitz (Spi). This is analogous to the AC/VU decision, in which the cell that does not receive LIN-12/Notch signaling produces EGF ligand.

Following R8 specification, the remaining photoreceptors are specified in a stereotyped pattern. Spi/EGF induces the immediate neighbors of R8 to differentiate into the R2 and R5 photoreceptor pair. R2 and R5 then secrete Spi which induces their immediate neighbors to differentiate into R3 and R4, respectively. Following a round of division by undifferentiated cells, R1 and R6 are specified in an EGFR dependent manner.

The differentiation of R1-R6 are, in general, examples of sequential signaling events: Notch signaling is initially required to prevent precocious photoreceptor differentiation followed by iterative EGFR signaling events which promote photoreceptor fate. The specification of R7, however, requires parallel input from EGFR and Notch, along with input from the RTK Sevenless (*sev*) (Cooper and Bray 2000; Tomlinson and Struhl 2001). A loss of Notch signaling in a R7 precursor causes it to be specified as a R1/R6 cell, whereas ectopic Notch activation in R1/R6 precursors promotes R7 differentiation (Tomlinson et al 2011).

Signaling by the Notch ligand Delta (*DI*) on the adjacent R1/R6 cells activates Notch in the presumptive R7 cell, promoting R7 differentiation (Cooper and Bray 2000; Tomlinson and Struhl 2001). Interestingly, in contrast to the VPCs, EGFR activity in photoreceptors drives upregulation of *DI* by relieving Su(H)-mediated repression of *DI* transcription (Tsuda *et al.* 2002). In this instance, it was proposed that EGFR activity, together with the nuclear protein Strawberry Notch and F-box protein Ebi, causes the corepressor SMRTER to be translocated from the nucleus.

It is conceivable that EGFR activity could upregulate genes via relief of LAG-1-mediated repression in *C. elegans*, although the available evidence is circumstantial. My analysis in Chapter 3 showed that LAG-1 is present in P6.p during induction along with SEL-10, which shares homology with Ebi. An investigation of *let-765*, a *C. elegans* Strawberry Notch homolog, found that a fosmid-based *let-765* transcriptional reporter was expressed in all VPCs and provides evidence that *let-765* promotes vulval induction (Simms and Baillie 2010); however, the investigators did not determine a cellular focus of action for *let-765* in vulval induction, and the loss-of-function vulval phenotype may be related to *let-765* activity in the AC. Additionally, SMRTER is not conserved in *C. elegans* and a LAG-1-associated corepressor that acts in the VPCs has not yet been identified. Interestingly, a computational screen identified a candidate gene that could be regulated by such a mechanism.

A screen for LIN-12/Notch target genes identified conserved LAG-1 binding sites (LBSs) in the 2 kb 5'-flanking region of the gene *Y46G5A.1/tbc-17*. A transcriptional reporter, containing

the immediate 4.9 kb 5'-flanking region of *tbc-17* driving *2xnl5-yfp*, was reported to be expressed at a basal level in all VPCs and upregulated specifically in P6.p following induction (Choi 2009). This observation is consistent with EGFR-dependent relief of LAG-1-mediated repression. An alternative explanation is that EGFR activity upregulate or activates some transcription factor required for *tbc-17* upregulation. Elk1 is a potential candidate, and a scan of the 2kb 5'-flanking region reveals a number of Elk1 consensus sequences. This explanation does not necessarily rule out a repressive role for LAG-1, and there are other examples of genes that are transcriptionally regulated by downstream effectors of both Notch and EGFR signaling.

Transcriptional activation of *D-Pax2* (also known as *shaven* and *sparkling*) in Cone Cell precursors requires parallel input of EGFR and Notch. In the absence of Notch and EGFR signaling *D-Pax2* is inhibited by Su(H) activity and the Ras-MAPK-target Ets factor Yan (Flores *et al.* 2000). Expression of *D-Pax2* requires Notch input to remove Su(H)-mediated repression, and EGFR input to alleviate Yan-mediated repression; EGFR activity also stimulates the activator Pointed-P2, another Ets factor (Flores *et al.* 2000; Swanson *et al.* 2010). While this type of regulatory mechanism has not been described in *C. elegans*, I discuss an example that shares some similarities below.

VPC expression from a transcriptional reporter, a 2.8 kb region upstream of *let-502* driving *nls-gfp*, was reported to be restricted to 2° VPCs. Like *D-Pax2*, this reporter required the presence of LIN-12/Notch activity and direct binding by an Ets-factor, LIN-1, for transcriptional activation (Farooqui *et al.* 2012). This investigation left many unanswered questions. For instance, it remains unclear what the mechanism for LIN-1-dependent transcriptional activation of this *let-502* reporter is, given that LIN-1 is predicted to be unphosphorylated and in repressor mode in a 2° VPC (Leight *et al.* 2015). A more thorough investigation into the transcriptional regulation of *let-502* and *tbc-17* may provide insight into how downstream targets of LIN-12/Notch and EGFR signaling are regulated.

## LIN-1 function in VPC specification

We found LIN-1 to be a critical factor in the establishment of resistance to LIN-12 activity in P6.p, and more generally for integrating LIN-12 and EGFR activity in the VPCs to produce discrete fates (discussed in more detail below). Our findings implicate SUR-2 and the CKM in the establishment of this resistance to LIN-12 activity as well; however, the mechanism of this resistance remains unknown.

One potential mechanism would be that these three factors function together to drive expression of a transcription factor that directly represses LIN-12 targets. My deletion analysis experiments of *Ist-5* cis-regulatory sequences, described in Chapter 4, identified a 354 bp region in the first intron of *Ist-5* that is required for repression of *Ist-5* in P6.p. Unfortunately, I could not continue this line of experiments to identify a more specific region, or any specific motifs (discussed later). A cursory scan of the 354 bp repressive region for transcription factor consensus motifs (Weirauch *et al.* 2014), reveals several candidate transcription factors that could be tested. If our hypothesis is correct, that a LIN-1-SUR-2-CKM complex transcriptionally activates a repressor that acts via a site in the 354 bp region, then we can narrow the list of candidate transcription factors by searching for putative LIN-1 binding sites, using the conserved Elk1 consensus sequences (Wei *et al.* 2010), or the less-stringent Ets core binding motif (Miley *et al.* 2004). We hypothesize that a LIN-1-SUR-2 complex is necessary for endocytic downregulation of LIN-12 in P6.p (Shaye and Greenwald 2002; Shaye and Greenwald 2005)(Chapter 2), and a comprehensive search for genes that contain LIN-1/Elk1 motifs may also help identify genes involved in this process.

Another possibility is that LIN-12 targets are repressed by LAG-1. Recent studies have identified phosphorylation sites in Su(H) that reduce DNA-binding affinity (Nagel *et al.* 2017), and ERK-directed phosphorylation sites that reduce the ability of Su(H) to transcriptionally activate target gene (Auer *et al.* 2015) when phosphorylated. These sites are conserved in LAG-1, and represent candidates for mutational analysis; however, transcriptional repression mediated by post-translational modification of LAG-1 does not account for the requirement of LIN-1, SUR-2,

and the CKM in the EGFR-mediated block in P6.p. A LIN-12-SUR-2-CKM complex could transcriptionally activate a co-repressor that interacts with LAG-1, and provides an additional reason to identify genes that are positively regulated by LIN-1.

### **LIN-1 integrates EGFR and LIN-12/Notch signaling in the VPCs**

*lin-1* has many roles in VPC specification. Lineage analysis of *lin-1* null mutants suggested that VPCs might be specified in an alternating 1<sup>o</sup>-2<sup>o</sup> pattern (Ferguson *et al.* 1987; Beitel *et al.* 1995), consistent with the pattern caused by mutations that ectopically activate the EGFR pathway. Beitel *et al.* (1995), however, noted the ambiguous nature of many lineages they observed, and indicated the presence of many “hybrid” fates. Transcriptional activation of lateral signal genes in 1<sup>o</sup> VPCs, does not require positive input from *lin-1* (Zhang and Greenwald 2011). While other studies showed that *lin-1* activity was required for expression of the 1<sup>o</sup>-fate marker *ayls4[egl-17::gfp]* (Tiensuu *et al.* 2005), this requirement does not appear to be direct (Cui and Han 2003). Genetic experiments revealed a positive role for *lin-1* in 1<sup>o</sup>-fate adoption redundant with the transcription factors *eor-1* and *eor-2* (Howard and Sundaram 2002).

We found two different 2<sup>o</sup>-fate reporters, both direct transcriptional targets of LIN-12, to be expressed in all VPCs in the absence of LIN-1. Expression of 2<sup>o</sup>-fate markers was not observed in a *lin-12(0); lin-1(0)* background, indicating that this expression in a *lin-1* mutant background still depends on LIN-12 activity. Additionally, normal endocytic downregulation of LIN-12-GFP in P6.p was not observed in *lin-1* mutants. Combined with the observations that 1<sup>o</sup>-fate markers are expressed in all VPCs (Zhang and Greenwald 2011), this suggests that VPCs have 1<sup>o</sup>- and 2<sup>o</sup>-fate characteristics in a *lin-1(0)* background, and is consistent with the hybrid fates described by (Beitel *et al.* 1995). We interpret this as indication that *lin-1* is a critical component for integration of EGFR and LIN-12 signaling.

### **Potential for autoregulation of *lag-1***

In *Drosophila* bristle cell development, high levels of Su(H) in the socket cell were found to be important for bristle physiology (Barolo *et al.* 2000). They found that levels of Su(H) above a certain threshold were required to initiate positive autoregulation, that is where high levels of

Su(H) could drive its own expression, without the requirement of activated Notch (Barolo *et al.* 2000; Liu and Posakony 2014). In *C. elegans* two cells are equally competent to adopt the fate of the AC or the VU (Sulston and Horvitz 1977). This is a stochastic decision determined by LIN-12 activity (Seydoux and Greenwald 1989). It has been observed that *lin-12* expression increases in the presumptive VU due to LIN-12 activation (Wilkinson *et al.* 1994), and *lag-1* and *lin-12* have been predicted to positively regulate each other and themselves (Wilkinson *et al.* 1994; Christensen *et al.* 1996). I observed LAG-1 protein levels to be low prior to AC/VU specification, and to rise in the presumptive VU rise and fall in the presumptive AC. This observation mirrors the expression pattern of *lin-12* and is consistent with LAG-1 autoregulation. Similarly, I observed that during VPC specification, LAG-1 accumulation correlated with LIN-12 activation. What is not known is whether the high levels of LAG-1 are sufficient to continue driving expression of *lag-1* without continued input from LIN-12 signaling.

An investigation of a transcriptional reporter of a roughly 1.5 kb sequence from the first intron of *lag-1* was reported to show an expression pattern (Choi *et al.* 2013) similar to the accumulation pattern of LAG-1-mKate2 in the AC/VU decision that I described in Chapter 3. This group showed that a cluster of LBSs in this transcriptional reporter was required for increased expression in the VUs, and reported similar observations using a *lin-12* transcriptional reporter. They proposed that LAG-1 represses *lin-12* and *lag-1* expression in the AC and promotes expression in the VU due to Notch activation (Choi *et al.* 2013; Park *et al.* 2013). This mirrors my observations of LAG-1-mKate2 accumulation in the AC/VU, and is consistent with my observations of LAG-1-mKate2 accumulation during VPC fate specification and with Su(H) accumulation in *Drosophila* lateral inhibition and socket cell specification. We could investigate this by generating an AID tag into the endogenous *lag-1* locus. This would allow us to knock-down LAG-1 specifically in the VUs or VPCs after specification has occurred, and test whether high LAG-1 levels need to be maintained in the VUs and 2° VPCs.

Another way to examine LAG-1 autoregulation, would be to generate a transgene that produces background levels of LAG-1. In their work dissecting the cis-regulatory regions of Su(H)

(Barolo *et al.* 2000), they removed a cluster of Su(H) sites in the 3' cis-regulatory region of a *Su(H)* rescue transgene. This transgene was able to rescue the *Su(H)* null phenotype, but was not expressed at high levels in the socket cell, thus allowing them to separate transcriptional upregulation of *Su(H)* from Notch activation. It would be possible to perform a similar experiment in *C. elegans*. The 5' cis-regulatory sequence of *let-858* is ubiquitously expressed, including in the germline, at a low level compared to other ubiquitously expressed regulatory elements. We could generate a single-copy transgene into the LGI or LGII site, chromosomal loci known to be germline permissive, that drives LAG-1 cDNA expression using the *let-858* regulatory sequence and test for rescue of a *lag-1* mutant. If this transgene rescued the mutant, we would be able to delete endogenous regulatory elements of *lag-1* without produces lethality, and we could test different *lag-1* cis-regulatory elements for their requirement in VPC and AC/VU specification.

### **Potential for different LAG-1 isoforms to affect VPC**

The first set of transgenic LAG-1 translational reporters I constructed contained *mcherry* inserted in-frame at the 5' end of what is now known to be the LAG-1a isoform. Two transgenes I examined did not produce a consistent expression pattern and was rarely visible in the VPCs or their descendants; however, both transgenes rescued *lag-1* null lethality. As discussed in Chapter 3, the inability to visualize LAG-1a could be due to issues with expression from multi-copy arrays or could suggest that N-terminally tagged LAG-1 is not stable in the VPCs.

After I conducted these experiments, the *lag-1* gene structure prediction was updated and presented an intriguing new possibility: a new isoform, LAG-1d, was predicted, which has been partially confirmed through cDNA (WormBase)(Chapter 3, Fig. 1A). The 5' exon of *lag-1d* is approximately 7kb downstream of the transcriptional start site of *lag-1a*. The two isoforms share the seven distal-most exons, and the first *lag-1d* exon is spliced directly to these common exons. This gene structure suggests that transcription of the different isoforms is due to alternate promoter choice [reviewed by (Zahler 2005)]. In this instance, only the LAG-1a isoform would be tagged. Thus, if the untagged LAG-1d is the most abundant isoform, it would explain lack of visible mCherry and the observed rescue by this fosmid reporter.

Analysis of the protein sequence of LAG-1a and LAG-1d reveal that the common distal exons encode 535 amino acids and contain functional core domains, *i.e.* the BTD, CTD, and NTD. These core domains are well-conserved, in both primary-sequence and structure, amongst members of the CSL family (Kovall and Blacklow 2010). The N-terminal region of LAG-1a is 138 aa while the N-terminal region of LAG-1D is 255 aa; sequence alignment of these two regions shows little similarity. A similar gene structure has not been predicted at the *lag-1* homolog genomic locus of other nematode species. That is to say, the first exon of *lag-1d* is not predicted in other nematode species; however, there is some evidence that this may be conserved: multiple-sequence alignment of the *lag-1* genomic locus of several nematode species (UCSC genome browser) shows the first exon of *lag-1d* has an increased level of conservation, at the nucleotide sequence level, compared to surrounding intronic regions; the consensus “GU” splice-donor dinucleotide of the 5' *lag-1d* exon is absolutely conserved across seven nematode species; and the top hits of tblastn searches of the LAG-1d N-terminal 255 aa sequence in the genomes of *C. brenneri*, *C. briggsae*, and *C. japonica* indicate the presence of an analogous *lag-1d* 5' exon in these species. (A tblastn searches a nucleotide database using a protein query.) These data provide evidence that the *lag-1d* isoform has been conserved in nematodes. I did not analyze the *lag-1* genomic loci of other species for the presence of ORFs in the putative *lag-1d* region.

The LAG-1d cDNA has been partially confirmed in WormBase. To verify this isoform, conventional methods like RT-PCR and 5' RACE could be used to isolate cDNA from whole animals; however, with the CRISPR techniques, the most efficient method may be to endogenously tag *lag-1d* at the 5' end. In general, the self-excising cassette (SEC) method described by (Dickinson *et al.* 2015) generates a conditional null allele when used to generate N-terminal tags, prior to excision of the SEC. In cases like *lag-1* which I suspect may have isoforms with different transcriptional start sites, this method would generate an isoform specific null. This approach would allow us to analyze the accumulation pattern of LAG-1d, and to query whether *lag-1d* is an essential isoform of *lag-1*.



Whether a LAG-1d isoform would be regulated differently or function differently than the LAG-1A isoform is difficult to predict. The N-terminal regions of CSL proteins in general are highly divergent in sequence, and there is no structural information (Kovall and Blacklow 2010). Consistent with this, there is little sequence conservation found the N-terminal regions of nematode LAG-1 homologs. This rapid divergence could indicate that the N-terminal regions have no important function, or it could indicate a regulatory region. The N-terminal regions of metazoan CSL proteins have not been found to have a function. Although Notch signaling is not conserved in fungus, homologous CSL genes and proteins have been identified in many fungal species, including *Schizosaccharomyces pombe* (Převorovský *et al.* 2007). Two CSL homologs in *S. pombe* have been shown to bind to a similar recognition motif and, notably, their N-terminal regions are enriched for phosphorylation sites and degradation domains, *i.e.* PEST domains (Převorovský *et al.* 2011).

Cursory bioinformatic searches for regulatory features, *e.g.* ubiquitination sites, nuclear localization signals (NLSs), PEST domains, phosphorylation sites, have not yielded any convincing results. For instance, I used two online NLS prediction tools, seqNLS and NLS mapper. NLS mapper predicts a strong monopartite NLS in the LAG-1A N-terminal region, and a weak bipartite NLS in LAG-1d; neither of these sites were predicted by seqNLS. A more comprehensive bioinformatic scan may reveal some motif of interest; however, confirming that the different LAG-1 isoforms are regulated differently, or have different requirements in development should be determined first.



















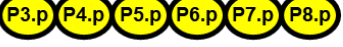

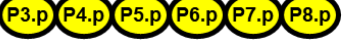




### **Issues resulting from use of multi-copy arrays**

My experiments using fosmid-based LAG-1 translational reporters did not see LAG-1 accumulation in the same pattern as the endogenous tags. The inability to visualize N-terminal mCherry-LAG-1 fusion may have other explanations, as discussed above. The C-terminal LAG-1-GFP fusion, however, consistently produced high levels of LAG-1-GFP in P6.p. As discussed earlier, the repetitive nature and other variables inherent to extrachromosomal arrays could be a factor here. Another possibility could be that, since the fosmid-produced LAG-1-GFP in addition

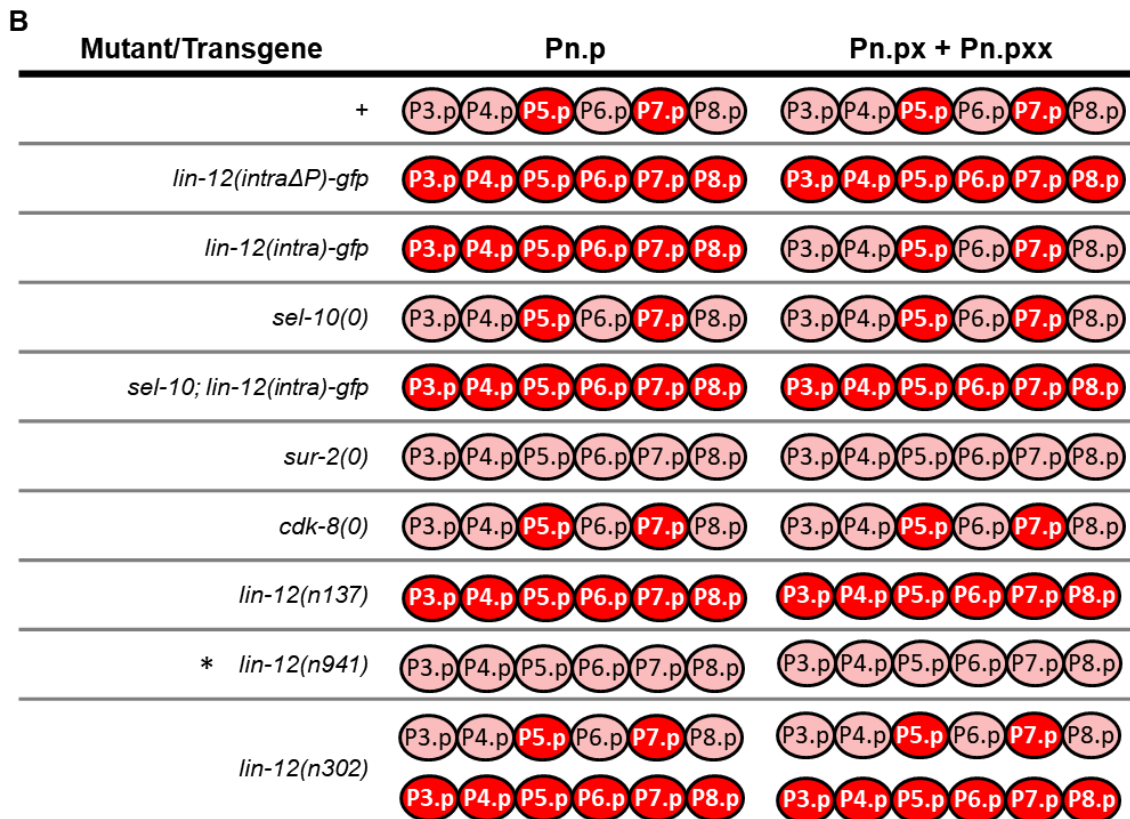
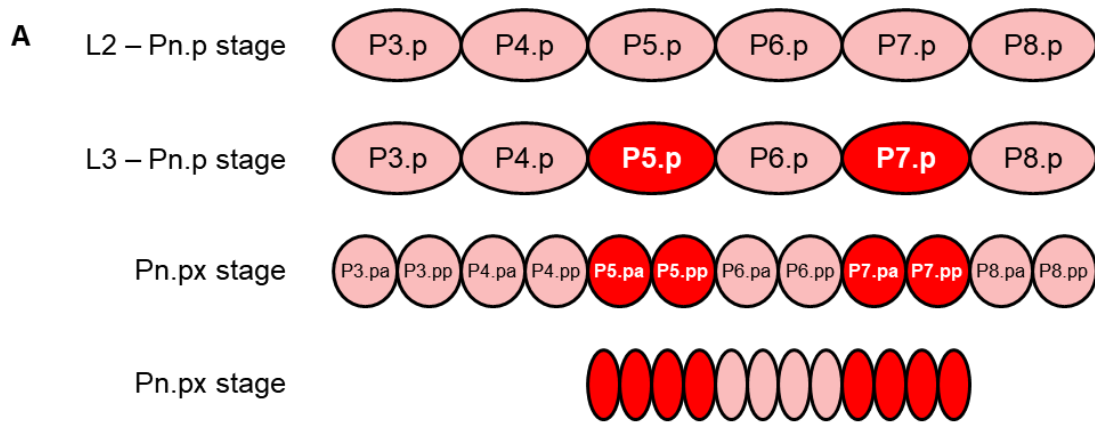
to endogenous LAG-1, the “extra” LAG-1-GFP could be ectopically activating LIN-12 target genes, including the *lag-1-gfp* fosmid gene itself, leading to high levels of LAG-1-GFP in P6.p. In *Drosophila*, it has been reported that repression of Notch targets by Hairless can be overcome by overexpression of Su(H) (Maier *et al.* 2013). It is interesting to note that animals carrying the LAG-1-GFP reporter fosmid arrays did not exhibit any noticeable defect in vulval induction, indicating that higher levels of LAG-1 in P6.p may not be deleterious to vulval induction. Additionally, it could suggest that LAG-1 levels are not regulated post-translationally, although it could be that the high levels of LAG-1-GFP are swamping a degradation system.

The dissection of the *Ist-5* regulatory sequences was also hindered by the use of multi-copy repetitive arrays. The reporter arrays exhibited many problems, most prominent were the variability of fluorescent reporter expression from transgene to transgene, and animal to animal. These variabilities made it difficult to score fluorescent expression in a consistent manner and to make accurate comparisons of different transgenes. This may be due to the *Ist-5* regulatory sequence itself. Fosmid-based LST-5-GFP reporter arrays did not produce visible expression. Single-copy *Ist-5p-2xnl5-yfp* reporters, first miniMos, and then using site-directed insertion methods, reporters were extremely dim or not visible at all. In an attempt to boost the signal from single-copy insertion transgenes, I used a method called “SunTag” (Tanenbaum *et al.* 2014) to allow for detection of weak expression. The SunTag amplification method worked, however a site-directed *Ist-5p::2xnl5-yfp-10xsuntag* was expressed in all VPCs and not in the LIN-12 dependent 2<sup>o</sup>-fate pattern, effectively ending this experimental pathway. The uniform pattern may be the result of the SunTag single-chain antibody stabilizing the epitope-tagged YFP. A CRISPR based method to tag *Ist-5* at the endogenous locus may be helpful, but my experiences thus far with endogenously tagged genes, and *Ist-5* reporters suggest that expression of an endogenous *Ist-5* reporter would be exceedingly dim. Due to this, I would endogenously tag LST-5 with a SunTag epitope to amplify the signal.

# Chapter 5. Figures

Genotype	No transgene	LIN-12-intra $\Delta$ P
<i>wt</i>		
<i>lin-1(0)</i>		No Data
<i>lin-1(gf)</i>		
<i>sur-2(0)</i>		
<i>cdk-8(0)</i>		
<i>cic-1(0)</i>		
<i>let-19(0)</i>		
<i>mdt-28(0)</i>		
<i>mdt-29(0)</i>		
<i>mdt-26(0)</i>		
<i>lin-31(0)</i>		
<i>lin-31(4T-&gt;A)</i>		
<i>lin-31(4T-&gt;E)</i>		

**Figure 1.** Summary of *arls116[lst-5p::2xnl5-yfp]* expression pattern in the absence and presence of activated LIN-12 provided by *arEx1080[lin-31p::lin-12(intra $\Delta$ P)]* for different mutant backgrounds. The following alleles were used: *lin-1(n304)*, *lin-1(n1790)*, *sur-2(ku9)*, *cdk-8(tm1238)*, *cic-1(tm3740)*, *let-19(os33)*, *mdt-28(tm1704)*, *mdt-29(tm2893)*, *mdt-26(tm6272)*, *lin-31(n301)*, *lin-31(cp1)*, *lin-31(cp3)*



**Figure 2.** Summary of LAG-1-mKate2 accumulation during development in different mutant backgrounds. (A) Summary of LAG-1-mKate2 accumulation in *wildtype* VPCs. During the L2 stage, LAG-1-mKate is initially equivalent in all VPCs at a basal level. During the L3 stage following induction, LAG-1-mKate2 levels in P5.p and P7.p are elevated in comparison to the remaining VPCs. This LAG-1-mKate2 accumulation pattern is maintained in the VPC daughters. Following the fusion of non-vulval VPC daughters with Hyp7, LAG-1-mKate2 levels remains

elevated in descendants of P5.p and P7.p compared to those of P6.p.(B) Summary of LAG-1-mKate2 accumulation patterning in VPCs compared to VPC descendants in several mutant and transgenic backgrounds. The following alleles were used: *sel-10(ok1632)*, *sur-2(ku9)*, *cdk-8(tm1238)*, *lin-12(n137)*, *lin-12(n302)*, *lin-12(n941)*. The following transgenes were used: *arTi120[lin-12(intra $\Delta$ P)-gfp]*, *arTi54[lin-12(intra)-gfp]*. *lin-12(n941)* animals were maintained over a derivative of *qC1* containing a GFP marker; *lin-12(n941)* homozygotes were selected by loss of GFP marker.

# References

- Ahier, A., and S. Jarriault, 2014 Simultaneous expression of multiple proteins under a single promoter in *Caenorhabditis elegans* via a versatile 2A-based toolkit. *Genetics* 196: 605-613.
- Akoulitchev, S., S. Chuikov and D. Reinberg, 2000 TFIID is negatively regulated by cdk8-containing mediator complexes. *Nature* 407: 102-106.
- Allen, B. L., and D. J. Taatjes, 2015 The Mediator complex: a central integrator of transcription. *Nature reviews. Molecular cell biology* 16: 155-166.
- Andersson, E. R., R. Sandberg and U. Lendahl, 2011 Notch signaling: simplicity in design, versatility in function. *Development* 138: 3593.
- Aroian, R. V., M. Koga, J. E. Mendel, Y. Ohshima and P. W. Sternberg, 1990 The *let-23* gene necessary for *Caenorhabditis elegans* vulval induction encodes a tyrosine kinase of the EGF receptor subfamily. *Nature* 348: 693-699.
- Auer, J. S., A. C. Nagel, A. Schulz, V. Wahl and A. Preiss, 2015 MAPK-dependent phosphorylation modulates the activity of Suppressor of Hairless in *Drosophila*. *Cellular Signalling* 27: 115-124.
- Bailey, A. M., and J. W. Posakony, 1995 Suppressor of hairless directly activates transcription of enhancer of split complex genes in response to Notch receptor activity. *Genes Dev* 9: 2609-2622.
- Barolo, S., T. Stone, A. G. Bang and J. W. Posakony, 2002 Default repression and Notch signaling: Hairless acts as an adaptor to recruit the corepressors Groucho and dCtBP to Suppressor of Hairless. *Genes Dev* 16: 1964-1976.
- Barolo, S., R. G. Walker, A. D. Polyanovsky, G. Freschi, T. Keil *et al.*, 2000 A notch-independent activity of suppressor of hairless is required for normal mechanoreceptor physiology. *Cell* 103: 957-969.
- Beitel, G. J., S. Tuck, I. Greenwald and H. R. Horvitz, 1995 The *Caenorhabditis elegans* gene *lin-1* encodes an ETS-domain protein and defines a branch of the vulval induction pathway. *Genes and Development* 9: 3149-3162.
- Berry, L. W., B. Westlund and T. Schedl, 1997 Germ-line tumor formation caused by activation of *glp-1*, a *Caenorhabditis elegans* member of the Notch family of receptors. *Development* 124: 925-936.
- Berset, T., E. F. Hoier, G. Battu, S. Canevascini and A. Hajnal, 2001 Notch inhibition of RAS signaling through MAP kinase phosphatase LIP-1 during *C. elegans* vulval development. *Science* 291: 1055-1058.
- Blumenthal, T., 2005 Trans-splicing and operons in *C. elegans*.
- Bond, S. R., and C. C. Naus, 2012 RF-Cloning. org: an online tool for the design of restriction-free cloning projects. *Nucleic acids research* 40: W209-W213.
- Borggreffe, T., and F. Oswald, 2009 The Notch signaling pathway: Transcriptional regulation at Notch target genes. *Cellular and Molecular Life Sciences* 66: 1631-1646.
- Boyer, T. G., M. E. Martin, E. Lees, R. P. Ricciardi and A. J. Berk, 1999 Mammalian Srb/Mediator complex is targeted by adenovirus E1A protein. *Nature* 399: 276-279.



- Bray, S. J., 2016 Notch signalling in context. *Nature Reviews Molecular Cell Biology* 17: 722-735.
- Brenner, S., 1974 The genetics of *Caenorhabditis elegans*. *Genetics* 77: 71-94.
- Brou, C., F. Logeat, M. Lecourtois, J. Vandekerckhove, P. Kourilsky *et al.*, 1994 Inhibition of the DNA-binding activity of *Drosophila* suppressor of hairless and of its human homolog, KBF2/RBP-J kappa, by direct protein-protein interaction with *Drosophila* hairless. *Genes & Development* 8: 2491-2503.
- Burdine, R. D., C. S. Branda and M. J. Stern, 1998 EGL-17(FGF) expression coordinates the attraction of the migrating sex myoblasts with vulval induction in *C. elegans*. *Development* 125: 1083.
- Carmi, I., J. B. Kopczyński and B. J. Meyer, 1998 The nuclear hormone receptor SEX-1 is an X-chromosome signal that determines nematode sex. *Nature* 396: 168-173.
- Castro, B., S. Barolo, A. M. Bailey and J. W. Posakony, 2005 Lateral inhibition in proneural clusters: cis-regulatory logic and default repression by Suppressor of Hairless. *Development* 132: 3333-3344.
- Chang, C., N. A. Hopper and P. W. Sternberg, 2000 *Caenorhabditis elegans* SOS-1 is necessary for multiple RAS-mediated developmental signals. *EMBO J* 19: 3283-3294.
- Chen, N., and I. Greenwald, 2004 The Lateral Signal for LIN-12/Notch in *C. elegans* Vulval Development Comprises Redundant Secreted and Transmembrane DSL Proteins. *Developmental Cell* 6: 183-192.
- Choi, M. S., 2009 Genes that act in specification of the vulval secondary fate in *Caenorhabditis elegans*, pp. 262. Columbia University, Ann Arbor.
- Choi, S. H., T. E. Wales, Y. Nam, D. O'Donovan, P. Sliz *et al.*, 2012 Conformational locking upon cooperative assembly of Notch transcription complexes. *Structure*(London, England:1993) 20: 340-349.
- Choi, V. N., S. K. Park and B. J. Hwang, 2013 Clustered LAG-1 binding sites in lag-1/CSL are involved in regulating lag-1 expression during lin-12/Notch-dependent cell-fate specification. *BMB reports* 46: 219-224.
- Christensen, S., V. Kodoyianni, M. Bosenberg, L. Friedman and J. Kimble, 1996 lag-1, a gene required for lin-12 and glp-1 signaling in *Caenorhabditis elegans*, is homologous to human CBF1 and *Drosophila* Su(H). *Development* 122: 1373-1383.
- Clark, S. G., A. D. Chisholm and H. R. Horvitz, 1993 Control of cell fates in the central body region of *C. elegans* by the homeobox gene lin-39. *Cell* 74: 43-55.
- Clark, S. G., M. J. Stern and H. R. Horvitz, 1992 *C. elegans* cell-signalling gene sem-5 encodes a protein with SH2 and SH3 domains. *Nature* 356: 340-344.
- Clayton, J. E., S. J. L. van den Heuvel and R. M. Saito, 2008 Transcriptional control of cell-cycle quiescence during *C. elegans* development. *Developmental Biology* 313: 603-613.
- Cochella, L., and O. Hobert, 2012 Embryonic priming of a miRNA locus predetermines postmitotic neuronal left/right asymmetry in *C. elegans*. *Cell* 151: 1229-1242.

- Cubas, P., J. F. de Celis, S. Campuzano and J. Modolell, 1991 Proneural clusters of achaete-scute expression and the generation of sensory organs in the *Drosophila* imaginal wing disc. *Genes Dev* 5: 996-1008.
- Cui, M., J. Chen, T. R. Myers, B. J. Hwang, P. W. Sternberg *et al.*, 2006 SynMuv genes redundantly inhibit lin-3/EGF expression to prevent inappropriate vulval induction in *C. elegans*. *Dev Cell* 10: 667-672.
- Cui, M., and M. Han, 2003 Cis regulatory requirements for vulval cell-specific expression of the *Caenorhabditis elegans* fibroblast growth factor gene egl-17. *Dev Biol* 257: 104-116.
- de la Cova, C., and I. Greenwald, 2012 SEL-10/Fbw7-dependent negative feedback regulation of LIN-45/braf signaling in *C. elegans* via a conserved phosphodegron. *Genes and Development* 26: 2524-2535.
- de la Cova, C., R. Townley, S. Regot and I. Greenwald, 2017 A Real-Time Biosensor for ERK Activity Reveals Signaling Dynamics during *C. elegans* Cell Fate Specification. *Developmental Cell*.
- de Souza, N., L. G. Vallier, H. Fares and I. Greenwald, 2007 SEL-2, the *C. elegans* neurobeachin/LRBA homolog, is a negative regulator of lin-12/Notch activity and affects endosomal traffic in polarized epithelial cells. *Development* 134: 691-702.
- Deng, Y., 2016 Novel negative regulation of LIN-12/Notch in *Caenorhabditis elegans*.
- Deng, Y., and I. Greenwald, 2016 Determinants in the LIN-12/Notch Intracellular Domain That Govern Its Activity and Stability During *Caenorhabditis elegans* Vulval Development. *G3: Genes|Genomes|Genetics* 6: 3663-3670.
- Dickinson, D. J., and B. Goldstein, 2016 CRISPR-Based Methods for *Caenorhabditis elegans* Genome Engineering. *Genetics* 202: 885-901.
- Dickinson, D. J., A. M. Pani, J. K. Heppert, C. D. Higgins and B. Goldstein, 2015 Streamlined Genome Engineering with a Self-Excising Drug Selection Cassette. *Genetics* 200: 1035-1049.
- Dickinson, D. J., J. D. Ward, D. J. Reiner and B. Goldstein, 2013 Engineering the *Caenorhabditis elegans* genome using Cas9-triggered homologous recombination. *Nat Methods* 10: 1028-1034.
- Doyle, T. G., C. Wen and I. Greenwald, 2000 SEL-8, a nuclear protein required for LIN-12 and GLP-1 signaling in *Caenorhabditis elegans*. *Proc Natl Acad Sci U S A* 97: 7877-7881.
- Eisenmann, D. M., J. N. Maloof, J. S. Simske, C. Kenyon and S. K. Kim, 1998 The beta-catenin homolog BAR-1 and LET-60 Ras coordinately regulate the Hox gene lin-39 during *Caenorhabditis elegans* vulval development. *Development* 125: 3667-3680.
- Fakhouri, T. H. I., J. Stevenson, A. D. Chisholm and S. E. Mango, 2010 Dynamic chromatin organization during foregut development mediated by the organ selector gene PHA-4/FoxA. *PLoS Genetics* 6.
- Farooqui, S., M. W. Pellegrino, I. Rimann, M. K. Morf, L. Müller *et al.*, 2012 Coordinated Lumen Contraction and Expansion during Vulval Tube Morphogenesis in *Caenorhabditis elegans*. *Developmental Cell* 23: 494-506.

- Felix, M. A., 2007 Cryptic quantitative evolution of the vulva intercellular signaling network in *Caenorhabditis*. *Curr Biol* 17: 103-114.
- Ferguson, E. L., and H. R. Horvitz, 1985 Identification and characterization of 22 genes that affect the vulval cell lineages of the nematode *Caenorhabditis elegans*. *Genetics* 110: 17-72.
- Ferguson, E. L., P. W. Sternberg and H. R. Horvitz, 1987 A genetic pathway for the specification of the vulval cell lineages of *Caenorhabditis elegans*. *Nature* 326: 259-267.
- Fitzgerald, K., H. A. Wilkinson and I. Greenwald, 1993 *glp-1* can substitute for *lin-12* in specifying cell fate decisions in *Caenorhabditis elegans*. *Development* 119: 1019-1027.
- Foehr, M. L., and J. Liu, 2008 Dorsoventral patterning of the *C. elegans* postembryonic mesoderm requires both LIN-12/Notch and TGFbeta signaling. *Dev Biol* 313: 256-266.
- Fortini, M. E., and S. Artavanis-Tsakonas, 1994 The suppressor of hairless protein participates in notch receptor signaling. *Cell* 79: 273-282.
- Freed, D. M., D. Alvarado and M. A. Lemmon, 2015 Ligand regulation of a constitutively dimeric EGF receptor. *6*: 7380.
- Friedland, A. E., Y. B. Tzur, K. M. Esvelt, M. P. Colaiacovo, G. M. Church *et al.*, 2013 Heritable genome editing in *C. elegans* via a CRISPR-Cas9 system. *Nat Methods* 10: 741-743.
- Friedmann, D. R., and R. A. Kovall, 2010 Thermodynamic and structural insights into CSL-DNA complexes. *Protein Science* 19: 34-46.
- Friedmann, D. R., J. J. Wilson and R. A. Kovall, 2008 RAM-induced allostery facilitates assembly of a notch pathway active transcription complex. *Journal of Biological Chemistry* 283: 14781-14791.
- Frøkjær-Jensen, C., M. W. Davis, M. Sarov, J. Taylor, S. Flibotte *et al.*, 2014 Random and targeted transgene insertion in *Caenorhabditis elegans* using a modified Mos1 transposon. *Nature Methods* 11: 529-534.
- Fryer, C. J., J. B. White and K. A. Jones, 2004 Mastermind Recruits CycC:CDK8 to Phosphorylate the Notch ICD and Coordinate Activation with Turnover. *Molecular Cell* 16: 509-520.
- Ghai, V., and J. Gaudet, 2008 The CSL transcription factor LAG-1 directly represses *hlh-6* expression in *C. elegans*. *Dev Biol* 322: 334-344.
- Gho, M., M. Lecourtois, G. Geraud, J. W. Posakony and F. Schweisguth, 1996 Subcellular localization of Suppressor of Hairless in *Drosophila* sense organ cells during Notch signalling. *Development* 122: 1673-1682.
- Gille, H., M. Kortjenann, O. Thomae, C. Moomaw, C. Slaughter *et al.*, 1995 ERK phosphorylation potentiates Elk-1-mediated ternary complex formation and transactivation. *EMBO J* 14: 951-962.
- Gille, H., A. D. Sharrocks and P. E. Shaw, 1992 Phosphorylation of transcription factor p62TCF by MAP kinase stimulates ternary complex formation at *c-fos* promoter. *Nature* 358: 414-417.

- Gleason, J. E., E. A. Szyleyko and D. M. Eisenmann, 2006 Multiple redundant Wnt signaling components function in two processes during *C. elegans* vulval development. *Developmental Biology* 298: 442-457.
- Grants, J. M., L. T. L. Ying, A. Yoda, C. C. You, H. Okano *et al.*, 2016 The mediator kinase module restrains epidermal growth factor receptor signaling and represses vulval cell fate specification in *Caenorhabditis elegans*. *Genetics* 202: 583-599.
- Greenwald, I., and R. Kovall, 2013 Notch signaling: genetics and structure. *WormBook*: 1-28.
- Greenwald, I., and G. Seydoux, 1990 Analysis of gain-of-function mutations of the *lin-12* gene of *Caenorhabditis elegans*. *Nature* 346: 197-199.
- Greenwald, I. S., P. W. Sternberg and H. R. Horvitz, 1983a The *lin-12* locus specifies cell fates in *caenorhabditis elegans*. *Cell* 34: 435-444.
- Greenwald, I. S., P. W. Sternberg and H. R. Horvitz, 1983b The *lin-12* locus specifies cell fates in *Caenorhabditis elegans*. *Cell* 34: 435-444.
- Gupta-Rossi, N., O. Le Bail, H. Gonen, C. Brou, F. Logeat *et al.*, 2001 Functional Interaction between SEL-10, an F-box Protein, and the Nuclear Form of Activated Notch1 Receptor. *Journal of Biological Chemistry* 276: 34371-34378.
- Haenlin, M., M. Kunisch, B. Kramatschek and J. A. Campos-Ortega, 1994 Genomic regions regulating early embryonic expression of the *Drosophila* neurogenic gene Delta. *Mech Dev* 47: 99-110.
- Han, M., A. Golden, Y. Han and P. W. Sternberg, 1993 *C. elegans* *lin-45* *raf* gene participates in *let-60* *ras*-stimulated vulval differentiation. *Nature* 363: 133-140.
- Han, M., and P. W. Sternberg, 1990 *let-60*, a gene that specifies cell fates during *C. elegans* vulval induction, encodes a *ras* protein. *Cell* 63: 921-931.
- Hart, A. H., R. Reventar and A. Bernstein, 2000 Genetic analysis of ETS genes in *C. elegans*. *Oncogene* 19: 6400-6408.
- Hermann, G. J., B. Leung and J. R. Priess, 2000 Left-right asymmetry in *C. elegans* intestine organogenesis involves a LIN-12/Notch signaling pathway. *Development* 127: 3429-3440.
- Hill, R. J., and P. W. Sternberg, 1992 The gene *lin-3* encodes an inductive signal for vulval development in *C. elegans*. *Nature* 358: 470-476.
- Hobert, O., 2011 Regulation of terminal differentiation programs in the nervous system. *Annual review of cell and developmental biology* 27: 681-696.
- Hopper, N. A., J. Lee and P. W. Sternberg, 2000 ARK-1 inhibits EGFR signaling in *C. elegans*. *Mol Cell* 6: 65-75.
- Horvitz, H. R., and J. E. Sulston, 1980 Isolation and genetic characterization of cell-lineage mutants of the nematode *Caenorhabditis elegans*. *Genetics* 96: 435-454.
- Howard, R. M., and M. V. Sundaram, 2002 *C. elegans* EOR-1/PLZF and EOR-2 positively regulate Ras and Wnt signaling and function redundantly with LIN-25 and the SUR-2 Mediator component. *Genes and Development* 16: 1815-1827.

- Howell, K., S. Arur, T. Schedl and M. V. Sundaram, 2010 EOR-2 is an obligate binding partner of the BTB-zinc finger protein EOR-1 in *Caenorhabditis elegans*. *Genetics* 184: 899-913.
- Hsieh, J. J. D., S. Zhou, L. Chen, D. B. Young and S. D. Hayward, 1999 CIR, a corepressor linking the DNA binding factor CBF1 to the histone deacetylase complex. *Proceedings of the National Academy of Sciences of the United States of America* 96: 23-28.
- Hu, P. J., 2007 Dauer. *WormBook: the online review of C. elegans biology*: 1-19.
- Hubbard, E. J., G. Wu, J. Kitajewski and I. Greenwald, 1997 *sel-10*, a negative regulator of *lin-12* activity in *Caenorhabditis elegans*, encodes a member of the CDC4 family of proteins. *Genes and Development* 11: 3182-3193.
- Jacobs, D., G. J. Beitel, S. G. Clark, H. R. Horvitz and K. Kornfeld, 1998 Gain-of-function mutations in the *Caenorhabditis elegans* *lin-1* ETS gene identify a C-terminal regulatory domain phosphorylated by ERK MAP kinase. *Genetics* 149: 1809-1822.
- Jacobs, D., D. Glossip, H. Xing, A. J. Muslin and K. Kornfeld, 1999 Multiple docking sites on substrate proteins form a modular system that mediates recognition by ERK MAP kinase. *Genes and Development* 13: 163-175.
- Kamath, R. S., and J. Ahringer, 2003 Genome-wide RNAi screening in *Caenorhabditis elegans*. *Methods* 30: 313-321.
- Karp, X., and I. Greenwald, 2013 Control of cell-fate plasticity and maintenance of multipotency by DAF-16/FoxO in quiescent *Caenorhabditis elegans*. *Proc Natl Acad Sci U S A* 110: 2181-2186.
- Katic, I., L. G. Vallier and I. Greenwald, 2005 New positive regulators of *lin-12* activity in *Caenorhabditis elegans* include the BRE-5/Brainiac glycosphingolipid biosynthesis enzyme. *Genetics* 171: 1605-1615.
- Keil, W., L. M. Kutscher, S. Shaham and E. D. Siggia, 2017 Long-Term High-Resolution Imaging of Developing *C. elegans* Larvae with Microfluidics. *Developmental Cell* 40: 202-214.
- Kim, H., T. Ishidate, K. S. Ghanta, M. Seth, D. Conte *et al.*, 2014 A Co-CRISPR strategy for efficient genome editing in *Caenorhabditis elegans*. *Genetics* 197: 1069-1080.
- Kimble, J., 1981 Alterations in cell lineage following laser ablation of cells in the somatic gonad of *Caenorhabditis elegans*. *Dev Biol* 87: 286-300.
- Kimble, J., and D. Hirsh, 1979 The postembryonic cell lineages of the hermaphrodite and male gonads in *Caenorhabditis elegans*. *Dev Biol* 70: 396-417.
- Knuesel, M. T., K. D. Meyer, C. Bernecky and D. J. Taatjes, 2009a The human CDK8 subcomplex is a molecular switch that controls Mediator coactivator function. *Genes and Development* 23: 439-451.
- Knuesel, M. T., K. D. Meyer, A. J. Donner, J. M. Espinosa and D. J. Taatjes, 2009b The human CDK8 subcomplex is a histone kinase that requires Med12 for activity and can function independently of mediator. *Molecular and Cellular Biology* 29: 650-661.
- Koch, U., and F. Radtke, 2011 Notch in T-ALL: new players in a complex disease. *Trends Immunol* 32: 434-442.

- Koppen, M., J. S. Simske, P. A. Sims, B. L. Firestein, D. H. Hall *et al.*, 2001 Cooperative regulation of AJM-1 controls junctional integrity in *Caenorhabditis elegans* epithelia. *Nat Cell Biol* 3: 983-991.
- Kornfeld, K., K. L. Guan and H. R. Horvitz, 1995 The *Caenorhabditis elegans* gene mek-2 is required for vulval induction and encodes a protein similar to the protein kinase MEK. *Genes Dev* 9: 756-768.
- Kovall, R. A., and S. C. Blacklow, 2010 Chapter Two - Mechanistic Insights into Notch Receptor Signaling from Structural and Biochemical Studies, pp. 31-71 in *Current Topics in Developmental Biology*, edited by K. Raphael. Academic Press.
- Kovall, R. A., B. Gebelein, D. Sprinzak and R. Kopan, 2017 The Canonical Notch Signaling Pathway: Structural and Biochemical Insights into Shape, Sugar, and Force. *Developmental Cell* 41: 228-241.
- Kovall, R. A., and W. A. Hendrickson, 2004 Crystal structure of the nuclear effector of Notch signaling, CSL, bound to DNA. *EMBO J* 23: 3441-3451.
- Kunisch, M., M. Haenlin and J. A. Campos-Ortega, 1994 Lateral inhibition mediated by the *Drosophila* neurogenic gene delta is enhanced by proneural proteins. *Proc Natl Acad Sci U S A* 91: 10139-10143.
- Kuroda, K., H. Han, S. Tani, K. Tanigaki, T. Tun *et al.*, 2003 Regulation of marginal zone B cell development by MINT, a suppressor of Notch/RBP-J signaling pathway. *Immunity* 18: 301-312.
- Lackner, M. R., and S. K. Kim, 1998 Genetic Analysis of the *Caenorhabditis elegans* MAP Kinase Gene *mpk-1*. *Genetics* 150: 103.
- Lackner, M. R., K. Kornfeld, L. M. Miller, H. R. Horvitz and S. K. Kim, 1994 A MAP kinase homolog, *mpk-1*, is involved in ras-mediated induction of vulval cell fates in *Caenorhabditis elegans*. *Genes Dev* 8: 160-173.
- Lambie, E. J., and J. Kimble, 1991 Two homologous regulatory genes, *lin-12* and *glp-1*, have overlapping functions. *Development* 112: 231-240.
- Larkin, M. A., G. Blackshields, N. P. Brown, R. Chenna, P. A. Mcgettigan *et al.*, 2007 Clustal W and Clustal X version 2.0. *Bioinformatics* 23: 2947-2948.
- Lecourtois, M., and F. Schweisguth, 1995 The neurogenic suppressor of hairless DNA-binding protein mediates the transcriptional activation of the enhancer of split complex genes triggered by Notch signaling. *Genes Dev* 9: 2598-2608.
- Leight, E. R., D. Glossip and K. Kornfeld, 2005 Sumoylation of LIN-1 promotes transcriptional repression and inhibition of vulval cell fates. *Development* 132.
- Leight, E. R., J. T. Murphy, D. A. Fantz, D. Pepin, D. L. Schneider *et al.*, 2015 Conversion of the LIN-1 ETS protein of *Caenorhabditis elegans* from a SUMOylated transcriptional repressor to a phosphorylated transcriptional activator. *Genetics* 199: 761-775.
- Lemmon, M. A., and J. Schlessinger, 2010 Cell Signaling by Receptor Tyrosine Kinases. *Cell* 141: 1117-1134.

- Levitan, D., and I. Greenwald, 1998a LIN-12 protein expression and localization during vulval development in *C. elegans*. *Development* 125: 3101-3109.
- Levitan, D., and I. Greenwald, 1998b LIN-12 protein expression and localization during vulval development in *C. elegans*. *Development* 125: 3101-3109.
- Li, J., 2011 *Temporal control of Vulval Precursor Cell fate patterning in Caenorhabditis elegans*. Columbia University.
- Li, J., and I. Greenwald, 2010 LIN-14 inhibition of LIN-12 contributes to precision and timing of *C. elegans* vulval fate patterning. *Current Biology* 20: 1875-1879.
- Li, N., A. Fassl, J. Chick, H. Inuzuka, X. Li *et al.*, 2014 Cyclin C is a haploinsufficient tumour suppressor. *Nature Cell Biology* 16: 1080-1091.
- Liu, F., and J. W. Posakony, 2014 An Enhancer Composed of Interlocking Sub-modules Controls Transcriptional Autoregulation of Suppressor of Hairless. *Developmental cell* 29: 88-101.
- Liu, W.-J., J. S. Reece-Hoyes, A. J. M. Walhout and D. M. Eisenmann, 2014 Multiple transcription factors directly regulate Hox gene *lin-39* expression in ventral hypodermal cells of the *C. elegans* embryo and larva, including the hypodermal fate regulators LIN-26 and ELT-6. *BMC Developmental Biology* 14: 17-17.
- Mahalak, K. K., A. M. Jama, S. J. Billups, A. T. Dawes and H. M. Chamberlin, 2017 Differing roles for *sur-2/MED23* in *C. elegans* and *C. briggsae* vulval development. *Dev Genes Evol* 227: 213-218.
- Maier, D., H. Praxenthaler, A. Schulz and A. Preiss, 2013 Gain of function notch phenotypes associated with ectopic expression of the Su(H) C-terminal domain illustrate separability of Notch and hairless-mediated activities. *PLoS One* 8: e81578.
- Maloof, J. N., and C. Kenyon, 1998 The Hox gene *lin-39* is required during *C. elegans* vulval induction to select the outcome of Ras signaling. *Development* 125: 181-190.
- Marais, R., J. Wynne and R. Treisman, 1993 The SRF accessory protein Elk-1 contains a growth factor-regulated transcriptional activation domain. *Cell* 73: 381-393.
- Mašek, J., and E. R. Andersson, 2017 The developmental biology of genetic Notch disorders. *Development* 144: 1743.
- Meister, P., S. Schott, C. Bedet, Y. Xiao, S. Rohner *et al.*, 2011 *Caenorhabditis elegans* Heterochromatin protein 1 (HPL-2) links developmental plasticity, longevity and lipid metabolism. *Genome Biol* 12: R123.
- Meister, P., B. D. Towbin, B. L. Pike, A. Ponti and S. M. Gasser, 2010 The spatial dynamics of tissue-specific promoters during *C. elegans* development. *Genes & development* 24: 766-782.
- Miley, G. R., D. Fantz, D. Glossip, X. Lu, R. M. Saito *et al.*, 2004 Identification of residues of the *Caenorhabditis elegans* LIN-1 ETS domain that are necessary for DNA binding and regulation of vulval cell fates. *Genetics* 167: 1697-1709.
- Miller, L. M., M. E. Gallegos, B. A. Morisseau and S. K. Kim, 1993 *lin-31*, a *Caenorhabditis elegans* HNF-3/fork head transcription factor homolog, specifies three alternative cell fates in vulval development. *Genes Dev* 7: 933-947.

- Mohler, W. A., G. Shemer, J. J. del Campo, C. Valansi, E. Opoku-Serebuoh *et al.*, 2002 The type I membrane protein EFF-1 is essential for developmental cell fusion. *Dev Cell* 2: 355-362.
- Morel, V., M. Lecourtois, O. Massiani, D. Maier, A. Preiss *et al.*, 2001 Transcriptional repression by Suppressor of Hairless involves the binding of a Hairless-dCtBP complex in *Drosophila*. *Current Biology* 11: 789-792.
- Mulligan, P., F. Yang, L. Di Stefano, J.-Y. Ji, J. Ouyang *et al.*, 2011 A SIRT1-LSD1 Co-repressor Complex Regulates Notch Target Gene Expression and Development. *Molecular cell* 42: 689-699.
- Myers, T. R., and I. Greenwald, 2005 *lin-35* Rb acts in the major hypodermis to oppose ras-mediated vulval induction in *C. elegans*. *Dev Cell* 8: 117-123.
- Myers, T. R., and I. Greenwald, 2007 Wnt signal from multiple tissues and *lin-3*/EGF signal from the gonad maintain vulval precursor cell competence in *Caenorhabditis elegans*. *Proceedings of the National Academy of Sciences of the United States of America* 104: 20368-20373.
- Nagel, A. C., J. S. Auer, A. Schulz, J. Pfannstiel, Z. Yuan *et al.*, 2017 Phosphorylation of Suppressor of Hairless impedes its DNA-binding activity. *Scientific Reports* 7: 11820.
- Nagel, A. C., A. Krejci, G. Tenin, A. Bravo-Patiño, S. Bray *et al.*, 2005 Hairless-mediated repression of notch target genes requires the combined activity of Groucho and CtBP corepressors. *Molecular and Cellular Biology* 25: 10433-10441.
- Nam, Y., P. Sliz, L. Song, J. C. Aster and S. C. Blacklow, 2006 Structural basis for cooperativity in recruitment of MAML coactivators to Notch transcription complexes. *Cell* 124: 973-983.
- Neves, A., K. English and J. R. Priess, 2007 Notch-GATA synergy promotes endoderm-specific expression of *ref-1* in *C. elegans*. *Development* 134: 4459-4468.
- Neves, A., and J. R. Priess, 2005 The REF-1 family of bHLH transcription factors pattern *C. elegans* embryos through Notch-dependent and Notch-independent pathways. *Dev Cell* 8: 867-879.
- Nilsson, L., X. Li, T. Tiensuu, R. Auty, I. Greenwald *et al.*, 1998 *Caenorhabditis elegans lin-25*: cellular focus, protein expression and requirement for *sur-2* during induction of vulval fates. *Development* 125: 4809-4819.
- Niu, W., Z. J. Lu, M. Zhong, M. Sarov, J. I. Murray *et al.*, 2011 Diverse transcription factor binding features revealed by genome-wide ChIP-seq in *C. elegans*. *Genome Res* 21: 245-254.
- Öberg, C., J. Li, A. Pauley, E. Wolf, M. Gurney *et al.*, 2001 The Notch Intracellular Domain Is Ubiquitinated and Negatively Regulated by the Mammalian Sel-10 Homolog. *Journal of Biological Chemistry* 276: 35847-35853.
- Oka, C., T. Nakano, A. Wakeham, J. L. de la Pompa, C. Mori *et al.*, 1995 Disruption of the mouse RBP-J kappa gene results in early embryonic death. *Development* 121: 3291.
- Oswald, F., U. Kostezka, K. Astrahantseff, S. Bourteele, K. Dillinger *et al.*, 2002 SHARP is a novel component of the Notch/RBP-Jkappa signalling pathway. *EMBO J* 21: 5417-5426.



- Park, S. K., V. N. Choi and B. J. Hwang, 2013 LIN-12/Notch regulates lag-1 and lin-12 expression during anchor cell/ventral uterine precursor cell fate specification. *Molecules and Cells* 35: 249-254.
- Patel, T., and O. Hobert, 2017 Coordinated control of terminal differentiation and restriction of cellular plasticity. *Elife* 6.
- Petcherski, A. G., and J. Kimble, 2000 LAG-3 is a putative transcriptional activator in the *C. elegans* Notch pathway. *Nature* 405: 364.
- Převorovský, M., S. R. Atkinson, M. Ptáčková, J. R. McLean, K. Gould *et al.*, 2011 N-Termini of Fungal CSL Transcription Factors Are Disordered, Enriched in Regulatory Motifs and Inhibit DNA Binding in Fission Yeast. *PLoS ONE* 6: e23650.
- Převorovský, M., F. Půta and P. Folk, 2007 Fungal CSL transcription factors. *BMC Genomics* 8: 233-233.
- Qiao, L., J. L. Lissemore, P. Shu, A. Smardon, M. B. Gelber *et al.*, 1995 Enhancers of glp-1, a gene required for cell-signaling in *Caenorhabditis elegans*, define a set of genes required for germline development. *Genetics* 141: 551-569.
- Ramos, A. I., and S. Barolo, 2013 Low-affinity transcription factor binding sites shape morphogen responses and enhancer evolution. *Philos Trans R Soc Lond B Biol Sci* 368: 20130018.
- Robinett, C. C., A. Straight, G. Li, C. Wilhelm, G. Sudlow *et al.*, 1996 In vivo localization of DNA sequences and visualization of large-scale chromatin organization using lac operator/repressor recognition. *The Journal of Cell Biology* 135: 1685.
- Rocheleau, C. E., R. M. Howard, A. P. Goldman, M. L. Volk, L. J. Girard *et al.*, 2002 A *lin-45* raf enhancer screen identifies *eor-1*, *eor-2* and unusual alleles of Ras pathway genes in *Caenorhabditis elegans*. *Genetics* 161: 121-131.
- Roiz, D., J. M. Escobar-Restrepo, P. Leu and A. Hajnal, 2016 The *C. elegans* hox gene *lin-39* controls cell cycle progression during vulval development. *Developmental Biology* 418: 124-134.
- Romani, S., S. Campuzano, E. R. Macagno and J. Modolell, 1989 Expression of achaete and scute genes in *Drosophila* imaginal discs and their function in sensory organ development. *Genes Dev* 3: 997-1007.
- Sallee, M. D., T. Aydin and I. Greenwald, 2015 Influences of LIN-12/Notch and POP-1/TCF on the Robustness of Ventral Uterine Cell Fate Specification in *Caenorhabditis elegans* Gonadogenesis. *G3: Genes|Genomes|Genetics* 5: 2775-2782.
- Sallee, M. D., and I. Greenwald, 2015 Dimerization-driven degradation of *C. elegans* and human E proteins. *Genes and Development* 29: 1356-1361.
- Salser, S. J., C. M. Loer and C. Kenyon, 1993 Multiple HOM-C gene interactions specify cell fates in the nematode central nervous system. *Genes Dev* 7: 1714-1724.
- Sarov, M., J. I. Murray, K. Schanze, A. Pozniakovski, W. Niu *et al.*, 2012 A genome-scale resource for in vivo tag-based protein function exploration in *C. elegans*. *Cell* 150: 855-866.
- Schindelin, J., I. Arganda-Carreras, I. Frise, V. Kaynig, M. Longair *et al.*, 2012 Fiji: an open-source platform for biological-image analysis. *Nature Methods* 9: 676-682.

- Schindelin, J., C. T. Rueden, M. C. Hiner and K. W. Eliceiri, 2015 The ImageJ ecosystem: An open platform for biomedical image analysis. *Molecular Reproduction and Development* 82: 518-529.
- Schmitz, C., P. Kinge and H. Hutter, 2007 Axon guidance genes identified in a large-scale RNAi screen using the RNAi-hypersensitive *Caenorhabditis elegans* strain *nre-1(hd20) lin-15b(hd126)*. *Proc Natl Acad Sci U S A* 104: 834-839.
- Schweisguth, F., 2015 Asymmetric cell division in the *Drosophila* bristle lineage: from the polarization of sensory organ precursor cells to Notch-mediated binary fate decision. *Wiley Interdiscip Rev Dev Biol* 4: 299-309.
- Schweisguth, F., and J. W. Posakony, 1992 Suppressor of Hairless, the *Drosophila* homolog of the mouse recombination signal-binding protein gene, controls sensory organ cell fates. *Cell* 69: 1199-1212.
- Schweisguth, F., and J. W. Posakony, 1994 Antagonistic activities of Suppressor of Hairless and Hairless control alternative cell fates in the *Drosophila* adult epidermis. *Development* 120: 1433-1441.
- Seydoux, G., and I. Greenwald, 1989 Cell autonomy of *lin-12* function in a cell fate decision in *C. elegans*. *Cell* 57: 1237-1245.
- Seydoux, G., T. Schedl and I. Greenwald, 1990 Cell-cell interactions prevent a potential inductive interaction between soma and germline in *C. elegans*. *Cell* 61: 939-951.
- Sharanya, D., C. J. Fillis, J. Kim, E. M. Zitnik, Jr., K. A. Ward *et al.*, 2015 Mutations in *Caenorhabditis briggsae* identify new genes important for limiting the response to EGF signaling during vulval development. *Evol Dev* 17: 34-48.
- Shaye, D. D., and I. Greenwald, 2002 Endocytosis-mediated downregulation of LIN-12/Notch upon Ras activation in *Caenorhabditis elegans*. *Nature* 420: 686-690.
- Shaye, D. D., and I. Greenwald, 2005 LIN-12/Notch trafficking and regulation of DSL ligand activity during vulval induction in *Caenorhabditis elegans*. *Development* 132: 5081-5092.
- Shaye, D. D., and I. Greenwald, 2011 OrthoList: a compendium of *C. elegans* genes with human orthologs. *PLoS One* 6: e20085.
- Shcherbo, D., C. S. Murphy, G. V. Ermakova, E. A. Solovieva, T. V. Chepurnykh *et al.*, 2009 Far-red fluorescent tags for protein imaging in living tissues. *Biochemical Journal* 418: 567-574.
- Shemer, G., and B. Podbilewicz, 2002 LIN-39/Hox triggers cell division and represses EFF-1/fusogen-dependent vulval cell fusion. *Genes and Development* 16: 3136-3141.
- Singh, N., and M. Han, 1995 *sur-2*, a novel gene, functions late in the *let-60* ras-mediated signaling pathway during *Caenorhabditis elegans* vulval induction. *Genes Dev* 9: 2251-2265.
- Sommer, R. J., 2012 Evolution of regulatory networks: nematode vulva induction as an example of developmental systems drift. *Adv Exp Med Biol* 751: 79-91.

- Sternberg, P. W., 1988 Lateral inhibition during vulval induction in *Caenorhabditis elegans*. *Nature* 335: 551-554.
- Sternberg, P. W., 2005 Vulval development. *WormBook*: 1-28.
- Sternberg, P. W., and H. R. Horvitz, 1986 Pattern formation during vulval development in *C. elegans*. *Cell* 44: 761-772.
- Sternberg, P. W., and H. R. Horvitz, 1989 The combined action of two intercellular signaling pathways specifies three cell fates during vulval induction in *C. elegans*. *Cell* 58: 679-693.
- Stevens, J. L., G. T. Cantin, G. Wang, A. A. Shevchenko, A. A. Shevchenko *et al.*, 2002 Transcription Control by E1A and MAP Kinase Pathway via Sur2 Mediator Subunit. *Science* 296: 755-758.
- Struhl, G., and A. Adachi, 1998 Nuclear access and action of notch in vivo. *Cell* 93: 649-660.
- Struhl, G., K. Fitzgerald and I. Greenwald, 1993 Intrinsic activity of the Lin-12 and Notch intracellular domains in vivo. *Cell* 74: 331-345.
- Struhl, G., and I. Greenwald, 1999 Presenilin is required for activity and nuclear access of Notch in *Drosophila*. *Nature* 398: 522-525.
- Subach, O. M., I. S. Gundorov, M. Yoshimura, F. V. Subach, J. Zhang *et al.*, 2008 Conversion of Red Fluorescent Protein into a Bright Blue Probe. *Chemistry and Biology* 15: 1116-1124.
- Sulston, J. E., and H. R. Horvitz, 1977 Post-embryonic cell lineages of the nematode, *Caenorhabditis elegans*. *Dev Biol* 56: 110-156.
- Sulston, J. E., and H. R. Horvitz, 1981 Abnormal cell lineages in mutants of the nematode *Caenorhabditis elegans*. *Dev Biol* 82: 41-55.
- Sulston, J. E., E. Schierenberg, J. G. White and J. N. Thomson, 1983 The embryonic cell lineage of the nematode *Caenorhabditis elegans*. *Dev Biol* 100: 64-119.
- Sulston, J. E., and J. G. White, 1980 Regulation and cell autonomy during postembryonic development of *Caenorhabditis elegans*. *Dev Biol* 78: 577-597.
- Sundaram, M., 2006 RTK/Ras/MAPK signaling. *WormBook*: 1-19.
- Sundaram, M., and I. Greenwald, 1993 Suppressors of a *lin-12* hypomorph define genes that interact with both *lin-12* and *glp-1* in *Caenorhabditis elegans*. *Genetics* 135: 765-783.
- Sundaram, M. V., 2013 Canonical RTK-Ras-ERK signaling and related alternative pathways. *WormBook*: 1-38.
- Sundaram, M. V., and M. Buechner, 2016 The *Caenorhabditis elegans* Excretory System: A Model for Tubulogenesis, Cell Fate Specification, and Plasticity. *Genetics* 203: 35-63.
- Swanson, C. I., D. B. Schwimmer and S. Barolo, 2011 Rapid evolutionary rewiring of a structurally constrained eye enhancer. *Curr Biol* 21: 1186-1196.

- Tan, P. B., M. R. Lackner and S. K. Kim, 1998 Map kinase signaling specificity mediated by the LIN-1 Ets/LIN-31 WH transcription factor complex during *C. elegans* vulval induction. *Cell* 93: 569-580.
- Tanenbaum, M. E., L. A. Gilbert, L. S. Qi, J. S. Weissman and R. D. Vale, 2014 A protein-tagging system for signal amplification in gene expression and fluorescence imaging. *Cell* 159: 635-646.
- Taniguchi, Y., T. Furukawa, T. Tun, H. Han and T. Honjo, 1998 LIM protein KyoT2 negatively regulates transcription by association with the RBP-J DNA-binding protein. *Mol Cell Biol* 18: 644-654.
- Tax, F. E., J. H. Thomas, E. L. Ferguson and H. R. Horvitz, 1997 Identification and characterization of genes that interact with *lin-12* in *Caenorhabditis elegans*. *Genetics* 147: 1675-1695.
- Tax, F. E., J. J. Yeagers and J. H. Thomas, 1994 Sequence of *C. elegans lag-2* reveals a cell-signalling domain shared with Delta and Serrate of *Drosophila*. *Nature* 368: 150-154.
- Tiensuu, T., M. K. Larsen, E. Verneris and S. Tuck, 2005 *lin-1* has both positive and negative functions in specifying multiple cell fates induced by Ras/MAP kinase signaling in *C. elegans*. *Developmental Biology* 286: 338-351.
- Tuck, S., and I. Greenwald, 1995 *lin-25*, a gene required for vulval induction in *Caenorhabditis elegans*. *Genes Dev* 9: 341-357.
- Tun, T., Y. Hamaguchi, N. Matsunami, T. Furukawa, T. Honjo *et al.*, 1994 Recognition sequence of a highly conserved DNA binding protein RBP-Jx. *Nucleic Acids Research* 22: 965-971.
- Tursun, B., L. Cochella, I. Carrera and O. Hobert, 2009 A Toolkit and Robust Pipeline for the Generation of Fosmid-Based Reporter Genes in *C. elegans*. *PLoS ONE* 4: e4625.
- Underwood, R., Y. Deng and I. Greenwald, 2017 Integration of EGFR and LIN-12/Notch Signaling by LIN-1/Elk1, the Cdk8 Kinase Module, and SUR-2/Med23 in Vulval Precursor Cell Fate Patterning in *Caenorhabditis elegans*. *Genetics*.
- Updike, D. L., and S. E. Mango, 2006 Temporal regulation of foregut development by HTZ-1/H2A.Z and PHA-4/FoxA. *PLoS Genetics* 2: 1500-1510.
- Wacker, S. A., C. Alvarado, G. Von Wichert, U. Knippschild, J. Wiedenmann *et al.*, 2011 RITA, a novel modulator of Notch signalling, acts via nuclear export of RBP-J. *The EMBO journal* 30: 43-56.
- Wagmaister, J. A., J. E. Gleason and D. M. Eisenmann, 2006 Transcriptional upregulation of the *C. elegans* Hox gene *lin-39* during vulval cell fate specification. *Mechanisms of Development* 123: 135-150.
- Wang, B. B., M. M. Muller-Immergluck, J. Austin, N. T. Robinson, A. Chisholm *et al.*, 1993 A homeotic gene cluster patterns the anteroposterior body axis of *C. elegans*. *Cell* 74: 29-42.
- Wang, G., M. A. Balamotis, J. L. Stevens, Y. Yamaguchi, H. Handa *et al.*, 2005 Mediator requirement for both recruitment and postrecruitment steps in transcription initiation. *Molecular Cell* 17: 683-694.

- Wei, G.-H., G. Badis, M. F. Berger, T. Kivioja, K. Palin *et al.*, 2010 Genome-wide analysis of ETS-family DNA-binding in vitro and in vivo. *The EMBO Journal* 29: 2147-2160.
- Weirauch, M. T., A. Yang, M. Albu, A. G. Cote, A. Montenegro-Montero *et al.*, 2014 Determination and Inference of Eukaryotic Transcription Factor Sequence Specificity. *Cell* 158: 1431-1443.
- Wen, C., M. M. Metzstein and I. Greenwald, 1997 SUP-17, a *Caenorhabditis elegans* ADAM protein related to *Drosophila* KUZBANIAN, and its role in LIN-12/NOTCH signalling. *Development* 124: 4759-4767.
- Weng, A. P., A. A. Ferrando, W. Lee, J. P. t. Morris, L. B. Silverman *et al.*, 2004 Activating mutations of NOTCH1 in human T cell acute lymphoblastic leukemia. *Science* 306: 269-271.
- Wilkinson, H. A., K. Fitzgerald and I. Greenwald, 1994 Reciprocal changes in expression of the receptor lin-12 and its ligand lag-2 prior to commitment in a *C. elegans* cell fate decision. *Cell* 79: 1187-1198.
- Wilson, J. J., and R. A. Kovall, 2006 Crystal structure of the CSL-Notch-Mastermind Ternary complex bound to DNA. *Cell* 124: 985-996.
- Wu, B., M. Ślabicki, L. Sellner, S. Dietrich, X. Liu *et al.*, 2017 MED12 mutations and NOTCH signalling in chronic lymphocytic leukaemia. *British Journal of Haematology*.
- Wu, G., S. Lyapina, I. Das, J. Li, M. Gurney *et al.*, 2001 SEL-10 Is an Inhibitor of Notch Signaling That Targets Notch for Ubiquitin-Mediated Protein Degradation. *Molecular and Cellular Biology* 21: 7403-7415.
- Wu, L., J. C. Aster, S. C. Blacklow, R. Lake, S. Artavanis-Tsakonas *et al.*, 2000 MAML1, a human homologue of *Drosophila* mastermind, is a transcriptional co-activator for NOTCH receptors. *Nature genetics* 26: 484.
- Wu, Y., and M. Han, 1994 Suppression of activated Let-60 ras protein defines a role of *Caenorhabditis elegans* Sur-1 MAP kinase in vulval differentiation. *Genes Dev* 8: 147-159.
- Yang, S.-H. H., E. Jaffray, R. T. Hay and A. D. Sharrocks, 2003 Dynamic interplay of the SUMO and ERK pathways in regulating Elk-1 transcriptional activity. *Molecular Cell* 12: 63-74.
- Yang, S. H., E. Vickers, A. Brehm, T. Kouzarides and A. D. Sharrocks, 2001 Temporal recruitment of the mSin3A-histone deacetylase corepressor complex to the ETS domain transcription factor Elk-1. *Molecular and Cellular Biology* 21: 2802-2814.
- Yochem, J., and I. Greenwald, 1989 *glp-1* and *lin-12*, genes implicated in distinct cell-cell interactions in *C. elegans*, encode similar transmembrane proteins. *Cell* 58: 553-563.
- Yochem, J., K. Weston and I. Greenwald, 1988 The *Caenorhabditis elegans* *lin-12* gene encodes a transmembrane protein with overall similarity to *Drosophila* Notch. *Nature* 335: 547-550.
- Yoo, A. S., C. Bais and I. Greenwald, 2004 Crosstalk Between the EGFR and LIN-12/Notch Pathways in *C. elegans* Vulval Development. *Science* 303.

- Yoo, A. S., and I. Greenwald, 2005 LIN-12/Notch Activation Leads to MicroRNA-Mediated Down-Regulation of Vav in *C. elegans*. *Science* 310: 1330-1333.
- Yu, H., A. S. Yoo and I. Greenwald, 2004 Cluster Analyzer for Transcription Sites (CATS): a C++-based program for identifying clustered transcription factor binding sites. *Bioinformatics* 20: 1198-1200.
- Yuzyuk, T., T. H. I. Fakhouri, J. Kiefer and S. E. Mango, 2009 The Polycomb Complex Protein *mes-2/E(z)* promotes the transition from developmental plasticity to differentiation in *C. elegans* embryos. *Developmental cell* 16: 699-710.
- Zahler, A. M., 2005 Alternative splicing in *C. elegans*.
- Zand, T. P., D. J. Reiner and C. J. Der, 2011 Ras effector switching promotes divergent cell fates in *C. elegans* vulval patterning. *Dev Cell* 20: 84-96.
- Zhang, L., J. D. Ward, Z. Cheng and A. F. Dernburg, 2015 The auxin-inducible degradation (AID) system enables versatile conditional protein depletion in *C. elegans*. *Development (Cambridge, England)* 142: 4374-4384.
- Zhang, X., and I. Greenwald, 2011 Spatial regulation of *lag-2* transcription during vulval precursor cell fate patterning in *Caenorhabditis elegans*. *Genetics* 188: 847-858.